Characterization of Photo-Induced Mechanical Responses in Azobenzene Polymers

Zahid S. Mahimwalla

Master of Science

Department of Chemistry,
McGill University,
Montreal
Quebec, Canada

A thesis submitted to McGill University in partial fulfillment of the requirements for the degree of Master of Science

Abstract

A cantilever based sensor system was adapted to characterize the photo-mechanical effect in thin films of azobenzene based polymers coated on silicon and mica cantilevers. The photomechanical effect is defined as a reversible molecular shape change upon absorption of light, resulting in a significant mechanical macroscopic deformation of the host material. The sensor was used to calculate cantilever bending, changes in surface stress, photo-mechanical energy, efficiency, and energy per unit volume for the polymers PDR1A, PDR13A and PMMA-co-PDR1A based on DR1 and DR12 dyes. The study demonstrated fast and significant cantilever bending as well as a robust, repeatable, and measurable photo-mechanical effect for the polymers studied. PDR1A exerted the largest forces and PMMA-co-PDR1A the greatest efficiency. This exhibits the ability of these thin polymer layers to act as strong light-driven 'artificial muscles' for larger mechanical systems, and the utility of the cantilever sensor platform for quantitative characterization of the photomechanical effect of azobenzene based polymers.

While micron-scale surface mass transport and formation of surface relief gratings in azobenzene polymers is a well-known phenomenon, a complete understanding of the underlying mechanism has yet to be achieved. Nanoindentation experiments were conducted to elucidate the changes in mechanical properties of PDR1A, a well-known covalent side-chain azo polymer and P4VP$(DY7)_{0.5}$, a hydrogen-bonded polymer-azobenzene complex, under irradiation. Material creep was characterized by calculation of the strain rate sensitivity m, of the two polymers for the dark and illuminated states. The experiments show a significant change in material creep between the dark and illuminated states of both materials. The measured strain rate sensitivity m increases from 0.021 to 0.038 (81%) for PDR1A and 0.086 to 0.192 (123%) for P4VP$(DY7)_{0.5}$ between the dark and illuminated states respectively. The correlation of experimental data describing photo-induced softening to the structure-property relationships of the two materials and their implications to understanding surface mass transport in azobenzene based materials is discussed.

Résumé

Un système de détection utilisant un micro-lévier fut adapté pour caractériser l'effet photomécanique dans des couches mince de polymères contenant de l'azobenzène sur des micro-lévier fabriqués de silicium et mica. L'effet photomécanique est défini comme un changement réversible de la forme moléculaire lors de l'absorption de la lumière, ce qui entraîne une déformation importante mécanique macroscopique du matériel. Ce capteur a été utilisé pour calculer la flexion du micro-lévier, les changements dans la tension de surface, l'énergie photomécanique, l'efficacité du système et l'énergie capté par unité de volume pour les polymères PDR1A, PDR13A et PMMA-co-PDR1A basé sur les chromophores DR1 et DR12. L'étude a démontré une flexion rapide ainsi que robuste du micro-lévier, basé sur des mesure reproductible photomécanique pour les polymères étudiés. Nous avons trouvé que les polymères PDR1A exercent la plus grande force et PMMA-co-PDR1A la plus grande efficacité. Ceci démontre la capacité de ces couches minces de polymères à agir en tant que «muscles artificiels» pour des systèmes mécaniques macroscopique, et l'utilité de la plate-forme du capteur micro-lévier pour la caractérisation de l'effet photomécanique des polymères à base d'azobenzène.

Bien que le transport de masse micrométrique et la formation des reliefs de surface dans les polymères d'azobenzène est un phénomène bien connu, une compréhension complète du mécanisme que mène a ceux-ci n'a pas encore été atteint. Des expériences de nanoindentation sous irradiation ont été menées pour élucider les changements dans les propriétés mécaniques de PDR1A, un polymère bien connu avec des chaînes latérales azoïques et $P4VP(DY7)_{0,5}$, un polymère complexé à l'aide de liens d'hydrogène. Du fluage de ces matériaux a été caractérisé par le calcul du rapport de la sensibilité de déformation (m) de ces deux polymères pour les états sombres et lumineux. Les expériences montrent un changement significatif du fluage des polymères entre les états sombres et lumineux de ces deux matériaux. Le taux de la sensibilité de déformation (m) mesuré augmente de 0,021 à 0,038 (81%) pour PDR1A et de 0,086 à 0,192 (123%) pour $P4VP(DY7)_{0,5}$ entre les états sombres et lumineux, respectivement. La corrélation des données expérimentales décrit l'adoucissement photo-induit basé sur les relations structure-propriété des deux matériaux, leurs implications pour la compréhension du transport de masse pour les matériaux à base d’azobenzène sont discutées.

Foreword

This thesis is in manuscript form, based upon a review book chapter, a review paper and two original research manuscripts. The review chapter and review paper have been published in 2012, with the latter forming the basis of the introduction and referenced below. Chapters 2 and 3 consist of manuscripts in the process of submission to peer-review journals.

Mahimwalla, Z., Yager, K., Mamiya, J.-i., Shishido, A., Priimagi, A., & Barrett, C. (**2012**). "Azobenzene photomechanics: prospects and potential applications." *Polymer Bulletin*, 1-40. *In Press*, doi: 10.1007/s00289-012-0792-0

Contributions of Authors

Chapter 1 is a comprehensive review of the photomechanical effect of azobenzene based materials. The review paper which forms the basis of the introduction was researched and written by the author with guidance from Prof. Christopher Barrett. The author wrote completely independently the sections relating to photomechanical actuation in thin films, amorphous azobenzene polymers, monolayers and interfacial films, applications in robotics and micromechanics, photomechanical crystalline bending and nanofabrication applications of photopatterning.

Chapter 2 describes the measurement and calculation of the photomechanical forces exerted by thin films of azobenzene polymers using a cantilever based sensor system. The results described in this chapter include collaborations with the group of Prof. Peter Grütter in the Dept. of Physics at McGill University. The initial silicon cantilever experiments were conducted with Dr. Yoshihiko Nagai of the Grütter Group. The sensor system was new, and built by the author, based upon a previously published system with technical assistance from Dr. Nagai. All sample preparation, experimental design, data acquisition, analysis, and interpretation as well as manuscript preparation was performed by the author under the supervision of Professor Christopher Barrett and with guidance from Professor Peter Grütter.

Chapter 3 describes the characterization of the strain rate sensitivity of two azobenzene based polymers. The results of this chapter include collaborations with Prof. Richard Chromik from the Department of Mining and Materials Engineering, McGill, and from Aalto University, Finland. All PDR1A sample preparation, design of sample irradiation in the indenter, data acquisition, and analysis using the Mayo and Nix methodology were carried out by the author under the supervision of Professors Christopher Barrett and Richard Chromik. The preparation of Poly4VP samples, design of the Dynamic Mechanical Analysis (DMA) experiments and related data acquisition and analysis were performed at McGill under the supervision of the author, with the assistance of Jaana Vapaavuori as a visiting student to McGill. The interpretation of data and preparation of the manuscript was performed by the author and Jaana Vapaavuori under the guidance of Professors Barrett, Chromik, Priimagi and Kaivola.

Acknowledgements

I would like to thank my thesis supervisor Professor Christopher Barrett for his support over the years. I’d like to say a heartfelt thank you for all the research and collaborative opportunities you have enabled, allowed me to participate in and experience. It has helped me improve as both a scientist and person. Your enthusiasm for science is contagious and your support and guidance will always be appreciated.

I’d like to make a very special thank you to Dr. Yoshihiko Nagai for his guidance, support and friendship during my graduate studies at McGill.

A giant thank you to all the members of the Barrett Group for their friendship, support, and providing me with an intellectually stimulating environment. In particular I’d like to acknowledge Miloslav, Alex, Tom, Janet, Yingshan, Annie, and Oleksandr for fond memories both in and out of the laboratory.

I would like to thank CSACS and Petr Fiurasek for critical support in the form of general scientific help, equipment training and travel funding.

I’d like to express my gratitude to YaoYao Ding for volunteering her time to train me on the nanoindenter, and providing support when things mysteriously stopped working, when I needed a sounding board for ideas or questions answered.

I’d also like to thank my friends and family in Montreal and elsewhere for their support, encouragement and many fond memories.

Finally I’d like to thank my parents, without your support, encouragement and guidance I would not be where I am today.

Thank You All

Table of Contents

Abstract i

Résumé ii

Foreword iv

Contributions of Authors iv

Acknowledgements vi

Table of Contents vii

List of Figures ix

List of Tables xi

Chapter 1: Introduction 1

- 1.1 Abstract 1
- 1.2 Azobenzene 2
  - 1.2.1 Azobenzene Photochemistry 5
  - 1.2.2 Photostationary State of Azobenzene 8
- 1.3 Photoinduced Motions and Movements 9
  - 1.3.1 Molecular Motion 10
  - 1.3.2 Macroscopic Motion 11
  - 1.3.3 Photo-Patterning and -Morphing 13
  - 1.3.4 Nanofabrication Applications of Photo-Patterning 16
- 1.4 Photomechanical Actuation 20
  - 1.4.1 Photo-Actuation in Monolayers and Interfacial Flms 20
  - 1.4.2 Photo-Actuation in Amorphous Thin Films 23
  - 1.4.3 Photo-Actuation in Liquid-Crystalline Polymers 26
- 1.5 Applications in Robotics and Micromechanics 30
- 1.6 Conclusions and Outlook, Scope of this Thesis 38
- 1.7 References 40

Chapter 2: Measuring the Photomechanical Effect in Thin Polymer Films of Azobenzene Using a Cantilever Based Sensor..................................68

2.1 Abstract..................................68

2.2 Introduction..................................69

2.3 Experimental..................................72

2.3.1 Materials..................................72

2.3.2 Coatings..................................72

2.3.3 Bending..................................72

2.4 Results and Discussion..................................74

2.5 Conclusions..................................81

2.6 References..................................82

Chapter 3: Measuring Photo-Induced Softening of Azobenzene Systems by Nanoidentation..................................86

3.1 Abstract..................................**Error! Bookmark not defined.**

3.2 Introduction..................................**Error! Bookmark not defined.**

3.3 Materials and Methods..................................**Error! Bookmark not defined.**

3.4 Results and Discussion..................................**Error! Bookmark not defined.**

3.5 References..................................**Error! Bookmark not defined.**

Chapter 4: Conclusions and Future Work..................................99

4.1 Conclusions..................................99

4.2 Future Work..................................100

List of Figures

Figure 1.1: Examples of azobenzene molecules of azobenzene-type , aminoazobenzene-type and pseudostilbene-type, and their absorption spectra measured from dilute tetrahydrofuran solution.. 7

Figure 1.2: AFM image of a typical surface relief grating (SRG) optically inscribed into an azo-polymer film.. 14

Figure 1.3: Schematic of the fabrication of the glucose-sensing hydrogel gratings [173] 18

Figure 1.4: SEM images of straight-walled (a upper) and mushroom-shaped (b lower) silicon nanopillar arrays. [176] 19

Figure 1.5: Photographs of the photodeformation of Keller's azobenzene-containing LCE before (a) and under (b) UV light irradiation, demonstrating a clear change in shape inducible [241] 27

Figure 1.6: Precise control of the bending direction of a film by linearly polarized light. Chemical structures of the LC monomer and crosslinker (top) used for preparation of the film, and photographic frames of the film in different directions in response to irradiation by linearly polarized light of different polarization directions (white arrows) at 366 nm, and bending flattened again by visible light longer than 540 nm [107] 29

Figure 1.7: Stress–strain curves for nonexposed and UV-irradiated films of three azo-CLCPs, denoted P20, P60, and P100. [252] 31

Figure 1.8: A light-driven plastic motor using the laminated azo-CLCP film. a) Schematic illustration of a light-driven plastic motor system, showing the relationship between light irradiation positions and a rotation direction. b) Series of photographs showing time profiles of the rotation of the light-driven plastic motor with the LCE laminated film induced by simultaneous irradiation with UV and visible light at room temperature. Reproduced from Ikeda *et al.* [193] 33

Figure 1.9: Series of photographs showing time profiles of the flexible robotic arm motion of a laminated azo-CLCP film, induced by irradiation with UVand visible light at room temperature. Arrows indicate the direction of light irradiation. Reproduced from Ikeda *et al.* [255] 34

Figure 1.10: The optical protocol for activating the light powered oscillation of a cantilever. The nematic director (n) is positioned parallel to the long axis of the polymer cantilever of dimension 5 mm x 1 mm x 50 mm. When exposed to light polarized orthogonal to n (E⊥n) bending occurs toward the laser source. Cycling the Ar+ laser from E⊥n to E//n can turn oscillation ''on'', while blocking the Ar+ or returning the polarization of the laser beam to E\n turns the oscillation ''off''. Reproduced from Bunning *et al* [189] 35

Figure 2.1: a) The *trans-cis* isomerization of azobenzene, b) the polymers (i) Poly Disperse Red 1 Acrylate (PDR1A), (ii) Poly Disperse Red 13 Acrylate (PDR13A) and (iii) Poly Methyl Methacrylate –co-Poly Disperse Red 1 Acrylate (PMMA-co-PDR1A)...... 70

Figure 2.2: Photographs of the silicon (left) and mica (right) cantilevers and their dimensions. 74

Figure 2.3: Schematic view of the cantilever bending in the sensor system. The polymer coating expands upon irradiation by the pump beam exerting a compressive surface stress upon the cantilever. 74

Figure 2.4: Top: Deflection (μm) and Photomechanical stress (N/m) plots of a silicon cantilever coated with PDR1A where the positive deflection is defined as a compressive stress exerted by the coating causing cantilever bending towards the probe beam (Fig. 3). Sample is irradiated for 200 s then allowed to relax for 200 s. Bottom: Repeat pump and relaxation cycles of sample. 76

Figure 2.5: Top: Deflection (μm) and photomechanical stress (N/m) plots of a mica cantilever coated with PDR1A and irradiated at 80 mW/cm^2. Sample is irradiated for 50 s then allowed to relax for 100 s. Bottom: Repeat pump and relaxation cycles of sample. 78

Figure 2.6: Surface stress changes of mica cantilevers coated with PDR1A, PDR1A with solvent, PDR13A, and PMMA-co-PDR1A to increasing pump beam power. 79

Figure 3.1: Structures of (a) PDR1a polymer and (b) P4VP(DY7)$_{0.5}$ polymer-azobenzene complex. .... **Error! Bookmark not defined.**

Figure 3.2: (a) The nanoindenter load as a function of the penetration depth and (b) the depth as a function of time for loading rate of 5 μN/s, under the illumination of 532 nm light (dashed line) and in darkness (solid line) .... **Error! Bookmark not defined.**

Figure 3.3: The stress strain-rate data pairs at the depth of 150 nm for (a) PDR1a and (b) P4VP(DY7)$_{0.5}$ under 532 nm light illumination (open circles) and in darkness (open squares). .... **Error! Bookmark not defined.**

List of Tables

Table 2.1: Summary of the photomechanical energy, efficiency and energy exerted per unit volume of film calculated from the photomechanical response of mica coated cantilevers at a beam power of 100 mW/cm^2. 80

Table 3.1: The values of fitted strain-rate sensitivities for both materials under the illumination of 532 nm light and in darkness. ....**Error! Bookmark not defined.**

Chapter 1: Introduction

This chapter provides a comprehensive introduction to the research relating to the photomechanical effect of azobenzene based materials. It is based upon a recently published literature review, with the text reprinted with permission from:

Mahimwalla, Z., Yager, K., Mamiya, J.-i., Shishido, A., Priimagi, A., & Barrett, C. (**2012**). "Azobenzene photomechanics: prospects and potential applications." *Polymer Bulletin*, 1-40. *In Press*, doi: 10.1007/s00289-012-0792-0

1.1 Abstract

The change in shape inducible in some photo-reversible molecules using light can effect powerful changes to a variety of properties of a host material. This class of reversible light-switchable molecules includes molecules that photo-dimerize, such as coumarins and anthracenes; those that allow intra-molecular photo-induced bond formation, such as fulgides, spiro-pyrans, and diarylethenes; and those that exhibit photo-isomerization, such as stilbenes, crowded alkenes, and azobenzenes. The most ubiquitous natural molecule for reversible shape change, however, and perhaps the inspiration for all artificial bio-mimics, is the rhodopsin/ retinal protein system that enables vision, and this is the quintessential reversible photo-switch for performance and robustness. Here, the small retinal molecule embedded in a cage of rhodopsin helices isomerizes from a *cis* geometry to a *trans* geometry around a C=C double bond with the absorption of just a single photon. The modest shape change of just a few angstroms is quickly amplified and sets off a cascade of larger shape and chemical changes, eventually culminating in an electrical signal to the brain of a vision event, the energy of the input photon amplified many thousands of times in the process. Complicated biochemical pathways then revert the *trans* isomer back to *cis*, and set the system back up for another cascade upon subsequent absorption. The reversibility is complete, and many subsequent cycles are possible. The reversion mechanism back to the initial *cis* state is complex and enzymatic, hence direct application of the retinal/rhodopsin photo-switch to engineering systems is difficult. Perhaps the best artificial mimic of this strong photo-switching effect however

in terms of reversibility, speed, and simplicity of incorporation, is azobenzene. *Trans* and *cis* states can be switched in microseconds with low-power light, reversibility of 10^5 and 10^6 cycles is routine before chemical fatigue, and a wide variety of molecular architectures is available to the synthetic materials chemist, permitting facile anchoring and compatibility, as well as chemical and physical amplification of the simple geometric change.

This review chapter focuses on photo-mechanical effect taking place in various material systems incorporating azobenzene. The photo-mechanical effect can be defined as reversible change in shape by absorption of light, which results in a significant macroscopic mechanical deformation, and reversible mechanical actuation, of the host material. Thus, we exclude simple thermal expansion effects, reversible but non-mechanical photo-switching or photo-chemistry, as well as the wide range of optical and electro-optical switching effects for which good reviews exist elsewhere. Azobenzene-based material systems are also of great interest for light energy harvesting applications across much of the solar spectrum, yet this emerging field is still in an early enough stage of research output as to not yet warrant review, but we hope that some of the ideas put forward here toward promising future directions of research, will help guide the field.

1.2 Azobenzene

Azobenzene, with two phenyl rings separated by an azo (–N=N–) bond, serves as the parent molecule for a broad class of aromatic azo compounds. These chromophores are versatile molecules, and have received much attention in research areas both fundamental and applied. The strong electronic absorption band can be tailored by ring substitution to fall anywhere from the ultraviolet to red-visible regions, allowing chemical fine-tuning of color. This, combined with the fact that the azo groups are relatively robust and chemically stable, has prompted extensive study of azobenzene-based structures as dyes and colorants. With appropriate electron-donor/acceptor ring substitution, the π electron delocalization of the extended aromatic structure can yield high optical nonlinearity, and azo chromophores have been extensively studied for nonlinear optical applications as well [1, 2]. One of the most interesting properties of these chromophores, however, and the main subject of this chapter, is the readily induced and reversible *trans–cis* photoisomerization of the azo bond and the geometric changes that result when azo chromophores are incorporated into polymers and other materials. This light-induced interconversion allows systems incorporating azobenzenes to be used as photo-switches, effecting rapid and reversible control over a variety of chemical, mechanical, electronic, and optical properties.

Examples of azobenzene-based photo-control have been demonstrated in photo-switchable phase changes [3], phase separation (or reversal of phase separation) [4, 5], solubility changes [6, 7], and crystallization [8]. These suggest a highly promising route toward novel functional materials: the incorporation of photo-physical effects into self-assembling systems. The inherent amplification of molecular order to macroscopic material properties can be coupled with molecular-scale photo-switching. For instance, in amphiphilic polypeptide systems, self-assembled micelles were stable in the dark, but could be disaggregated with light irradiation [9]. This construct can act as a trans-membrane structure, where the reversible formation and disruption of the aggregate enabled photo-switchable ion transport [10]. In another example, cyclic peptide rings connected by a *trans*-azo unit would hydrogen-bond with their neighbors, forming extended chains. The *cis* azo analog, formed upon irradiation, participates in intra-molecular hydrogen bonding, forming discrete units, and thereby disrupting the higher-order network [11, 12]. A system of hydrogen-bonding azobenzene rosettes was also found to spontaneously organize into columns and these columns to assemble into fibers. Upon UV irradiation, this extended ordering was disrupted [13], converting a solid organogel into a fluid. Similarly, large changes in viscosity can be elicited by irradiating a solution of azo polyacrylate associated with the protein–bovine serum albumin [14]. In a liquid crystal systems, light can be used to induce a glass-to-LC phase transition [15, 16]. A wide variety of applications (such as microfluidics) is possible for functional materials that change phase upon light stimulus.

The primary and secondary shapes of azo-containing self-assembled structures in solution can also be controlled with light. Azo block-copolymers can be used to create photo-responsive micelles [17–21], and vesicles [22]. The isomerization-induced change in azo dipole moment plays a critical role in determining the difference between the aggregations in the two states, and can be optimized to produce a highly efficient photo-functional vesicle system [23]. The use of azo photo-isomerization to disrupt self-assembled systems may be particularly valuable when coupled with biological systems. With biomaterials, one can exploit the powerful and efficient biochemistry of natural systems, yet impose the control of photo-activation. The azobenzene unit in particular has been applied to photobiological experiments with considerable success [24, 25]. Order–disorder transitions can also be photo-induced in biopolymers. Azo-modified polypeptides may undergo transitions from ordered chiral helices to disordered solutions [26–28], or even undergo reversible a-helix to b-sheet conversions [29]. In many cases catalytic activity can be regulated due to the presence of the azo group. A cyclodextrin with a histidine and azobenzene pendant, for example, was normally inactive because the *trans*-azobenzene would bind inside the cyclodextrin pocket, whereas the photo-generated *cis*-azobenzene liberated the catalytic site [30]. Thus, the ability to create biomaterials whose biological functions are activated or inhibited on demand via light is of interest for fundamental biological studies, and, possibly, for dynamic biomedical implants [25, 31].

Perhaps ranging as widely as the interesting phenomena displayed by azo aromatic compounds, is the variety of molecular systems into which these chromophores can be incorporated. In addition to liquid-crystalline (LC) media and amorphous glasses, azobenzenes can be incorporated into self-assembled monolayers and superlattices, sol–gel silica glasses, and various biomaterials. The photochromic or photo-switchable nature of azobenzenes can also be used to control the properties of novel small molecules, such as crown-ethers [32], cyclodextrins [33, 34], proteins such as bacteriorhodopsin [35], and 3D polycyclics such as cubane [36], and adamantane [37]. Typically, however, azo chromophores are embedded into a solid matrix for studies and real devices. As a result, matrix effects are inescapable: the behavior of the chromophore is altered due to the matrix, and in turn the chromophore alters the matrix [38, 39]. Although either could be viewed as a hindrance, both can in fact be quite useful: the chromophore can be used as a delicate probe of the matrix (free volume, polarizability, mobility, morphology, viscoelasticity, etc.), and when the matrix couples to chromophore motion, molecular motions can be translated to larger length scales, for example using nanometer ‘‘command surfaces’’ of azo chromophores to re-orient surrounding micron-sized layers of inert liquid crystals [38]. Thus, the incorporation strategy can be extremely valuable for transferring and amplifying azobenzene’s photo-reversible effects.

As the above examples illustrate, azobenzene is a unique and powerful molecular switch, the function of which can be amplified such that also larger-scale material properties are switched or altered in response to light. Therefore, azo-containing materials exhibit a number of fascinating photo-mechanical effects. Herein, we present an attempt at a comprehensive review on these photo-mechanical effects in various material systems, and on their exploitation in designing photo-mobile and photo-deformable materials. The motions covered range from 1D motion on flat surfaces and 2D mass transport, to micro-and macro-scale 3D motions and their applications in micro-actuation and robotics.

1.2.1 Azobenzene Photochemistry

In this chapter ‘‘azobenzene’’ and ‘‘azo’’ are used in a general way: to refer to the class of compounds that exhibit the core azobenzene structure, with different ring substitution patterns (even though, strictly, these compounds should be referred to as ‘‘diazenes’’). There are many properties common to nearly all azobenzene molecules. The most obvious is the strong electronic absorption of the conjugated π system. This absorption spectrum can be tailored, via ring substitution, to lie anywhere from the ultraviolet to the visible-red region. Based on the absorption spectrum, azobenzenes can be classified into three spectroscopic classes [40]: azobenzene-type molecules, aminoazobenzene-type molecules, and pseudo-stilbenes (Fig. 1.1). Azobenzene-type molecules exhibit absorption characteristics similar to the unsubstituted azobenzene archetype and a long half-life. Adding ortho- or para- substituents with an electron-donating group (usually an amino, –NH_2), results in a red-shifted absorbance spectrum and a shorter half-life, describing the aminoazobenzene-type spectroscopic class. Substitution of azobenzene at the 4 and 4′ positions with an electron-donor and -acceptor (such as an amino and a nitro, –NO_2, group) leads to a strongly asymmetric electron distribution (often referred to as a ‘‘push/pull’’ substitution pattern) and defines the third spectroscopic class, the pseudo-stilbenes. Pseudo-stilbenes are significantly red-shifted and have shorter half-lives.

The most startling and intriguing characteristic of the azobenzenes is their highly efficient and fully reversible photo-isomerization. Azobenzenes have two stable geometric isomer states: a thermally stable elongated *trans* configuration, and a meta-stable bent *cis* form. Remarkably, the azo chromophore can interconvert between these two isomers upon absorption of just a single photon, as the quantum yield in many systems approaches unity. For most azobenzenes, the molecule can be optically isomerized from *trans* to *cis* with light anywhere within the broad absorption band in the near UV and Visible, and the molecule will subsequently thermally relax back to the *trans* state on a timescale dictated by the substitution pattern.

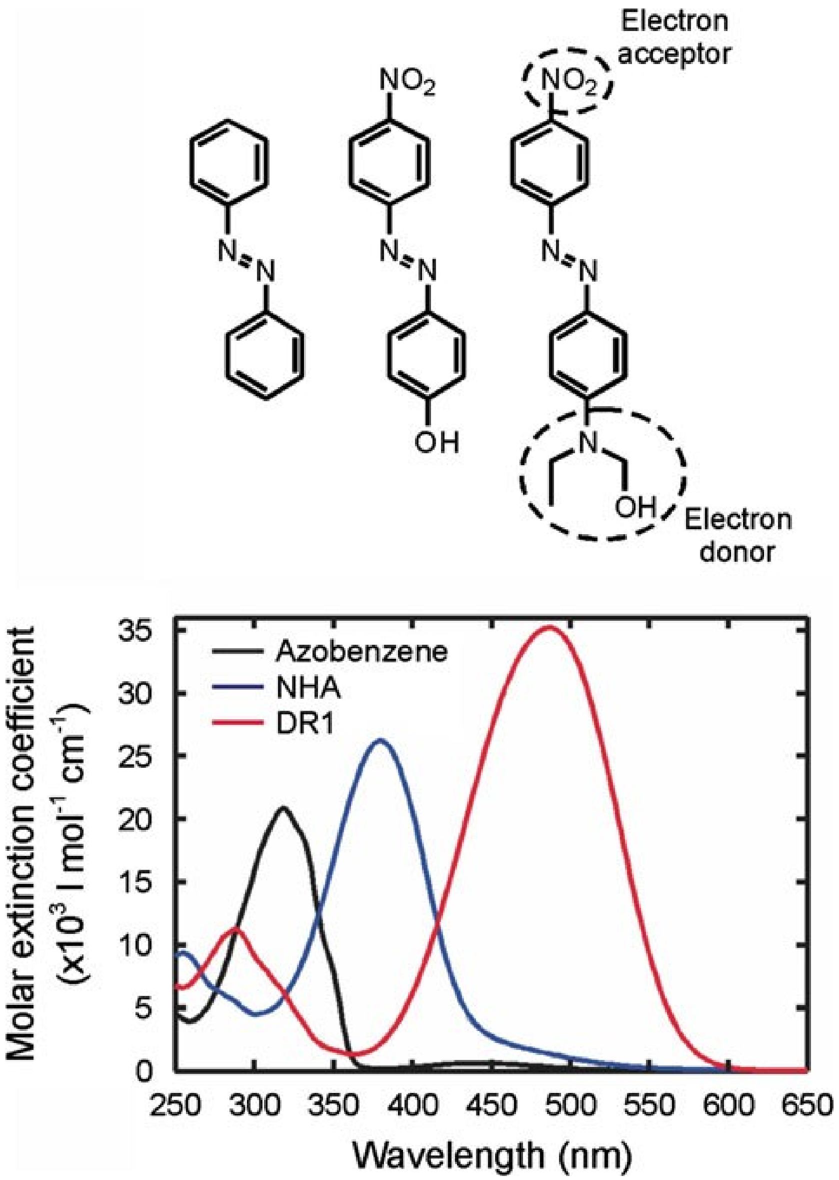

Figure 1.1: Examples of azobenzene molecules of azobenzene-type (unsubstituted azobenzene, upper left), aminoazobenzene-type (4-nitro-4´-hydroxyazobenzene (NHA), upper center), and pseudostilbene-type (Disperse Red 1 (DR1), upper right), and their absorption spectra measured from dilute tetrahydrofuran solution. Note that the azobenzene classification rests on the absorption spectrum rather than the chemical structure of the compound. Hence, molecules with weak push-pull character such as NHA can be classified into the aminoazobenzene category.

Azobenzene photo-isomerization is completely reversible and free from side reactions. The *trans* isomer is more stable by approximately 50–100 kJ/mol [41, 42], and the energy barrier to the photo-excited state (barrier to isomerization) is on the order of 200 kJ/mol [43]. In the dark, azobenzene molecules will be found initially in the *trans* form. Upon absorption of a photon (with a wavelength in the *trans* absorption band), the azobenzene will convert, with high efficiency, into the *cis* isomer. A second wavelength of light (corresponding to the *cis* absorption band) can cause the back-conversion, and both these forward and reverse photoisomerizations typically exhibit picosecond timescales [44, 45]. Alternately, azos will thermally reconvert from the *cis* to *trans* state, with a timescale ranging from milliseconds to hours, or even days, depending on the substitution pattern and local environment. More specifically, the lifetimes for azobenzenes, aminoazobenzenes, and pseudo-stilbenes are usually on the order of hours, minutes, and seconds, respectively. The energy barrier for thermal isomerization is on the order of 100–150 kJ/mol [46, 47]. In addition, one can also generate a system that starts in the *cis* state, and where isomerization (in either direction) is completely hindered. For instance, attachment to a surface [48], direct synthesis of ring-like azo molecules [49], and crystallization of the *cis* form [50, 51] can be used to maintain one state, but such systems are not bistable photo-switches, nor are they reversible.

1.2.2 Photostationary State of Azobenzene

A bulk azo sample or solution under illumination will reach a photostationary state, with a steady-state *trans/cis* composition based on the competing effects of photoisomerization into the *cis* state, thermal relaxation back to the *trans* state, and *cis* reconversion upon light absorption. The steady-state composition is unique to each system, as it depends on the quantum yields for the two processes (*trans* and *cis*) and the thermal relaxation rate constant. The composition also thus depends upon irradiation intensity, wavelength, temperature, and the chromophore environment. Azobenzenes are photochromic, since the effective absorption spectrum (a combination of the *trans* and *cis* spectra) changes with light intensity. Thus absorption spectroscopy can be conveniently used to measure the *cis* fraction in the steady-state [52, 53], and the subsequent thermal relaxation to an all-*trans* state [54–57]. NMR spectroscopy can also be used [58]. Under moderate irradiation, the composition of the photostationary state is predominantly *cis* for azobenzenes, mixed for aminoazobenzenes, and predominantly *trans* for pseudo-stilbenes. In the dark, the *cis* fraction is below most detection limits, and the sample can be considered to be in an all-*trans* state. The ring substitution pattern affects both the *trans* and the *cis* absorption spectra, and for certain patterns, the absorption spectra of the two isomers overlap significantly (notably for the pseudo-stilbenes). In these cases, a single wavelength of light activates both the forward and reverse reactions, leading to a mixed stationary state, and continual inter-conversion of the molecules. For some interesting azobenzene photo-motions, this rapid and efficient cycling of chromophores is advantageous, whereas in cases where the azo chromophore is being used as a switch, it is clearly undesirable.

The mechanism of isomerization has undergone considerable debate [59–63]. Isomerization takes place either through a rotation about the activated N–N single bond, with rupture of the π bond, or through inversion, with a semi-linear and hybridized transition state, where the π-bond remains intact. The thermal back-relaxation is generally agreed to proceed via rotation, whereas for the photochemical isomerization, both mechanisms appear viable with a different one dominating depending on the particular chromophore and environment [64]. Furthermore, *ab initio* and density functional theory calculations indicate that both pathways are energetically accessible, although inversion is preferred [65, 66]. The availability of the inversion mechanism explains how azos are able to isomerize easily even in rigid matrices, such as glassy polymers, since the inversion mechanism usually has a much smaller free volume requirement than the rotation.

1.3 Photoinduced Motions and Movements

Light irradiation produces geometric changes in azobenzenes, and under appropriate conditions, these changes can translate into larger-scale motions and even macroscopic movements of the material system. These motions can take place at various size scales [67], but as the motion on any size-scale invariably affects (and is affected by) other scales, clear divisions do not exist, and these effects are often concurrent and inter-dependent. The most relevant motion to eventual actuation applications is expansion and contraction due to the photo-mechanical effect and this effect will be highlighted in this review. The related effect of all-optical surface patterning (‘‘photo-morphing’’), which occurs when an azo-polymer film is exposed to a light intensity gradient, will also be reviewed and discussed [1, 67–69].

1.3.1 Molecular Motion

The root fundamental molecular photo-motion in azobenzenes is the geometrical change that occurs upon absorption of light. In *cis*-azobenzene, the phenyl rings are twisted at 90° relative to the C–N=N–C plane [60, 70]. Isomerization reduces the distance between the 4 and 4′ positions from 0.99 nm in the *trans* state to 0.55 nm for the *cis* state [71–73]. This geometric change creates or increases the dipole moment: whereas the *trans* form has no dipole moment in parent azobenzene, the *cis* form has a dipole moment of 3.1 D [50]. The free volume requirement of the *cis* can be much larger than the *trans* [74], and the free volume required to ‘‘cycle between’’ these two states larger still. It has been estimated that the minimum free volume pocket required to allow isomerization to proceed through a transition state via the inversion pathway is 0.12 nm^3 [60, 75], and via the rotation pathway approximately 0.38 nm^3 [76]. The effects of matrix free volume constraints on photochemical reactions in general have been considered [77]. The geometrical changes in azobenzene are very large, by molecular standards, and it is thus no surprise that isomerization modifies a wide host of material properties. More recent measurements via high-pressure spectroscopy (10^4–10^5 atm) on the force applied and energy exerted through this isomerization suggest that azobenzene is indeed an extremely powerful little artificial muscle, and application optimization for actuators depends largely on clever engineering of the mechanical advantage provided, and is not inherently materials-limited.

This molecular shape change generates a significant nanoscale force, which has been measured in single-molecule force spectroscopy experiments [78, 79], and compared well to theory [80]. In these experiments, illumination causes contraction of an azobenzene-polymer, showing that each chromophore can exert pN to nN molecular forces on demand. This force can be further engineered into an on-off or ‘‘ratchet motion’’ switch bridging the gap between force and simple machinery, such as that demonstrated by an ingenious two-state pseudo-rotaxane that could be reversibly threaded–dethreaded using light which Stoddart and co-workers [81, 82] called an ‘‘artificial molecular-level machine’’. The ability to activate and power molecular-level devices using light is of course attractive in many applications, since it circumvents the limitations inherent to diffusion or wiring, and permits a remote (or even quite distant) power supply. The fast response and lack of waste products in azo isomerization are also advantageous. Coupling these molecular-scale motions to do actual human-scale useful work is of course the next challenging step. Encouraging progress in this direction is evident, however, from a wide variety of molecular switches that have been synthesized. For example, an azo linking two porphyrin rings enabled photo-control of electron transfer [83], and in another example, dramatically different hydrogen-bonding networks (intermolecular and intramolecular) could be favored based on the isomeric state of the azo group linking two cyclic peptides [11, 12]. Other recently reported examples include osmotic pressure pumps [84], created by the photo-controlled solubility of azobenzene, analytical columns that increase the effluent rate of developing solvents [85], reversible light-controlled conductance switching [86], and photoresponsive gold nanoparticle solvation [87], and network formation [88].

1.3.2 Macroscopic Motion

While it is important to study the nm-scale azobenzene molecular conformational changes that give rise to macroscopic phenomena, by far the most useful applications to actuation are the reversible changes that can result macroscopic motions over the μm to cm size-scale. The first consideration is perhaps whether the host material can expand or contract to an appreciable extent. In floating monolayers at a liquid surface, it is well-established that the larger molecular size of the *cis* isomer leads to a corresponding lateral expansion of tens of percent [89], which can modify other bulk properties. For instance, this allows photo-modulation of a monolayer’s water contact angle [90], or surface potential [91]. Using fluorinated azo-polymers, good photo-control over photo-patterning [92, 93], and wettability has been demonstrated [94–96]. A monolayer of azo-modified calixarene, when irradiated with a light gradient, produced a gradient in surface energy sufficient to move a macroscopic oil droplet [97]. In more recent work surfactants of azobenzene were used to create a liquid–liquid interface between oleic acid droplets in an aqueous solution [98]. Photoisomerization of the azobenzene surfactant created a wavelength-dependent interfacial tension capable of inducing interfacial flow, and this interfacial flow then generated large-scale droplet motion in a direction opposite to the gradient. The photo-controlled droplet motion was thus used to direct droplets into various trajectories. It also suggests possible applications of the above materials to microfluidics. Modest photo-induced contact angle changes for thin polymer films have also been reported [99]. Recently an azobenzene copolymer assembled into polyelectrolyte multilayer showed a modest 2º change in contact angle with UV light irradiation. However, when the same copolymer was assembled onto a patterned substrate, the change in contact angle upon irradiation was enhanced to 70º [96]. The fact that surface roughness plays a role in contact angle is well-established, and shows that many systems can be optimized to give rise to a large change in surface properties through clever amplification.

In layered inorganic systems with intercalated azobenzenes, reversible photoinduced changes in the basal spacing (on the order of 4%) can be achieved [100, 101]. In polymer films, there is evidence that the film thickness increases, as measured by *in situ* single-wavelength ellipsometry, atomic force microscopy (AFM), and *in situ* neutron reflectometry [102–104]. Photo-contraction for semicrystalline main-chain azos has been measured, [105, 106] where the extent and direction (expansion or contraction) of photo-mechanical change can be tuned by using ambient temperature as demonstrated by variable-temperature neutron reflectometry experiments. The experiments demonstrated unambiguously that both photo-expansion and photo-contraction could be optimized in a single azo-material merely by varying the dominance of these two competing effects with low and high extremes of temperature, respectively.

The most convincing demonstration of macroscopic motion due to azo isomerization is the mechanical bending and unbending of a free-standing LC polymer film [107, 108]. The macroscopic bending direction may be selected either with polarized light, or by homogeneously aligning the mesogens within the polymer network. Bending occurs in these relatively thick films because the free surface (which absorbs light) contracts, whereas the interior of the film (which is not irradiated owing to the strong absorption of the upper part of the film) does not contract. Because the direction of bending can be controlled with polarized light, the materials enable full directional photomechanical control [109]. One can also invert the coupling of mechanical and optical effects: by stretching an elastomeric azo film containing a grating, one can affect its wavelength-selection properties and orient chromophores [110]. Much of this bending and related motion at the macroscale are invariably related to or have possible applications in actuation and will be discussed further later in the chapter.

1.3.3 Photo-Patterning and -Morphing

In 1995, an unexpected and unprecedented optical effect was discovered in polymer thin films. The Natansohn/Rochon research team [111], and the Tripathy/Kumar collaboration [112], simultaneously and independently discovered a large-scale surface mass transport when the films were irradiated with a light interference pattern. The mass transport takes place when two coherent laser beams, with a wavelength within the azo absorption band, are intersected at the sample surface. The sample usually consists of a thin spin-cast film (10–1,000 nm) of an amorphous azo-polymer on a transparent substrate. The sinusoidal light interference pattern at the sample surface leads to a sinusoidal surface pattern, often referred to in the literature as a surface relief grating (SRG), However, the azo-initiated surface mass transport is not limited to just gratings and can produce arbitrary structures, dictated by the spatial intensity and polarization pattern of the incident light. Hence, the phenomenon might more accurately and generally be called photo-patterning, -transport, or -morphing. The SRGs were found to be extremely large, up to hundreds of nanometers, as confirmed by AFM (Fig. 1.2), suggesting that light triggers the polymer chains to ‘‘walk’’ across the substrate surface over a distance of hundreds of nm. The SRGs diffract light very cleanly and efficiently, and in retrospect it is clear that many reports of large diffraction efficiency prior to 1995, attributed to birefringence, were in fact due to surface gratings unbeknownst to the experimenters. The process occurs readily at room temperature (well below the T_g of the amorphous polymers used) with moderate irradiation (1–100 mW/cm^2) over seconds to minutes. The phenomenon is caused by reversible mass transport, not irreversible material ablation, since a flat film with the original thickness is recovered upon heating above T_g. Importantly, the photo-patterning of amorphous azo-polymers is strongly polarization-dependent: efficient gratings are formed when an interference pattern formed by two *p*-polarized or counter-circularly polarized light beams, whereas *s*-polarized beams produce essentially no grating [68]. This evidences that neither thermal effects nor photodegradation play a significant role in the light-induced mass transport, and that what appears to be essential for efficient surface patterning is an ‘‘electric-field gradient’’ in the direction of the grating vector [113, 114].

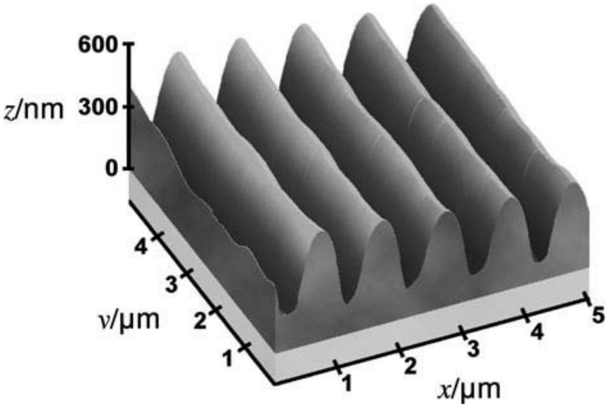

Figure 1.2: AFM image of a typical surface relief grating (SRG) optically inscribed into an azo-polymer film. Grating amplitudes of hundreds of nanometers, on the order of the original film thickness, are easily obtained. In this image, the approximate location of the film-substrate interface has been set to z = 0, based on knowledge of the film thickness.

The all-optical patterning unique to azobenzenes has been studied intensively since its discovery and many reviews of the remarkable body of experimental results are available [1, 67, 69, 115]. Critically, it requires the presence and isomerization of azobenzene chromophores, as other absorbing but non-isomerizing chromophores do not produce SRGs. Concomitant with the inscription of a surface relief is a photo-orientation of the azo chromophores, which depends on the polarization of the incident beam(s). The chromophore orientation has been measured using polarized Raman confocal microspectrometry [116–118], and the strong surface orientation has been confirmed by photoelectron spectroscopy [119]. It is found is that the chromophores orient perpendicular to the local polarization vector of the impinging interference pattern. Thus, for a (+45º, –45º) two-beam interference: in the valleys ($x = 0$) the electric field is aligned in the *y*-direction (see Fig. 1.2 for the coordinate axes), so the chromophores orient in the x-direction; in the peaks ($x = \Lambda/2$) the chromophores orient in the y-direction; in the slope regions ($x = \Lambda/4$) the electric field is circularly polarized and thus the chromophore distribution are nearly in-plane isotropic. For a (*p, p*) two-beam interference, the chromophores are primarily oriented in the *y*-direction everywhere, since the impinging light pattern is always linearly polarized in the *x*-direction. Recent theoretical studies concerning the origin of the SRG formation relate the photo-orientation and the resultant entropy decrease to the photoinduced deformation of the polymer system [120, 121]. Recent experiments, on the other hand, seem to suggest that efficient photo-orientation is not a prerequisite for efficient mass transport, and that collaborative effects can suppress the SRG formation on azo-polymer films [122].

The anisotropy grating that is submerged below a surface relief grating apparently also leads to the formation of a density grating under appropriate conditions. It was found that upon annealing, which erases the surface grating and restores a flat film surface, a density grating began growing beneath the surface (and into the film bulk) [123, 124]. This density grating only develops where the SRG was originally inscribed, and it appears that the photo-orientation and mass transport leads to the nucleation of ''seeding aggregates'' that are thermally grown into larger-scale density variations. The thermal erasure of the SRG, with concomitant growth of the density grating, has been both measured [125], and modeled [126].

It was recognized early on that the gratings do not form in systems of small molecules (for instance, comparing unreacted monomers to their corresponding polymers). The polymer molecular weight (M_W), however, must not be too large [127]. Presumably a large M_W eventually introduces entanglements, which act as crosslinks, hindering polymer motion. Thus, intermediate molecular weight polymers ($M_W \sim 10^3$, arguably oligomers) are optimal [128]. That having been said, there are many noteworthy counter-examples. Weak SRGs can be formed in polyelectrolyte multilayers, which are essentially crosslinked polymer systems [118, 129–131], and efficient SRGs have been inscribed in high-molecular-weight azobenzene-polyelectrolyte complexes [132].

Efficient grating formation has also been demonstrated using an azo-cellulose with ultra-high molecular weight ($M_W \sim 10^7$) [133, 134]. In a high molecular weight polypeptide ($M_W \sim 10^5$), gratings could be formed but the grating amplitude-depended strongly on the polymer conformation [135], and restricted conformations (a-helices and b-sheets) hindered SRG formation. More recently, high modulation-depth surface patterns have been inscribed in amorphous azobenzene molecular glasses [136, 137], and polymer systems employing spiropyran photo-chromic compounds [138, 139]. These observations serve to highlight that the fundamental mechanism of this complex photomechanical effect is not comprehensively understood up to date.

1.3.4 Nanofabrication Applications of Photo-Patterning

The rapid, facile, reversible, and single-step all-optical surface patterning effect discovered in a wide variety of azobenzene systems has been suggested as the basis for numerous applications. The surface structures are erasable, but on the other hand, one may use a system where crosslinking enables permanent fixation of the surface patterns [140, 141]. It is also possible to remove the azobenzene moieties from the material system after the grating inscription, resulting in thermally stable colorless gratings with unaltered periodicity but somewhat lowered grating modulation depth [142, 143]. Many proposed applications are optical, and fit well with azobenzene's already extensive list of optical capabilities. The gratings have been demonstrated as optical polarizers [144], angular or wavelength filters [145–147], and couplers for optical devices [148]. They have also been suggested as photonic bandgap materials [149], and have been used to create polymeric lasers where emission wavelength is tunable via grating pitch [150–152]. The process has also been suggested as an optical data storage and holographic recording mechanism [153, 154]. The high-speed and single-step holographic recording has been suggested to enable ‘‘instant holography’’ [155], with obvious applications for industry or end consumers. Since the hologram is topographical, it can easily be used as a master to create replicas via molding. This technique has been recently employed to enhance the light trapping, and hence to improve the device efficiency, of polymeric solar cells [156]. The surface patterning also allows multiple holograms to be superimposed into hierarchical structures. This has been used to create multilayered structures [157], with phase correlation between layers of the active azobenzene and an alternating spacer layer, to form 3D linear, tetragonal, and hexagonal relief gratings with a hierarchical structure. Another suggestion is to use the holographic patterning for rapid prototyping of optical elements [158]. Optical elements could be generated or modified quickly and during device operation. They could thereafter be replaced with permanent components, if required.

The physical structure of the surface relief can be exploited to organize other systems. For instance, it can act as a command layer, aligning neighboring liquid crystal phases [159–163]. The grating can be formed after the LC cell has been assembled, and can be subsequently erased and rewritten. The surface relief can also be used to organize fluorophores into various 2D micropatterns [164, 165]. Colloids can also be arranged into the grooves of an SRG, thereby templating higher-order structures [166, 167], and these lines of colloids can then be sintered to form wires [168]. Another advantage of holographic patterning is that there is guaranteed registry between features over macroscopic distances. This is especially attractive as technologies move toward wiring nanometer-sized components. Examples in this direction involved evaporating metal onto an SRG, and then annealing. This formed a large number of very long (several mm) but extremely thin (200 nm) parallel metal wires [169]. More recently, similar concept was applied for fabricating well-ordered TiO_2 nanowire arrays and nanostructures [170]. Lastly, SRGs can be used to optically control the alignment of cylindrical nanodomains in block copolymer thin films. Uniquely, such ‘‘optically directed self-assembly’’ provides both in-plane and out-of-plane control of the micro-phase separated nanostructure without any modification of the substrate or mechanical manipulation [171].

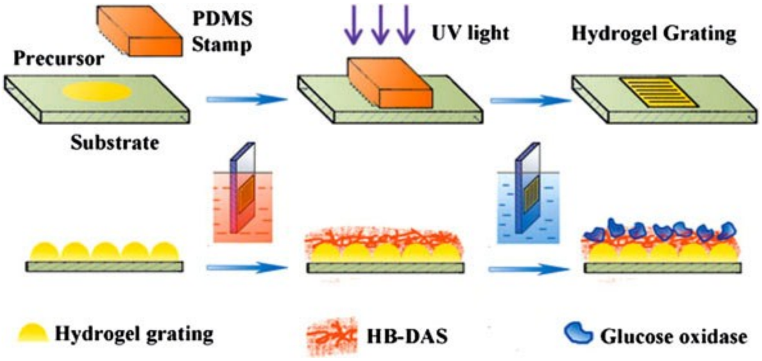

Figure 1.3: Schematic of the fabrication of the glucose-sensing hydrogel gratings [173]

The photoinduced surface structuring renders azo-polymers amenable to a variety of optical-lithography patterning schemes. Soft-lithographic approaches of replica molding using PDMS stamps to reproduce the gratings on a variety of substrates [172] and have been used to fabricate analyte sensors. These sensors were based upon the observed change in the diffraction efficiency of a grating upon analyte absorption. In a recent example [173], diffraction grating on an azobenzene-based material was transferred onto a stimuli responsive hydrogel functionalized with glucose oxidase and has been used to demonstrate glucose sensors capable of quantitative and continuous measurements in solution (see Fig. 1.3). Another recent example, referred to as ‘‘directional photofluidization lithography’’, employs micromolding for the fabrication of pristine 1D or 2D azo-polymer patterns, which are then post-modified using light-induced azo-polymer movement [174, 175]. By properly optimizing the irradiation conditions, this technique allows fabricating circular, ellipsoidal, and even rectangular nanostructures with feature sizes as small as 30 nm. As the latest example, SRGs have been used as masks for fabricating large-area silicon nanostructures [176]. They provide an intriguing alternative for conventional PMMA-based photoresists, and silicon nanopillar arrays of various shape and with feature size as small as 65 nm have been successfully fabricated (Fig. 1.4). Similarly, surface patterning can be used to immobilize various compounds, themselves acting as a mask. In a recent example, a tobacco mosaic virus was used as such a mask by placing it on an azobenzene surface. Subsequent irradiation resulted in virus immobilization by the formation of complementary grooves [177].

Of interest for next-generation patterning techniques is the fact that the azo surface modification is amenable to near-field patterning, which enables high-resolution nanopatterning by circumventing the usual diffraction limit of far-field optical systems. Proof of principle was demonstrated by irradiating through polystyrene spheres assembled on the surface of an azo film. The results in a polarization-dependent surface topography pattern [178], and a corresponding surface density pattern [179]. Using this technique, resolution on the order of 20 nm was achieved [180]. This process appears to be enhanced by the presence of gold nano-islands [181]. It was also shown that volume is not strictly conserved in these surface deformations [182]. In addition to being useful as a sub-diffraction limit patterning technique, it has been shown that the azo-polymer surface deformation is also a useful technique for photochemical imaging the near-field of various optical interactions [183], especially in mapping the hot spots of plasmonic nanostructures [184, 185].

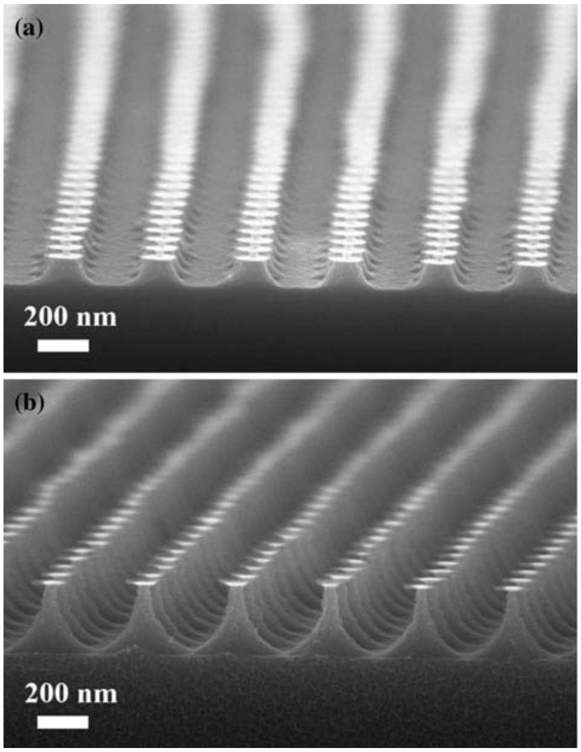

Figure 1.4: SEM images of straight-walled (a upper) and mushroom-shaped (b lower) silicon nanopillar arrays. The structures are fabricated by reactive ion etching through a mask fabricated using azo-polymer surface deformation, and changing the etching parameters can control the shape of the pillars [176]

1.4 Photomechanical Actuation

If an actuator is defined as an energy transducer converting an input energy into mechanical motion, then azobenzene-based systems are excellent candidates for photo-mechanical actuation for many niche applications involving small size, localized actuation, remoteness of the power source, and freedom from the encumbrance of batteries, electrons, and internal moving parts, where advantageous. The most convincing demonstration of macroscopic motion due to azo isomerization is the mechanical bending and unbending of a free-standing polymer thin film [107, 108]. Bending occurs in these films through surface contraction while the thick inner layer does not contract as it is not irradiated. As the direction of bending can be controlled via the polarization of the light, the materials enable full directional photomechanical control [107, 109], and have been used to drive macroscopic motion of a floating film [186]. The contraction of these materials (as opposed to expansion) appears again to be related to the main-chain azo groups, and may also be related to the LC nature of the crosslinked gels. For a thin film floating on a water surface, a contraction in the direction of polarized light was seen for LC materials, whereas an expansion was seen for amorphous materials [187]. A related amplification of azo motion to macroscopic motion is the photo-induced bending of cantilevers coated with an azobenzene monolayer [188]. Other examples include macroscopic bending and three dimensional control of cantilevers made of azobenzene liquid-crystalline elastomers [189–191], light-driven microvalves [192], and full plastic motors [193]. In this section, a survey summary of various manifestations of the photomechanical effect leading to macroscale actuation with various azobenzene-based materials will be described.

1.4.1 Photo-Actuation in Monolayers and Interfacial Flms

Monolayers of azobenzene polymers are easily prepared at the air/water interface, and much of the earliest work focussed on these simple systems. In the monolayer state, changes in the molecular shape and orientation can be directly related to the film properties such as film area and surface pressure, providing further ease of direct molecular interpretation of results. Thus, azobenzene monolayer films are ideal for studying macroscopic deformations in terms of molecular-level processes. When azo-polymer monolayers are prepared at interfaces, the motion of azobenzene moieties occurring at a molecular level is transferred directly and efficiently, and can be readily amplified to a macroscopic material. Photomechanical effects of a monolayer consisting of polyamides with azobenzene moieties in the main chain were first reported by Blair *et al.* in 1980 [194, 195]. At the air/water interface, a decrease in stress was observed upon UV light irradiation of the monolayer, indicating a contraction of the monolayer. In the dark, the stress increased again, and the cycle could be repeated many times. For these main-chain type monolayers, the azobenzene moieties were considered to lie flat on the water surface. The photomechanical effects were then simply attributed to the *trans–cis* isomerization of the azobenzene moieties, which occupy a larger area at the interface when they are in the more linear *trans* form than in the *cis* form.

Polypeptide monolayers of two a-helical poly(a-methyl L-glutamate) rods linked by an azobenzene moiety were prepared by Higuchi *et al.* [89]. The *trans–cis* photoisomerization and the consequent change in geometry of the azobenzene produced a 140° bending of the main chain of the molecule, and a decrease in the limiting area per molecule. An important finding here was that the photoinduced changes in the area of the monolayer occurred more slowly than the spectral changes of the azobenzene moieties, and that the photoinduced changes in the surface area may arise from the rearrangement of the bent molecules, induced by photoisomerization of the azobenzene moieties in the main chain. The intermolecular interaction in the condensed monolayer may have served to slow down the rate of their rearrangement process.

In monolayers of side-chain type polymers, photo-mechanical effects of related azobenzene-containing polypeptides were also investigated by Menzel *et al.* [196]. They prepared poly(L-glutamate)s with azobenzene groups in the side chains coupled to the backbone via alkyl spacers. The resulting monolayers showed a photoresponsive behavior that was opposite to the above-mentioned systems, however, as they expanded when exposed to UV light, and shrank when exposed to visible light. This was perhaps the first observation of curious opposite expansion/ contraction behavior from the same class of chromophores. The *trans–cis* photoisomerization of the azobenzene moiety upon

UV light irradiation in this study led to a large increase in the dipole moment of this unit, however, and this gain in affinity to a water surface was proposed to be responsible for the net contraction [197]. In perhaps the first set of studies into quantifying the effect generally, and optimizing some photo-mechanical systems, Seki *et al.* prepared poly(vinyl alcohol)s-containing azobenzene side chains and observed photoinduced changes in areas on a water surface in an excellent series of papers beginning in 1993 [198–207]. These monolayers at the air/water interface exhibited a three-fold expansion in area upon UV light irradiation and reversibly shrunk by visible-light irradiation. The mechanism of the photoinduced changes in area was interpreted in terms of the change in polarity of the azobenzene moiety: the *trans–cis* photoisomerization led to an increase in dipole moment, bringing about a higher affinity of the *cis*-azobenzene to the water surface and the expansion of the monolayers. *Cis–trans* back isomerization by visible-light irradiation then gave rise to a recovery of the monolayers to the initial structure. By analyzing the XRD data, it was shown that the thickness of the monolayer becomes larger for the *trans* form than the *cis* form. The resulting change in the thickness by 0.2–0.3 nm due to the *trans–cis* isomerization in the hydrophobic side chain was then directly observed *in situ* on the water surface [204]. These results with azo monolayers indicate that the photoinduced deformations of the azobenzene-containing monolayers can depend strongly on the location of the azobenzene moieties in the dark: when the azobenzenes are on or in the water subphase, the structural response of the monolayers is determined by the geometrical change of the photochromic units. On the other hand, the change in polarity of the azobenzene moieties is more important when they are away from the water subphase in the dark. The potential of azobenzene monolayers for actuation based applications has been demonstrated by Ji *et al.* [188] through the amplification of azo motion in monolayers to macroscopic motion. A monolayer of thiol-terminated azobenzene derivative was deposited onto a gold-coated microcantilver, and exposure to UV-light resulted in the reversible deflection of the microcantilever due to molecular repulsion in the monolayer. Other examples of systems composed of azobenzene self-assembled monolayers of planar and curved inorganic surfaces has been excellently presented in a recent review by Klajn [208].

1.4.2 Photo-Actuation in Amorphous Thin Films

Azo-polymers offer advantages over azo monolayers as superior materials in view of higher processability, the ability to form good free-standing films with a variety of thicknesses from nanometer to centimeter scales, in addition to flexibility in molecular design, and precisely controlled synthesis. Hence, azo-polymers have emerged as the azo material of choice for most applications. From this point of view, polymer actuators capable of responding to external stimuli and deforming are most desirable for practical applications, either amorphous or organized (such as liquid crystalline). Various chemical and physical stimuli have been applied such as temperature [209], electric field [210, 211], and solvent composition [212], to induce deformation of polymer actuators.

The use of structural changes of photoisomerizable chromophores for a macroscopic change in size of polymers was first proposed by Merian in 1966 [213], when he observed that a nylon filament fabric dyed with an azobenzene derivative shrank upon photoirradiation. This effect was postulated to involve the photochemical structural change of the azobenzene group absorbed on the nylon fibers, yet these fibrous systems were sufficiently complex that the real mechanism could only be speculated upon. The observed shrinkage was also quite small, only about 0.1 %, which made it further difficult to draw firm conclusions. Following this interesting study, however, much effort was made to find new photomechanical systems with an enhanced efficiency [105, 214, 215]. Matejka *et al.* for example, synthesized several types of photochromic polymers based on a copolymer of maleic anhydride with styrene-containing azobenzene moieties both in the side chains and in the crosslinks of the polymer network [216–218]. The photomechanical effect observed here was enhanced with an increase in the content of photochromic groups, and for a polymer with 5.4 mol% of the azobenzene moieties, a photoinduced contraction of the sample of 1 % was achieved. Most recently, the photoinduced expansion of thin films of acrylate polymers-containing azobenzene chromophores was tracked directly in real time by Barrett and co-workers [102, 103, 219] using a variety of techniques including *in situ* single-wavelength ellipsometry, AFM, and *in situ* neutron reflectometry. An initial expansion of the azobenzene-polymer films was found to be irreversible with an extent of relative expansion observed of 1.5–4 % in films of thickness ranging from 25 to 140 nm, then a subsequent and reversible expansion was observed with repeated irradiation cycles, achieving a relative extent of expansion of 0.6–1.6 %. The extent and direction (expansion or contraction) of photo-mechanical change could be tuned for the first time just by using ambient temperature, suggesting that competing dynamic effects exist during isomerization. These variable-temperature neutron reflectometry experiments demonstrated unambiguously that both photo-expansion and -contraction could be induced in a single azo-material merely by varying the dominance of these two competing effects by changing the temperature. This implicates a fundamental competition of mechanisms, and helps unify both the photo-contraction and -expansion literature. In particular, it now appears that most azo materials exhibit photo-expansion below a well-defined cross-over temperature, and photo-contraction above this temperature. Highly mobile materials will thus be above their cross-over temperature at ambient conditions, whereas rigid materials will be below.

As another technique to measure the photomechanical effect directly, recent developments of single-molecule force spectroscopy by AFM have enabled one quite successfully to measure mechanical force produced at a molecular level. Gaub and co-workers [78, 79] for example synthesized a polymer with azobenzene moieties in its main chain, then coupled the ends of the polymer covalently to the AFM tip and a supporting glass substrate by heterobifunctional methods to insure stable attachment, and investigated the force (pN) and extension (nm) produced in a single polymer in total internal reflection geometry using the slide glass as a wave guide. This clever excitation geometry proved very useful to avoid thermo-mechanical effects on the cantilever. They were thus able to photochemically lengthen and contract individual polymer chains by switching the azobenzene moieties between their *trans* and *cis* forms by irradiation with UV (365 nm) and visible (420 nm) light, respectively. The mechanical work executed by the azobenzene-polymer strand by *trans–cis* photoisomerization could then be estimated directly as $W \approx 4.5 \times 10^{-20}$ J. This mechanical work observed at the molecular level resulted from a macroscopic photo-excitation, and the real quantum efficiency of the photomechanical work for the given cycle in their AFM setup was only on the order of 10^{-18}. However, a theoretical maximum efficiency of the photomechanical energy conversion at a molecular level can be estimated as 0.1, if it is assumed that each switching of a single azobenzene unit is initiated by a single photon carrying an energy of 5.5×10^{-19} J [78, 79].

Photoinduced reversible changes in elasticity of semi-interpenetrating network films bearing azobenzene moieties were achieved recently by UV and Vis light irradiation [220]. These network films were prepared by cationic copolymerization of azobenzene-containing vinyl ethers in a linear polycarbonate matrix. The network film showed reversible deformation by switching the UV light on and off, and the photomechanical effect was attributed to a reversible change between the highly aggregated and dissociated state of the azobenzene groups [220–222]. In other studies similar films of azobenzene-containing vinyl ethers films with polycaprolactone have achieved rapid (0.1 min) anisotropic deformation and recovery. The films, placed under constant tensile stress were stretched perpendicular and parallel to the tensile stress before irradiation. Photoisomerization of these films resulted in film contraction for stretching parallel to the tensile stress and film elongation for stretching perpendicular to the tensile stress. The photomechanical response was observed to increase with film stretching and speculated to arise from anisotropic responses caused by the isomerization-induced vibration of azobenzene molecules which decreases the modulus of the deformed amorphous area [223]. Other polymer films that exhibit high bending intensity and large bending angles (90°) have also been reported [224].

The photomechanical expansion of azobenzene has been used to create a simple UV sensor [225, 226], and has been proposed for applications in mechanically tunable filters and switching devices. The sensor, based upon a fiber bragg grating coated with an azobenzene polymer, measured UV-light intensity by monitoring the center wavelength shift in the fiber bragg grating. Upon photoisomerization (proportional to incoming UV light) the encapsulating azobenzene material applied a photomechanical axial strain upon the fiber bragg grating proportionally shifting its center wavelength. Another interesting and similar mode of deformation of polymer colloidal particles by light was reported by Wang *et al.* [17, 227–231]. They observed that spherical polymer particles-containing azobenzene moieties changed their shape from a sphere to an ellipsoid upon exposure to interfering linearly polarized laser beams, and the elongation of the particles was induced along the polarization direction of the incident laser beam. They also reported the deformation of the micellar structure between spherical and rod-like particles under alternating UV and visible-light irradiation. Gels of polymer films containing azobenzenes are also potential materials for applications, however, in general the gels reported have a disadvantage in that the response is slow, and the degree of deformation of the polymer films is too small to be practically utilized. It is generally agreed now that it is crucial to develop only photomechanical systems that can undergo fast and large deformations.

1.4.3 Photo-Actuation in Liquid-Crystalline Polymers

The previously described monolayer, gel, and amorphous polymer films are generally without microscopic or macroscopic order. Hence the photo-mechanical deformations mostly occur in an isotropic and uniform way, i.e., there is no preferential direction for deformation. If materials with anisotropic physical properties are instead used, the mechanical power produced can increase significantly, and more control can be realized. A particularly promising class of materials for efficient photoinduced actuation is liquid-crystalline elastomers (LCEs). LCEs are lightly crosslinked polymers in which the high alignment order of the mesogens can be coupled with the motions of the highly elastic polymer network. This coupling gives rise to many characteristic properties of LCEs. Upon heating, the alignment order of the LCE films decreases, and when the LC–isotropic phase transition temperature is exceeded, the films exhibit a contraction along the mesogen alignment direction. Such anisotropic deformation can be very large, and along with the versatile mechanical properties of the polymer network and the reversibility of the process (upon cooling, LCE films revert back to their original size), LCEs show great potential as artificial muscles [232–237].

Incorporation of photochromic moieties into LCEs allows one to trigger the reduction in the LC alignment order, and in an extreme case to induce the LC-isotropic phase transition, with light. The photoinduced contraction of LCE films was first demonstrated by Finkelmann *et al.* who observed a 20 % contraction in monodomain nematic LCEs consisting of a polysiloxane main chain and azobenzene crosslinks by irradiating the samples with UV light [238]. From the viewpoint of the photomechanical effect, the subtle variation in nematic order by *trans–cis* isomerization causes a significant uniaxial deformation of LCs along the director axis, if the LC molecules are strongly associated by covalent crosslinking to form a 3D polymer network. Terentjev and co-workers [239, 240] have incorporated a wide range of azobenzene derivatives into LCEs as photoresponsive triggers, examined their deformation behavior upon exposure to UV light, and performed detailed analysis on the photomechanical effects taking place. Furthermore, Keller and co-workers [241] developed monodomain nematic side-on elastomers with large (up to 18 %) and rapid (less than 1 min) contraction upon UV irradiation as illustrated in Fig. 1.5.

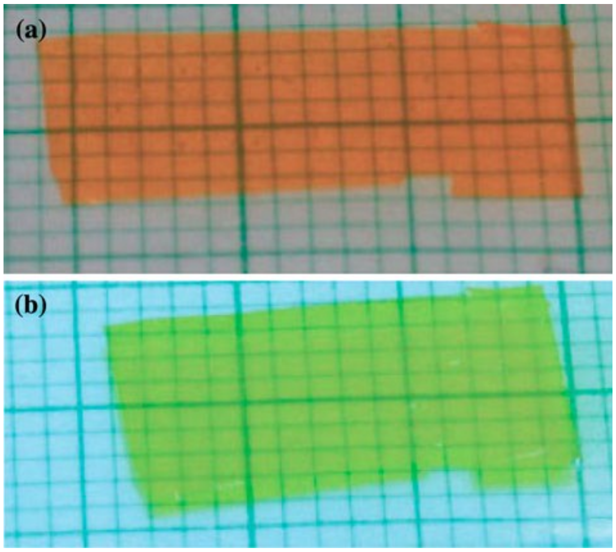

Figure 1.5: Photographs of the photodeformation of Keller's azobenzene-containing LCE before (a) and under (b) UV light irradiation, demonstrating a clear change in shape inducible [241]

The large-amplitude actuation controlled by external stimulus in room temperature was obviously highly intriguing from the viewpoint of, e.g., micro-pumps and artificial muscles. The application potential of photocontrolled actuators was further promoted when Ikeda and co-workers [107, 108, 242] reported on photoinduced 3D motions (bending) of azobenzene LC gels and elastomers. The bending is driven by gradient in the isomerization-induced reduction in the LC alignment order: majority of the incident UV irradiation is absorbed within a relatively thin surface layer of the film, which generates asymmetric strain and subsequent deformation. The process is reversible: UV irradiation destructs the mesogen alignment through *trans–cis* isomerization and causes the sample to bend, whereas irradiation with visible-green light restores the azobenzenes to the *trans*-form and the film regains its original unbent state. The nature of bending depends strongly on the details of the material system. Homogeneously aligned polymer systems bend in the mesogen alignment direction [242], whereas the bending direction of polydomain LCEs can be controlled by linearly polarized light (Fig. 1.6) [107]. The latter serves as an example for repeatable and precisely controlled photoinduced deformation along any chosen direction, enabling full photo-mechanical directional control. It is an important step toward practical applicability of light-driven actuators. Another example of direction control is provided by artificial muscle-like photochromic fibers, the bending direction of which can be controlled by changing the location of the illuminating source [243, 244]. Conversely, homeotropically aligned crosslinked LC polymer films were observed to exhibit a completely different bending behavior; upon exposure to UV light they bent away from the actinic light source, due to isotropic expansion of the sample surface upon *trans–cis* isomerization [245]. The initial chromophore alignment is not the only way to control the directionality of the photoinduced bending: Tabiryan *et al.* [246] demonstrated that the bending direction can be controlled with the polarization direction of the excitation beam, which was attributed to light-induced reorientation of the azobenzene moieties. More recently, van Oosten *et al.* [247] showed that the bending direction can be controlled by designing the material to bear internal composition gradients within the LC polymer network, and as the latest example, Shishido and co-workers [248] showed that the bending direction can also be dictated by the nature of bonding between the azobenzene moieties and the crosslinked polymer network.

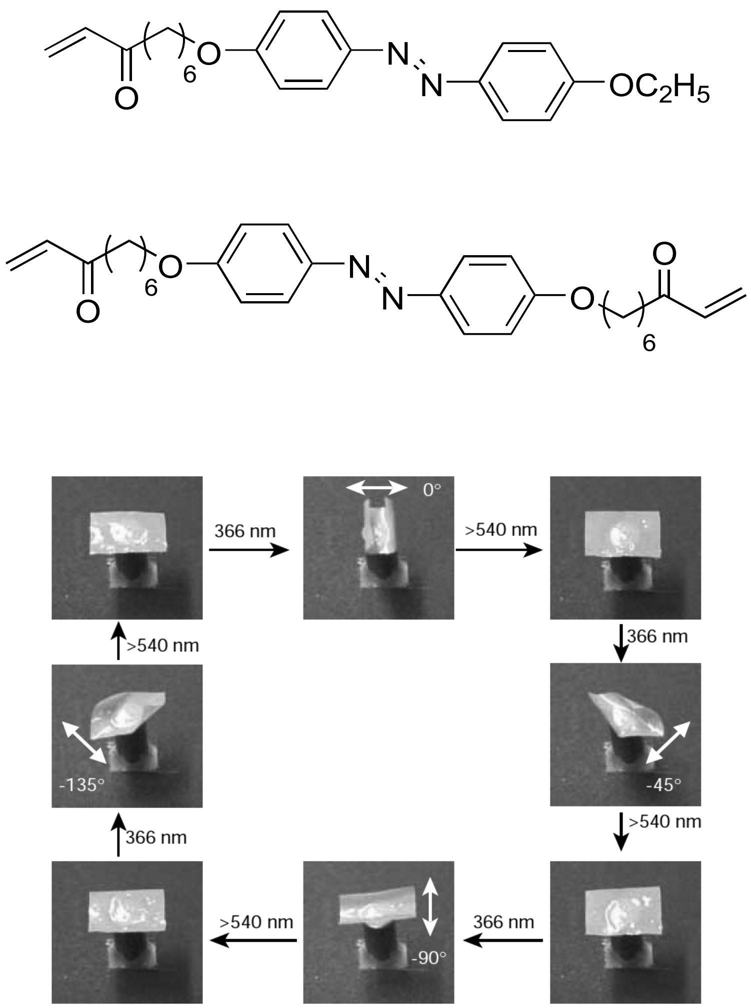

Figure 1.6: Precise control of the bending direction of a film by linearly polarized light. Chemical structures of the LC monomer and crosslinker (top) used for preparation of the film, and photographic frames of the film in different directions in response to irradiation by linearly polarized light of different polarization directions (white arrows) at 366 nm, and bending flattened again by visible light longer than 540 nm [107]

The above-mentioned studies employed azo-containing crosslinked LC polymers (azo-CLCPs) consisting of azobenzene mesogens only. In such systems, practically all of the incident irradiation is absorbed within the surface region with a thickness of 1–2 μm. As typical film thicknesses used are in the order of 10–20 μm, majority of the azobenzene moieties in the bulk of the film remain unaffected by incident light. As a result, the efficiency of the photomechanical effect generated in such plain-azobenzene actuators is far from optimal. This was first addressed by Broer and co-workers [249] who designed densely crosslinked high-elastic-modulus polymer actuators with relatively low azobenzene concentration. Indeed, as shown by Palffy-Muhoray and co-workers [186] as early as in 2004, even non-photoresponsive LCEs doped with low concentration of azobenzene dyes can exhibit remarkable and unprecedented photoinduced deformation behavior. In fact, it has been recently shown that the optimum photoinduced response (in terms of the stress generated) is achieved using moderate concentration of azobenzene moieties, supplemented with higher concentration of non-photoactive mesogens [250]. The largest mechanical force generated by photoirradiation of the various films was measured as 2.6 MPa. Detailed studies have also been performed on the crosslinker concentration dependence of low-azo-concentration CLCPs. The crosslinking density changes the elastic modulus and the thermomechanical properties of the material system in a delicate manner, playing an important role in the mobility of the polymer segments, and in general, low crosslinker concentration is favorable for optimizing the photoinduced/thermally induced deformation of crosslinked LC polymers whereas high crosslinker concentration (high modulus) is preferable for high photoinduced stress generation [236, 251, 252]. Lastly, a recent observation of Shishido and co-workers [252] suggests that the photoinduced bending of azo-CLCPs is accompanied by a significant, 2.5-fold, decrease in the Young's modulus of the sample upon UV irradiation (Fig. 1.7). Such ''photosoftening'' was observed to be the most pronounced in a low-crosslinker-concentration (and low modulus) sample, which also exhibited the most efficient photoinduced bending. Upon increasing the crosslinker concentration (and the modulus), both photoinduced bending and the photosoftening effect became less efficient, indicating that there might be a profound connection between the ''photosoftening'' and the photo-mechanical properties and azo-CLCPs.

1.5 Applications in Robotics and Micromechanics

Azobenzene-containing LC polymers are ideal candidates for photo-robotics applications as they are capable of strong and efficient mechanical actuation powered remotely by light energy, without the need for additional components such as batteries or wires. They also possess the additional advantages of high processability, easy fabrication, relatively low weight density, low cost as well as low environmental impact of polymeric materials [253, 254]. With appropriate engineering, the photo-induced deformations (expansion/contraction and bending) can be translated into ‘‘real-life’’ actuation, to design proof-of-principle micromachines capable of producing applicable work. As the first example of such engineering, Ikeda with Barrett, and co-workers [193] translated the photoinduced deformations of an azo-CLCP film into rotational motion. They laminated the azobenzene film with a thin polyethylene sheet, joined two ends of the laminated film to create a continuous ring, and mounted it onto a pulley system. The belt was then simultaneously irradiated with both UV and visible light (Fig. 1.8a), which drove the pulleys into counter-clockwise rotational motion, as shown in Fig. 1.8b. As the azobenzene mesogens were aligned parallel to the long axis of the belt, such simultaneous irradiation caused both the local contraction and the expansion forces, the combination of which gave rise to the observed photoinduced motion. The rotation then exposed new (yet unirradiated) sections of the belt to irradiation, continuing the photo-contraction and -expansion and thus resulting in continuous rotation of the pulleys. This was the first demonstration of a light-fuelled motor.

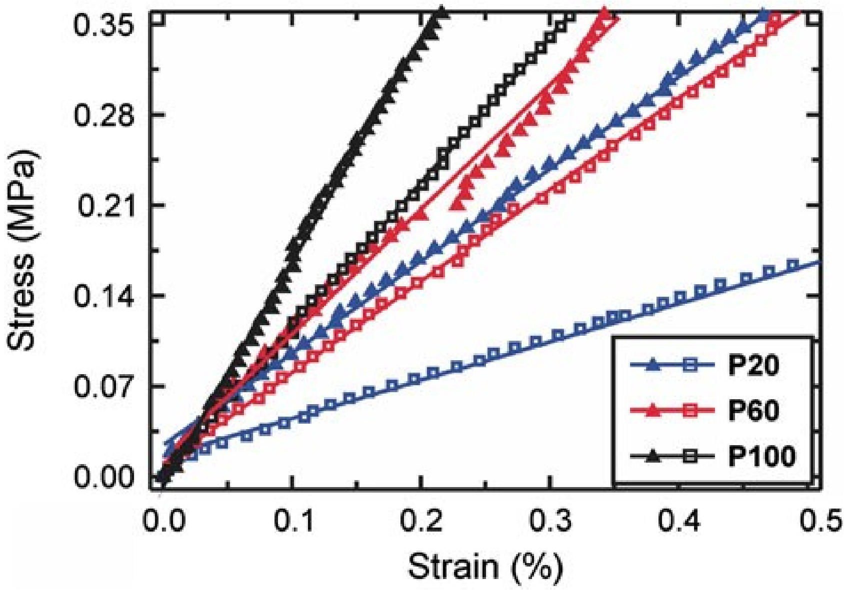

Figure 1.7: Stress–strain curves for nonexposed (filled triangles) and UV-irradiated (empty squares; 5 min irradiation, 365 nm, 10 mW/cm^2) films of three azo-CLCPs, denoted P20, P60, and P100. Each sample bears a modest (5 mol%) azobenzene concentration, whereas their overall crosslinker concentrations are 20, 60, and 100, respectively. The solid lines are linear fits to the experimental data, the slope of which are used to determine the Young’s moduli of the samples [252]

Other recent examples by the same research group include an ‘‘inchworm’’ locomotion achieved by attaching a sheet of azo-CLCP on a flexible polyethylene (PE) substrate with asymmetric sliding friction [255]. In this application the film undergoes photomechanical contraction while the asymmetric end shapes on the PE films act as a ratchet, directing the motion of the film. Robotic arm-like actuation of flexible PE sheets was also demonstrated by using azo-polymer hinges (Fig. 1.9). Different sections of a flexible PE film were laminated with azo-CLCPs, which enabled-specific optical control (expansion or contraction) at various individually addressable positions of the film. The sections containing the azo-CLCPs thus acted as hinge joints, acting as ‘‘arms’’ with remote control over ‘‘elbows’’, and ‘‘wrists’’. The latest advancement addressed an important problem inherent to the laminated azo-CLCP films: even if their mechanical strength is improved by the flexible polymer substrate, the adhesive between the two layers prevents efficient deformation transfer from the photoactive layer to the polymer substrate. This can be overcome by connecting the active and passive layers by chemical bonding (using e-beam crosslinking) [256]. The durability of such adhesive-free bilayer structures was significantly improved as compared to adhesive-containing laminated films, and they might provide a route toward increasing the optical–mechanical energy conversion efficiency of the light-driven motors.

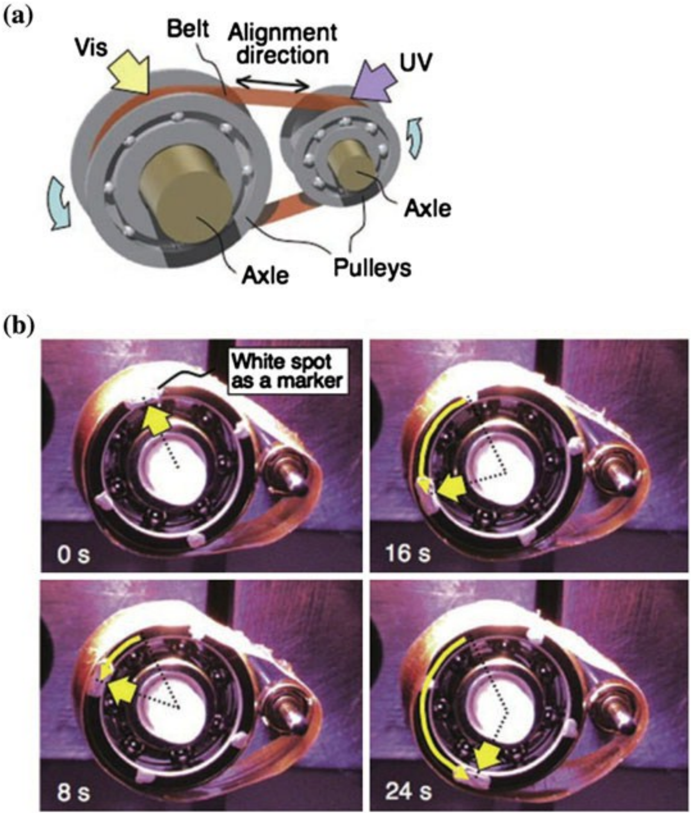

Figure 1.8: A light-driven plastic motor using the laminated azo-CLCP film. a) Schematic illustration of a light-driven plastic motor system, showing the relationship between light irradiation positions and a rotation direction. b) Series of photographs showing time profiles of the rotation of the light-driven plastic motor with the LCE laminated film induced by simultaneous irradiation with UV (366 nm, 240 mW cm^{-2}) and visible light (540 nm, 120 mWcm^{-2}) at room temperature. Diameter of pulleys: 10 mm (left), 3 mm (right). Size of the belt: 36 x 5.5 mm^{2}. Thickness of the layers of the belt: PE, 50 mm; LCE, 18 mm. Reproduced from Ikeda *et al.* [193]

In the previous examples of photo-driven motions, the primary energy source was the combination of UV and visible-light sources, which gave rise to locally addressable photoinduced contraction/expansion of the photoactive polymer films. UV light is harmful to many living organisms, thus it is important to develop photodriven actuators driven by visible light, and ultimately sunlight. The first sunlight-driven photomobile materials, employing photoresponsive azotolane moieties, were developed by Yu *et al.* [257], who also fabricated visible-light-driven microrobots capable of lifting up and moving an object weighing 10 mg, ten times the weight of the robotic arm itself [258, 259]. This robot consisted of several azo-CLCP films on PE substrates connected by joints to mimic the arm, wrist, hand and even fingers of the human arm. The robotic arm could be bent and manipulated to perform complex actions by individually addressing the various photoactive sections, for instance an object could be picked up or dropped by addressing the fingers, while the entire arm could be moved by addressing it at different locations. Later on, White and co-workers [260] demonstrated photo-fuelled catapult motion, capable of launching an object at a rate of 0.3 m/s using moderate-intensity blue-light irradiation, and as the most recent advancement, Yu and co-workers [261] designed a clever composite material, in which upconverting nanophosphors allowed inducing the photoinduced deformation using near-infrared (980 nm) light.

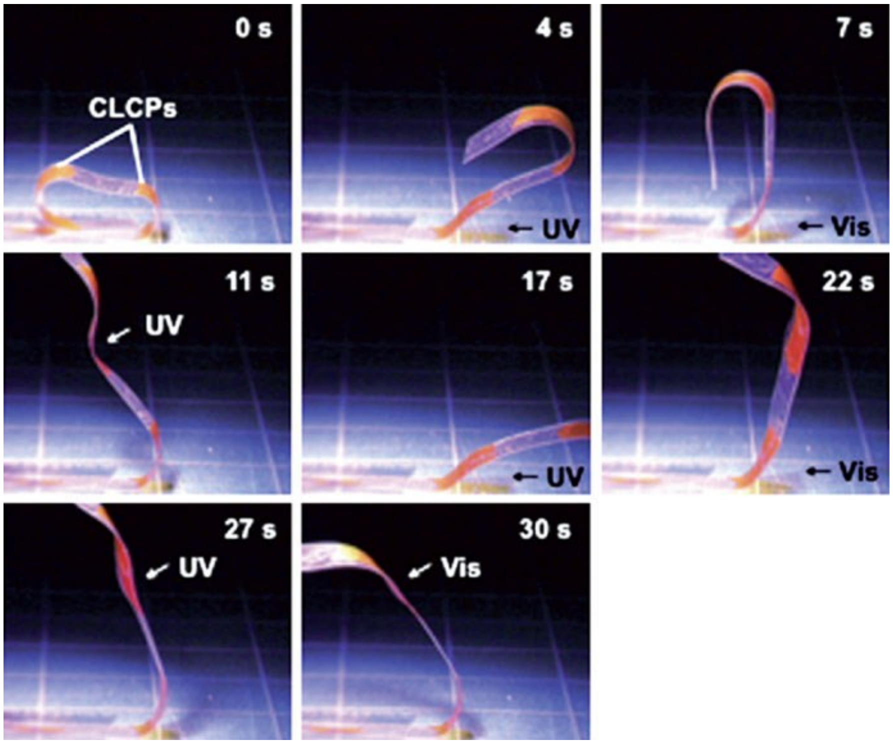

Figure 1.9: Series of photographs showing time profiles of the flexible robotic arm motion of a laminated azo-CLCP film, induced by irradiation with UV (366 nm, 240 mW cm^{-2}) and visible light ([540 nm, 120 mW cm^{-2}) at room temperature. Arrows indicate the direction of light irradiation. Reproduced from Ikeda *et al.* [255]

White, Bunning, and co-workers [189–191] have designed ingenious high-frequency photo-driven oscillators. They designed LC azo-polymer cantilevers capable of achieving oscillation frequencies as high as 270 Hz and an energy conversion efficiency of 0.1 % upon irradiation with focused blue laser beam, with a range of motion close to 180° (Fig. 1.10). The cantilevers possessed a storage modulus ranging from 1.3 to 1.7

GPa and were shown to bend faster and attain larger bending angles with monodomain orientation, increasing azobenzene concentration, and reduced thickness. The bending angle was also dependent upon the polarization of incoming light as well as atmospheric pressure. These azopolymer cantilevers also exhibited oscillation under a focused beam of sunlight [191], and thus offer the potential for remotely triggered photoactuation, adaptive optics, and most importantly energy harvesting. Such high-frequency oscillator could power a miniaturized micro-opto-mechanical system as it contains both the force generation component (azobenzene) and the kinematic structure (cantilever) in a single unit.

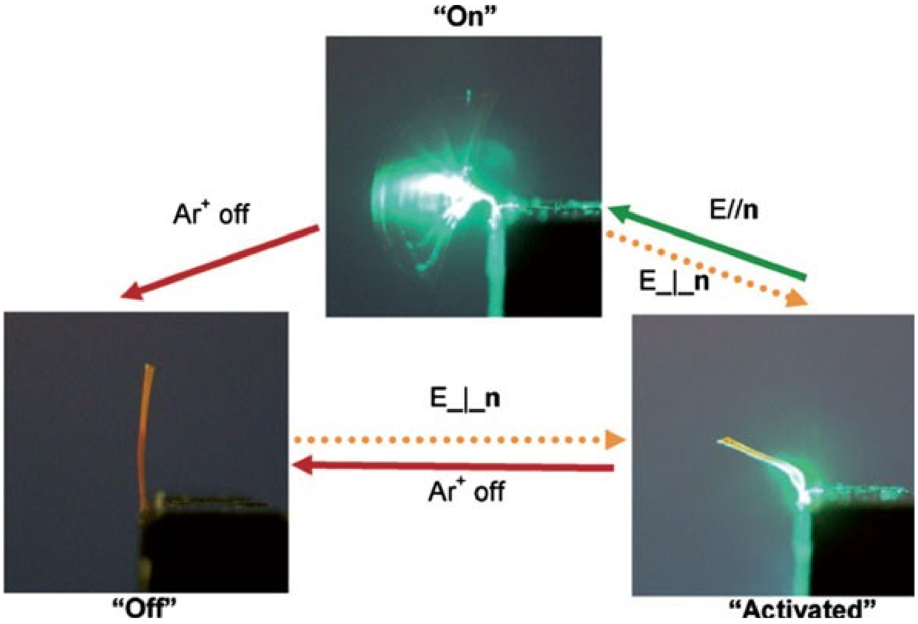

Figure 1.10: The optical protocol for activating the light powered oscillation of a cantilever. The nematic director (n) is positioned parallel to the long axis of the polymer cantilever of dimension 5 mm x 1 mm x 50 mm. When exposed to light polarized orthogonal to n (E⊥n) bending occurs toward the laser source. Cycling the Ar+ laser from E⊥n to E//n can turn oscillation ''on'', while blocking the Ar+ or returning the polarization of the laser beam to E\n turns the oscillation ''off''. Reproduced from Bunning *et al* [189]

Other important proof-of-principle applications of azo-CLCPs include the design and fabrication of microvalves [192], and micropumps [262]. The microvalves were created by fitting a CLCP film over an inlet valve in a sealed valve chamber, where the film in this state completely blocks the inlet preventing flow [263]. Upon irradiation, the bending of the film results in unblocking of the inlet valve as well as a concave cavity under the bent film that allows solution to flow from the inlet to the nearby outlet. In the case of micropumps [262], the CLCP film is placed on the outside of a membrane covering a sealed cavity. Upon irradiation the CLCP film bends, forcing the membrane downwards, reducing cavity volume and increasing the cavity pressure. Thus, fluid flows out through the outlet valve. Upon film contraction, the membrane is pulled upwards increasing the cavity volume, decreasing cavity pressure and forcing fluid inflow through the inlet valve. Related to possible microfluidic applications, van Oosten *et al.* [264] have reported the design and construction of bio-inspired artificial cilia for microfluidic pumping and mixing applications. Using commercial inkjet printing technology, droplets of reactive azo LC monomers were deposited onto a film of poly vinyl alcohol (PVA) and a thin layer of rubbed polyamide for LC alignment. After self-assembly and crosslinking of the LC monomers another layer of the same or different azobenzene monomer-based ink is added to create mono or bicomponent cilia capable of responding to different wavelengths of light. Dissolving the PVA releases the cilia, which are capable of intensity-dependent upward bending when irradiated with UV light from above. The bicomponent cilia were capable of different bending properties due to their separately addressable sections, and the activation of these two components in sequence with different wavelengths of light would thus imply a non-reciprocal motion, permitting the cilia to pump fluids [265].

While most azobenzene photomechanical systems are based upon amorphous or liquid-crystalline polymers there are also some very recent reports of photomechanical crystals of azobenzene in the literature. There have been reports of numerous solid-state reactions in molecular crystals [266, 267], and of these, crystalline photo-reactions are especially interesting as they are often accompanied by molecular motion and morphological changes at the crystal surfaces [268–271]. Irie and co-workers [272, 273] were among the first to report on these crystalline photoreactions in diarylethene microcrystals accompanied by a rapid, reversible shape change of the crystal under alternating UV-and visible-light irradiation. In contrast to the diarylethene derivatives, the photoisomerization of azobenzene, requiring a larger free volume, is hindered in the bulk crystal. An early AFM study demonstrated the reversible alteration of the layered structure of an azobenzene crystal under UV-and visible-light suggesting that the topmost bilayers of the azobenzene crystal are capable of isomerization [274]. Conclusive evidence of reversible photoismerization in azobenzene crystals has only been recently reported through a reversible 3.5 % reduction in particle size of azobenzene crystals dispersed in water [275], and the fraction of the *cis* isomer was determined to level off at 30 % in the photostationary state. In further work, photoinduced particle size deformation of crystalline azobenzene and silica nano-hybrids fabricated by dry grinding was also reported [276].

In other examples, photoisomerization in crystalline azobenzene was demonstrated by the formation of a surface relief grating upon single crystal azobenzene derivatives [277–279], and the observation of photoinduced vitrification near the surfaces of the single crystals of azobenzene-based molecular materials possessing a glass-forming ability [280]. In further work [281], the reversible mechanical bending of plate-like microcrystals of azobenzene derivatives has been reported. Here, photoisomerization of the *trans* azobenzene molecules on the (001) crystal surface elongates the unit cell length near the (001) surface giving rise to uneven features. As the inner unit cells do not undergo photoisomerization their dimensions remain constant and thus, result in crystal bending.

More recently, Kyu and coworkers [282] have observed variously the ‘‘swimming’’, sinking and stationary floating of azobenzene crystals in a triacrylate solution (TA). The authors explain such motion through the creation of concentration/surface tension gradients formed around the liquid crystal interface by the rejection of TA solvent from the growing crystal fronts. When these gradients act on different facets in an unbalanced manner the crystal is propelled forward and ‘‘swims’’. Solvent rejection in the vertical direction causes crystal flotation while balanced forces on all facets results in stationary crystal growth. In addition, stationary rhomboidal crystals of azobenzene were shown to swim (move away from the UV-light source) upon irradiation. This has been attributed by the authors to the generation of a mechanical torque within the crystal by higher isomerisation rates in the sections closer to the UV light. In addition, isomerisation-induced changes in the polarity and thus solubility of the azobenzene crystals could result in system instability, driving phase segregation, and greater solvent rejection rates from the crystal front closer to the UV light.

1.6 Conclusions and Outlook, Scope of this Thesis

The azobenzene chromophore is a unique and powerful molecular switch, exhibiting a clean and reversible photo-isomerization that induces a reversible change in geometry. This motion can be exploited directly as a photo-switch, and can also be further amplified so that larger-scale material properties are switched or altered in response to light. Thus, azo materials offer a promising potential as photo-mechanical materials. Light is an efficient power source for many of these applications, a direct transfer of photonic energy into mechanical motion with no moving parts, and light is also an ideal triggering mechanism, since it can be localized (in time and space), selective, non-damaging, and allows for remote activation and remote delivery of energy to a system. Thus for sensing, actuation, and motion, photo-functional materials are of great interest. Azo materials have demonstrated a wide variety of switching behavior, from altering optical properties, to surface energy changes, to even eliciting bulk material phase changes. Azobenzene is the arguable leader amongst the small class of photo-reversible molecules, and soft azopolymers can be considered promising materials for next-generation photo-mechanical applications because of their ease of incorporation, and efficient and robust photochemistry. Herein we have described the photomechanical effects observed in monolayers, thin films, gels, crystals, amorphous polymers, and crosslinked liquid-crystalline polymers containing azobenzene. In various systems, full macroscopic light-driven actuation has been achieved; however, the mechanical forces produced thus far and energy conversion efficiency are still far from optimal. Crosslinked liquid-crystalline polymers in particular are promising materials for artificial muscles and motors driven by light, and in these systems not only two-dimensional but 3D motions have now been achieved, which are competitive and promising for many applications as soft actuators. Many problems also still remain unsolved, however, such as fatigue resistance and biocompatibility of these materials, which need further intensive investigation.

Overall, azobenzene materials might still be viewed more as ‘‘solutions in need of a problem to solve’’, as material development has far outpaced useful applications. For the field to progress now, it requires creative and inspired engineering, continuing on from this body of excellent and successful science, to identify the major unique niches in actuation where azobenzene-based materials and photo-actuation in general are capable of becoming a competitive solution. This introduction has identified various strengths, properties, and possibilities that azobenzene-based systems are capable of as well as the ability to incorporate azobenzene into various materials and systems. It still, however, lacks unifying problems or application areas where it can display its inherent advantages and potential, such as in energy harvesting and storage. Indeed, these azo materials have been seldom investigated for solar energy conversion and storage applications, despite an inherent strong potential interaction with sunlight. The *trans* to *cis* conversion is exceptionally high quantum yield, and the energy harvested can be more than 50 kJ/mol. Unlike most fast relaxations too after absorption, this energy-rich *cis* form persists, for hours or even days, offering a tantalizing opportunity for scientists and engineers to seize advantage of this harvested sunlight, and transduce or store it, even just thermally. The few recent ‘‘proof-of-principle’’ applications described in the last section, however, have provided much encouragement and confidence, however, as the first important steps toward the ability of azobenzene-based materials to fabricate real macro-and micro-scale robots amenable to remote operation and control, as well as the advantages offered in design simplification and scale-down afforded by the replacement of electrons by photons. Driving actuation with light by this powerful emerging class of photo-energy harvesting materials can offer important and significant advantages that warrant much further study of these materials into their full potential.

Improving our understanding of the photo-mechanical effect, exhibited by azobenzene molecules upon light absorption is vital to the improvement and design of novel photo-responsive materials and systems. It is also of interest from a fundamental material science perspective. The focus of this thesis is the characterization of the photomechanical response of azobenzene polymers with a view towards improving our understanding of the mechanism underlying photo-actuation and the structure-property relationships driving the photomechanical effect and photo-induced flow.

Chapter 2 describes the methodology and measurements with a cantilever based sensor system to create a general framework capable of measuring changes in surface stress, photomechanical energy, efficiency and energy per unit volume of multiple azobenzene based polymers. These measurements demonstrate the ability of these polymer films to act as light driven artificial muscles in larger mechanical systems and are used as a basis to infer structure, processing and material response relationships through comparison of the polymers PDR1A, PDR13A and PMMA-co-PMMA studied.

Nanoindentation experiments described in Chapter 3 are then used to investigate changes in the mechanical properties of azobenzene polymers under irradiation, namely photo-induced creep and photosoftening. The strain rate sensitivity of PDR1A and $P4VP(DY7)_{0.5}$ in the dark and under irradiation is measured. The correlation of experimental data describing photo-induced softening to the structure-property relationships of the two materials and their implications to understanding surface mass transport in azobenzene based materials is discussed. Finally, concluding remarks and directions for future research based upon the experimental work and interpretations of this thesis are presented in Chapter 4.

1.7 References

1. Delaire JA, Nakatani K (2000) Linear and Nonlinear Optical Properties of Photochromic Molecules and Materials. Chemical Reviews 100 (5):1817-1846.
2. Yesodha SK, Sadashiva Pillai CK, Tsutsumi N (2004) Stable polymeric materials for nonlinear optics: A review based on azobenzene systems. Progress in Polymer Science 29 (1):45-74.

3. Aoki Ki, Nakagawa M, Ichimura K (2000) Self-Assembly of Amphoteric Azopyridine Carboxylic Acids: Organized Structures and Macroscopic Organized Morphology Influenced by Heat, pH Change, and Light. Journal of the American Chemical Society 122 (44):10997-11004.
4. Kadota S, Aoki K, Nagano S, Seki T (2005) Photocontrolled Microphase Separation of Block Copolymers in Two Dimensions. Journal of the American Chemical Society 127 (23):8266-8267.
5. Effing JJ, Kwak JCT (1995) Photoswitchable phase separation in hydrophobically modified polyacrylamide/surfactant systems. Angewandte Chemie, International Edition 34 (1):88-90.
6. Yamamoto H, Nishida A, Takimoto T, Nagai A (1990) Photoresponsive peptide and polypeptide systems. VIII. Synthesis and reversible photochromism of azo aromatic poly(L-ornithine). Journal of Polymer Science, Part A: Polymer Chemistry 28 (1):67-74.
7. Arai K, Kawabata Y (1995) Changes in the sol-gel transformation behavior of azobenzene moiety-containing methyl cellulose irradiated with UV light. Macromolecular Rapid Communications 16 (12):875-880.
8. Ebralidze TD, Mumladze AN (1990) Light-induced anisotropy in azo-dye-colored materials. Applied Optics 29 (4):446-447.
9. Higuchi M, Minoura N, Kinoshita T (1994) Photocontrol of micellar structure of an azobenzene containing amphiphilic sequential polypeptide. Chemistry Letters (2):227-230.
10. Higuchi M, Minoura N, Kinoshita T (1995) Photoinduced Structural and Functional Changes of an Azobenzene Containing Amphiphilic Sequential Polypeptide. Macromolecules 28 (14):4981-4985.
11. Steinem C, Janshoff A, Vollmer MS, Ghadiri MR (1999) Reversible Photoisomerization of Self-Organized Cylindrical Peptide Assemblies at Air-Water and Solid Interfaces. Langmuir 15 (11):3956-3964.
12. Vollmer MS, Clark TD, Steinem C, Ghadiri MR (1999) Photoswitchable Hydrogen-Bonding in Self-Organized Cylindrical Peptide Systems. Angewandte Chemie, International Edition 38 (11):1598-1601.

13. Yagai S, Nakajima T, Kishikawa K, Kohmoto S, Karatsu T, Kitamura A (2005) Hierarchical Organization of Photoresponsive Hydrogen-Bonded Rosettes. Journal of the American Chemical Society 127 (31):11134-11139.
14. Pouliquen G, Tribet C (2005) Light-Triggered Association of Bovine Serum Albumin and Azobenzene-Modified Poly(acrylic acid) in Dilute and Semidilute Solutions. Macromolecules 39 (1):373-383.
15. Camorani P, Fontana MP (2006) Optical control of structural morphology in azobenzene containing polymeric liquid crystals. Phys Rev E 73 (1):011703-011706.
16. Norikane Y, Hirai Y, Yoshida M (2011) Photoinduced isothermal phase transitions of liquid-crystalline macrocyclic azobenzenes. Chemical Communications 47 (6):1770-1772.
17. Wang G, Tong X, Zhao Y (2004) Preparation of Azobenzene-Containing Amphiphilic Diblock Copolymers for Light-Responsive Micellar Aggregates. Macromolecules 37 (24):8911-8917.
18. Ravi P, Sin SL, Gan LH, Gan YY, Tam KC, Xia XL, Hu X (2005) New water soluble azobenzene-containing diblock copolymers: synthesis and aggregation behavior. Polymer 46 (1):137-146.
19. Sin SL, Gan LH, Hu X, Tam KC, Gan YY (2005) Photochemical and thermal isomerizations of azobenzene-containing amphiphilic diblock copolymers in aqueous micellar aggregates and in film. Macromolecules 38 (9):3943-3948.
20. Yoshida E, Ohta M (2005) Preparation of light-stable micelles with azo dyes from a nonamphiphilic random block copolymer. Colloid and Polymer Science 283 (8):872-879.
21. Yoshida E, Ohta M (2005) Preparation of micelles with azobenzene at their coronas or cores from nonamphiphilic diblock copolymers. Colloid and Polymer Science 283 (5):521-531.
22. Sakai H, Matsumura A, Saji T, Abe M (2001) Active control of vesicle formation with photoelectrochemical switching. Studies in Surface Science and Catalysis 132:505-508.

23. Tong X, Wang G, Soldera A, Zhao Y (2005) How Can Azobenzene Block Copolymer Vesicles Be Dissociated and Reformed by Light? Journal of Physical Chemistry B 109 (43):20281-20287.

24. Willner I, Rubin S (1996) Control of the structure and functions of biomaterials by light. Angewandte Chemie, International Edition 35 (4):367-385.

25. Beharry AA, Woolley GA (2011) Azobenzene photoswitches for biomolecules. Chemical Society Reviews 40 (8):4422-4437.

26. Montagnoli G, Pieroni O, Suzuki S (1983) Control of peptide chain conformation by photoisomerising chromophores: Enzymes and model compounds. Polymer Photochemistry 3 (4):279-294.

27. Yamamoto H, Nishida A (1991) Photoresponsive peptide and polypeptide systems. Part 9. Synthesis and reversible photochromism of azo aromatic poly(L-a,g-diaminobutyric acid). Polymer International 24 (3):145-148.

28. Fissi A, Pieroni O, Balestreri E, Amato C (1996) Photoresponsive Polypeptides. Photomodulation of the Macromolecular Structure in Poly(N((phenylazophenyl)sulfonyl)-L-lysine). Macromolecules 29 (13):4680-4685.

29. Fissi A, Pieroni O, Ciardelli F (1987) Photoresponsive Polymers - Azobenzene-Containing Poly(L-Lysine). Biopolymers 26 (12):1993-2007.

30. Lee W-S, Ueno A (2001) Photocontrol of the Catalytic Activity of a beta-Cyclodextrin Bearing Azobenzene and Histidine Moieties as a Pendant Group. Macromolecular Rapid Communications 22 (6):448-450.

31. Pearson D, Downard AJ, Muscroft-Taylor A, Abell AD (2007) Reversible photoregulation of binding of α-chymotrypsin to a gold surface. Journal of the American Chemical Society 129 (48):14862-14863.

32. Shinkai S, Minami T, Kusano Y, Manabe O (1983) Photoresponsive crown ethers. 8. Azobenzenophane-type switched-on crown ethers which exhibit an all-or-nothing change in ion-binding ability. Journal of the American Chemical Society 105 (7):1851-1856.

33. Jung JH, Takehisa C, Sakata Y, Kaneda T (1996) p-(4-Nitrophenylazo)phenol dye-bridged permethylated a-cyclodextrin dimer: synthesis and self-aggregation in dilute aqueous solution. Chemistry Letters (2):147-148.

34. Yamamura H, Kawai H, Yotsuya T, Higuchi T, Butsugan Y, Araki S, Kawai M, Fujita K (1996) A cyclodextrin derivative with cation carrying ability: heptakis(3,6-anhydro)-b-cyclodextrin 2-O-p-phenylazobenzoate. Chemistry Letters (9):799-800.
35. Singh AK, Das J, Majumdar N (1996) Novel Bacteriorhodopsin Analogs Based on Azo Chromophores. Journal of the American Chemical Society 118 (26):6185-6191.
36. Chen SH, Mastrangelo JC, Shi H, Blanton TN, Bashir-Hashemi A (1997) Novel Glass-Forming Organic Materials. 3. Cubane with Pendant Nematogens, Carbazole, and Disperse Red 1. Macromolecules 30 (1):93-97.
37. Chen SH, Mastrangelo JC, Shi H, Bashir-Hashemi A, Li J, Gelber N (1995) Novel Glass-Forming Organic Materials. 1. Adamantane with Pendant Cholesteryl, Disperse Red 1, and Nematogenic Groups. Macromolecules 28 (23):7775-7778.
38. Ichimura K (2000) Photoalignment of Liquid-Crystal Systems. Chemical Reviews 100 (5):1847-1873.
39. Kumar GS, Neckers DC (1989) Photochemistry of azobenzene-containing polymers. Chemical Reviews 89 (8):1915-1925.
40. Rau H (1990) Photoisomerization of Azobenzenes. In: Rebek J (ed) Photochemistry and Photophysics, vol 2. CRC Press, Boca Raton, FL, pp 119-141.
41. Schulze FW, Petrick HJ, Cammenga HK, Klinge H (1977) Thermodynamic properties of the structural analogs benzo[c]cinnoline, trans-azobenzene, and cis-azobenzene. Zeitschrift fuer Physikalische Chemie 107 (1):1-19.
42. Mita I, Horie K, Hirao K (1989) Photochemistry in Polymer Solids. 9. Photoisomerization of Azobenzene in a Polycarbonate Film. Macromolecules 22 (2):558-563.
43. Monti S, Orlandi G, Palmieri P (1982) Features of the photochemically active state surfaces of azobenzene. Chemical Physics 71 (1):87-99.
44. Kobayashi T, Degenkolb EO, Rentzepis PM (1979) Picosecond spectroscopy of 1-phenylazo-2-hydroxynaphthalene. Journal of Physical Chemistry 83 (19):2431-2434.

45. Lednev IK, Ye T-Q, Hester RE, Moore JN (1996) Femtosecond Time-Resolved UV-Visible Absorption Spectroscopy of trans-Azobenzene in Solution. Journal of Physical Chemistry 100 (32):13338-13341.
46. Brown EV, Granneman GR (1975) Cis-Trans Isomerism in Pyridyl Analogs of Azobenzene - Kinetic and Molecular-Orbital Analysis. Journal of the American Chemical Society 97 (3):621-627.
47. Haberfield P, Block PM, Lux MS (1975) Enthalpies of Solvent Transfer of Transition-States in Cis-Trans Isomerization of Azo-Compounds - Rotation Vs Nitrogen Inversion Mechanism. Journal of the American Chemical Society 97 (20):5804-5806.
48. Kerzhner BK, Kofanov VI, Vrubel TL (1983) Photoisomerization of aromatic azo compounds adsorbed on a hydroxylated surface. Zhurnal Obshchei Khimii 53 (10):2303-2306.
49. Funke U, Gruetzmacher HF (1987) Dithiadiaza[n.2]paracyclophenes. Tetrahedron 43 (16):3787-3795.
50. Hartley GS (1937) Cis form of azobenzene. Nature 140:281.
51. Hartley GS (1938) Cis form of azobenzene and the velocity of the thermal cis- trans conversion of azobenzene and some derivatives. Journal of the Chemical Society, Abstracts:633-642.
52. Fischer E (1967) Calculation of photostationary states in systems A-B when only A is known. Journal of Physical Chemistry 71 (11):3704-3706.
53. Rau H, Greiner G, Gauglitz G, Meier H (1990) Photochemical quantum yields in the A-B system when only the spectrum of A is known. The Journal of Physical Chemistry 94 (17):6523-6524.
54. Gabor G, Fischer E (1971) Spectra and cis-trans isomerism in highly dipolar derivatives of azobenzene. Journal of Physical Chemistry 75 (4):581-583.
55. Eisenbach CD (1980) Cis-Trans Isomerization of Aromatic Azo Chromophores, Incorporated in the Hard Segments of Poly(ester urethane)s. Macromolecular Rapid Communications 1 (5):287-292.

56. Hair SR, Taylor GA, Schultz LW (1990) An Easily Implemented Flash-Photolysis Experiment for the Physical-Chemistry Laboratory - The Isomerization of 4-Anilino-4'-Nitroazobenzene. Journal of Chemical Education 67 (8):709-712.
57. Beltrame PL, Paglia ED, Castelli A, Tantardini GF, Seves A, Marcandalli B (1993) Thermal Cis-Trans-Isomerization of Azo Dyes in Poly(Methyl Methacrylate) Matrix - A Kinetic-Study. Journal of Applied Polymer Science 49 (12):2235-2239.
58. Magennis SW, Mackay FS, Jones AC, Tait KM, Sadler PJ (2005) Two-photon-induced photoisomerization of an azo dye. Chemistry of Materials 17 (8):2059-2062.
59. Rau H, Lueddecke E (1982) On the rotation-inversion controversy on photoisomerization of azobenzenes. Experimental proof of inversion. Journal of the American Chemical Society 104 (6):1616-1620.
60. Naito T, Horie K, Mita I (1991) Photochemistry in polymer solids. 11. The effects of the size of reaction groups and the mode of photoisomerization on photochromic reactions in polycarbonate film. Macromolecules 24 (10):2907-2911.
61. Liu ZF, Morigaki K, Enomoto T, Hashimoto K, Fujishima A (1992) Kinetic studies on the thermal cis-trans isomerization of an azo compound in the assembled monolayer film. Journal of Physical Chemistry 96 (4):1875-1880.
62. Altomare A, Ciardelli F, Tirelli N, Solaro R (1997) 4-Vinylazobenzene: Polymerizability and Photochromic Properties of Its Polymers. Macromolecules 30 (5):1298-1303.
63. Ho C-H, Yang K-N, Lee S-N (2001) Mechanistic study of trans-cis isomerization of the substituted azobenzene moiety bound on a liquid-crystalline polymer. Journal of Polymer Science, Part A: Polymer Chemistry 39 (13):2296-2307.
64. Xie S, Natansohn A, Rochon P (1993) Recent developments in aromatic azo polymers research. Chemistry of Materials 5 (4):403-411.
65. Jursic BS (1996) Ab initio and density functional theory study of the diazene isomerization. Chemical Physics Letters 261 (1-2):13-17.
66. Angeli C, Cimiraglia R, Hofmann H-J (1996) On the competition between the inversion and rotation mechanisms in the cis-trans thermal isomerization of diazene. Chemical Physics Letters 259 (3-4):276-282.

67. Natansohn A, Rochon P (2002) Photoinduced Motions in Azo-Containing Polymers. Chemical Reviews 102 (11):4139-4176.
68. Viswanathan NK, Balasubramanian S, Li L, Tripathy SK, Kumar J (1999) A detailed investigation of the polarization-dependent surface-relief-grating formation process on azo polymer films. Japanese Journal of Applied Physics 38 (10):5928-5937.
69. Yager KG, Barrett CJ (2001) All-optical patterning of azo polymer films. Current Opinion in Solid State & Materials Science 5 (6):487-494.
70. Uznanski P, Kryszewski M, Thulstrup EW (1991) Linear dichroism and trans-cis photo-isomerization studies of azobenzene molecules in oriented polyethylene matrix. European Polymer Journal 27 (1):41-43.
71. de Lange JJ, Robertson JM, Woodward I (1939) X-ray crystal analysis of trans-azobenzene. Proceedings of the Royal Society A: Mathematical, Physical and Engineering Sciences 171:398-410.
72. Hampson GC, Robertson JM (1941) Bond length and resonance in the cis-azobenzene molecule. Journal of the Chemical Society, Abstracts:409-413.
73. Brown CJ (1966) A refinement of the crystal structure of azobenzene. Acta Cryst 21 (1):146-152.
74. Naito T, Horie K, Mita I (1993) Photochemistry in polymer solids: 12. Effects of main-chain structures and formation of hydrogen bonds on photoisomerization of azobenzene in various polymer films. Polymer 34 (19):4140-4145.
75. Paik CS, Morawetz H (1972) Photochemical and Thermal Isomerization of Azoaromatic Residues in the Side Chains and the Backbone of Polymers in Bulk. Macromolecules 5 (2):171-177.
76. Lamarre L, Sung CSP (1983) Studies of physical aging and molecular motion by azochromophoric labels attached to the main chains of amorphous polymers. Macromolecules 16 (11):1729-1736.
77. Weiss RG, Ramamurthy V, Hammond GS (1993) Photochemistry in organized and confining media: a model. Accounts of Chemical Research 25 (10):530-536.
78. Hugel T, Holland NB, Cattani A, Moroder L, Seitz M, Gaub HE (2002) Single-Molecule Optomechanical Cycle. Science 296 (5570):1103-1106.

79. Holland NB, Hugel T, Neuert G, Cattani-Scholz A, Renner C, Oesterhelt D, Moroder L, Seitz M, Gaub HE (2003) Single Molecule Force Spectroscopy of Azobenzene Polymers: Switching Elasticity of Single Photochromic Macromolecules. Macromolecules 36 (6):2015-2023.

80. Neuert G, Hugel T, Netz RR, Gaub HE (2005) Elasticity of Poly(azobenzene-peptides). Macromolecules 39 (2):789-797.

81. Asakawa M, Ashton PR, Balzani V, Brown CL, Credi A, Matthews OA, Newton SP, Raymo FM, Shipway AN, Spencer N, Quick A, Stoddart JF, White AJP, Williams DJ (1999) Photoactive Azobenzene-Containing Supramolecular Complexes and Related Interlocked Molecular Compounds. Chemistry--A European Journal 5 (3):860-875.

82. Balzani V, Credi A, Marchioni F, Stoddart JF (2001) Artificial molecular-level machines. Dethreading-rethreading of a pseudorotaxane powered exclusively by light energy. Chemical Communications 18:1860-1861.

83. Tsuchiya S (1999) Intramolecular Electron Transfer of Diporphyrins Comprised of Electron-Deficient Porphyrin and Electron-Rich Porphyrin with Photocontrolled Isomerization. Journal of the American Chemical Society 121 (1):48-53.

84. Masiero S, Lena S, Pieraccini S, Spada GP (2008) The Direct Conversion of Light into Continuous Mechanical Energy by Photoreversible Self-Assembly: A Prototype of a Light-Powered Engine. Angewandte Chemie International Edition 47 (17):3184-3187.

85. Fujiwara M, Akiyama M, Hata M, Shiokawa K, Nomura R (2008) Photoinduced acceleration of the effluent rate of developing solvents in azobenzene-tethered silica gel. ACS Nano 2 (8):1671-1681.

86. Pakula C, Zaporojtchenko V, Strunskus T, Zargarani D, Herges R, Faupel F (2010) Reversible light-controlled conductance switching of azobenzene-based metal/polymer nanocomposites. Nanotechnology 21 (46).

87. Raimondo C, Reinders F, Soydaner U, Mayor M, Samorì P (2010) Light-responsive reversible solvation and precipitation of gold nanoparticles. Chemical Communications 46 (7):1147-1149.

88. Kimoto A, Iwasaki K, Abe J (2010) Formation of photoresponsive gold nanoparticle networks via click chemistry. Photochemical and Photobiological Sciences 9 (2):152-156.
89. Higuchi M, Minoura N, Kinoshita T (1995) Photo-Responsive Behavior of a Monolayer Composed of an Azobenzene Containing Polypeptide in the Main-Chain. Colloid and Polymer Science 273 (11):1022-1027.
90. Siewierski LM, Brittain WJ, Petrash S, Foster MD (1996) Photoresponsive monolayers containing in-chain azobenzene. Langmuir 12 (24):5838-5844.
91. Stiller B, Knochenhauer G, Markava E, Gustina D, Muzikante I, Karageorgiev P, Brehmer L (1999) Self-assembled monolayers of novel azobenzenes for optically induced switching. Materials Science and Engineering: C 8-9:385-389.
92. Moller G, Harke M, Motschmann H, Prescher D (1998) Controlling microdroplet formation by light. Langmuir 14 (18):4955-4957.
93. Feng CL, Zhang YJ, Jin J, Song YL, Xie LY, Qu GR, Jiang L, Zhu DB (2001) Reversible Wettability of Photoresponsive Fluorine-Containing Azobenzene Polymer in Langmuir-Blodgett Films. Langmuir 17 (15):4593-4597.
94. Chen T, Xu S, Zhang F, Evans DG, Duan X (2009) Formation of photo- and thermo-stable layered double hydroxide films with photo-responsive wettability by intercalation of functionalized azobenzenes. Chemical Engineering Science 64 (21):4350-4357.
95. Delorme N, Bardeau J-F, Bulou A, Poncin-Epaillard F (2005) Azobenzene-Containing Monolayer with Photoswitchable Wettability. Langmuir 21 (26):12278-12282.
96. Jiang WH, Wang GJ, He YN, Wang XG, An YL, Song YL, Jiang L (2005) Photo-switched wettability on an electrostatic self-assembly azobenzene monolayer. Chemical Communications (28):3550-3552.
97. Ichimura K, Oh S-K, Nakagawa M (2000) Light-Driven Motion of Liquids on a Photoresponsive Surface. Science 288 (5471):1624-1626.
98. Diguet A, Guillermic R-M, Magome N, Saint-Jalmes A, Chen Y, Yoshikawa K, Baigl D (2009) Photomanipulation of a Droplet by the Chromocapillary Effect. Angewandte Chemie International Edition 48 (49):9281-9284.

99. Sarkar N, Sarkar A, Sivaram S (2001) Isomerization behavior of aromatic azo chromophores bound to semicrystalline polymer films. Journal of Applied Polymer Science 81 (12):2923-2928.
100. Fujita T, Iyi N, Klapyta Z (1998) Preparation of azobenzene-mica complex and its photoresponse to ultraviolet irradiation. Materials Research Bulletin 33 (11):1693-1701.
101. Fujita T, Iyi N, Klapyta Z (2001) Optimum conditions for photoresponse of azobenzene-organophilic tetrasilicic mica complexes. Materials Research Bulletin 36 (3-4):557-571.
102. Yager KG, Tanchak OM, Godbout C, Fritzsche H, Barrett CJ (2006) Photomechanical effects in azo-polymers studied by neutron reflectometry. Macromolecules 39 (26):9311-9319.
103. Tanchak OM, Barrett CJ (2005) Light-induced reversible volume changes in thin films of azo polymers: The photomechanical effect. Macromolecules 38 (25):10566-10570.
104. Yager KG, Tanchak OM, Barrett CJ, Watson MJ, Fritzsche H (2006) Temperature-controlled neutron reflectometry sample cell suitable for study of photoactive thin films. Review of Scientific Instruments 77 (4).
105. Eisenbach CD (1980) Isomerization of aromatic azo chromophores in poly(ethyl acrylate) networks and photomechanical effect. Polymer 21 (10):1175-1179.
106. Agolini F, Gay FP (1970) Synthesis and properties of azoaromatic polymers. Macromolecules 3 (3):349-351.
107. Yu Y, Nakano M, Ikeda T (2003) Photomechanics: Directed bending of a polymer film by light. Nature 425:145.
108. Ikeda T, Nakano M, Yu Y, Tsutsumi O, Kanazawa A (2003) Anisotropic Bending and Unbending Behavior of Azobenzene Liquid-Crystalline Gels by Light Exposure. Advanced Materials 15 (3):201-205.
109. Yu YL, Nakano M, Maeda T, Kondo M, Ikeda T (2005) Precisely direction-controllable bending of cross-linked liquid-crystalline polymer films by light. Molecular Crystals and Liquid Crystals 436:1235-1244.

110. Bai S, Zhao Y (2001) Azobenzene-Containing Thermoplastic Elastomers: Coupling Mechanical and Optical Effects. Macromolecules 34 (26):9032-9038.

111. Rochon P, Batalla E, Natansohn A (1995) Optically induced surface gratings on azoaromatic polymer films. Applied Physics Letters 66 (2):136-138.

112. Kim DY, Tripathy SK, Li L, Kumar J (1995) Laser-induced holographic surface relief gratings on nonlinear optical polymer films. Applied Physics Letters 66 (10):1166-1168.

113. Bian S, Li L, Kumar J, Kim DY, Williams J, Tripathy SK (1998) Single laser beam-induced surface deformation on azobenzene polymer films. Applied Physics Letters 73 (13):1817-1819.

114. Kumar J, Li L, Jiang XL, Kim DY, Lee TS, Tripathy S (1998) Gradient force: The mechanism for surface relief grating formation in azobenzene functionalized polymers. Applied Physics Letters 72 (17):2096-2098.

115. Viswanathan NK, Kim DY, Bian S, Williams J, Liu W, Li L, Samuelson L, Kumar J, Tripathy SK (1999) Surface relief structures on azo polymer films. Journal of Materials Chemistry 9 (9):1941-1955.

116. Labarthet FL, Bruneel JL, Buffeteau T, Sourisseau C (2004) Chromophore orientations upon irradiation in gratings inscribed on azo-dye polymer films: A combined AFM and confocal Raman microscopic study. Journal of Physical Chemistry B 108 (22):6949-6960.

117. Lagugne-Labarthet F, Bruneel JL, Rodriguez V, Sourisseau C (2004) Chromophore orientations in surface relief gratings with second-order nonlinearity as studied by confocal polarized Raman microspectrometry. Journal of Physical Chemistry B 108 (4):1267-1278.

118. Labarthet FL, Bruneel JL, Buffeteau T, Sourisseau C, Huber MR, Zilker SJ, Bieringer T (2000) Photoinduced orientations of azobenzene chromophores in two distinct holographic diffraction gratings as studied by polarized Raman confocal microspectrometry. Physical Chemistry Chemical Physics 2 (22):5154-5167.

119. Henneberg O, Geue T, Pietsch U, Saphiannikova M, Winter B (2004) Investigation of azobenzene side group orientation in polymer surface relief gratings by means of photoelectron spectroscopy. Applied Physics Letters 84 (9):1561-1563.

120. Saphiannikova M, Neher D (2005) Thermodynamic theory of light-induced material transport in amorphous azobenzene polymer films. Journal of Physical Chemistry B 109 (41):19428-19436.

121. Toshchevikov V, Saphiannikova M, Heinrich G (2009) Microscopic theory of light-induced deformation in amorphous side-chain azobenzene polymers. Journal of Physical Chemistry B 113 (15):5032-5045.

122. Vapaavuori J, Valtavirta V, Alasaarela T, Mamiya JI, Priimagi A, Shishido A, Kaivola M (2011) Efficient surface structuring and photoalignment of supramolecular polymer-azobenzene complexes through rational chromophore design. Journal of Materials Chemistry 21 (39):15437-15441.

123. Pietsch U, Rochon P, Natansohn A (2000) Formation of a buried lateral density grating in azobenzene polymer films. Advanced Materials 12 (15):1129-1132.

124. Geue T, Henneberg O, Grenzer J, Pietsch U, Natansohn A, Rochon P, Finkelstein K (2002) Formation of a buried density grating on thermal erasure of azobenzene polymer surface gratings. Colloids and Surfaces a-Physicochemical and Engineering Aspects 198-200:31-36.

125. Geue TM, Saphiannikova MG, Henneberg O, Pietsch U, Rochon PL, Natansohn AL (2003) X-ray investigations of formation efficiency of buried azobenzene polymer density gratings. Journal of Applied Physics 93 (6):3161-3166.

126. Pietsch U (2002) X-ray and visible light scattering from light-induced polymer gratings. Phys Rev B 66 (15):155430.

127. Barrett CJ, Natansohn AL, Rochon PL (1996) Mechanism of Optically Inscribed High-Efficiency Diffraction Gratings in Azo Polymer Films. Journal of Physical Chemistry 100 (21):8836-8842.

128. Priimagi A, Lindfors K, Kaivola M, Rochon P (2009) Efficient Surface-Relief Gratings in Hydrogen-Bonded Polymer−Azobenzene Complexes. ACS Applied Materials & Interfaces 1 (6):1183-1189.

129. Wang X, Balasubramanian S, Kumar J, Tripathy SK, Li L (1998) Azo Chromophore-Functionalized Polyelectrolytes. 1. Synthesis, Characterization, and Photoprocessing. Chemistry of Materials 10 (6):1546-1553.

130. He J-A, Bian S, Li L, Kumar J, Tripathy SK, Samuelson LA (2000) Surface relief gratings from electrostatically layered azo dye films. Applied Physics Letters 76 (22):3233-3235.

131. Lee S-H, Balasubramanian S, Kim DY, Viswanathan NK, Bian S, Kumar J, Tripathy SK (2000) Azo Polymer Multilayer Films by Electrostatic Self-Assembly and Layer-by-Layer Post Azo Functionalization. Macromolecules 33 (17):6534-6540.

132. Zhang Q, Wang X, Barrett CJ, Bazuin CG (2009) Spacer-free ionic dye-polyelectrolyte complexes: Influence of molecular structure on liquid crystal order and photoinduced motion. Chemistry of Materials 21 (14):3216-3227.

133. Yang SZ, Li L, Cholli AL, Kumar J, Tripathy SK (2001) Photoinduced surface relief gratings on azocellulose films. Journal of Macromolecular Science - Pure and Applied Chemistry 38 (12):1345-1354.

134. Yang S, Jacob MM, Li L, Yang K, Cholli AL, Kumar J, Tripathy SK (2002) Azobenzene-Modified Cellulose. Polymer News 27:368-372.

135. Yang SZ, Li L, Cholli AL, Kumar J, Tripathy SK (2003) Ambenzene-modified poly(L-glutamic acid) (AZOPLGA): Its conformational and photodynamic properties. Biomacromolecules 4 (2):366-371.

136. Nakano H, Tanino T, Takahashi T, Ando H, Shirota Y (2008) Relationship between molecular structure and photoinduced surface relief grating formation using azobenzene-based photochromic amorphous molecular materials. Journal of Materials Chemistry 18 (2):242-246.

137. Walker R, Audorff H, Kador L, Schmidt HW (2009) Synthesis and structure-property relations of a series of photochromic molecular classes for controlled and efficient formation of surface relief nanostructures. Advanced Functional Materials 19 (16):2630-2638.

138. Ubukata T, Takahashi K, Yokoyama Y (2007) Photoinduced surface relief structures formed on polymer films doped with photochromic spiropyrans. Journal of Physical Organic Chemistry 20 (11):981-984.

139. Ubukata T, Fujii S, Yokoyama Y (2009) Reversible phototriggered micromanufacturing using amorphous photoresponsive spirooxazine film. Journal of Materials Chemistry 19 (21):3373-3377.
140. Zettsu N, Ubukata T, Seki T, Ichimura K (2001) Soft crosslinkable azo polymer for rapid surface relief formation and persistent fixation. Advanced Materials 13 (22):1693-1697.
141. Li W, Nagano S, Seki T (2009) Photo-crosslinkable liquid-crystalline azo-polymer for surface relief gratings and persistent fixation. New Journal of Chemistry 33 (6):1343-1348.
142. Goldenberg LM, Kulikovsky L, Kulikovska O, Stumpe J (2009) New materials with detachable azobenzene: Effective, colourless and extremely stable surface relief gratings. Journal of Materials Chemistry 19 (43):8068-8071.
143. Zettsu N, Ogasawara T, Mizoshita N, Nagano S, Seki T (2008) Photo-triggered surface relief grating formation in supramolecular liquid crystalline polymer systems with detachable azobenzene units. Advanced Materials 20 (3):516-521.
144. Tripathy SK, Viswanathan NK, Balasubramanian S, Kumar J (2000) Holographic fabrication of polarization selective diffractive optical elements on azopolymer film. Polymers for Advanced Technologies 11 (8-12):570-574.
145. Rochon P, Natansohn A, Callendar CL, Robitaille L (1997) Guided mode resonance filters using polymer films. Applied Physics Letters 71 (8):1008-1010.
146. Stockermans RJ, Rochon PL (1999) Narrow-band Resonant Grating Waveguide Filters Constructed with Azobenzene Polymers. Applied Optics 38 (17):3714-3719.
147. Alasaarela T, Zheng D, Huang L, Priimagi A, Bai B, Tervonen A, Honkanen S, Kuittinen M, Turunen J (2011) Single-layer one-dimensional nonpolarizing guided-mode resonance filters under normal incidence. Optics Letters 36 (13):2411-2413.
148. Paterson J, Natansohn A, Rochon P, Callendar CL, Robitaille L (1996) Optically inscribed surface relief diffraction gratings on azobenzene-containing polymers for coupling light into slab waveguides. Applied Physics Letters 69 (22):3318-3320.
149. Nagata T, Matsui T, Ozaki M, Yoshino K, Kajzar F (2001) Novel optical properties of conducting polymer-photochromic polymer systems. Synthetic Met 119 (1-3):607-608.

150. Dumarcher V, Rocha L, Denis C, Fiorini C, Nunzi J-M, Sobel F, Sahraoui B, Gindre D (2000) Polymer thin-film distributed feedback tunable lasers. Journal of Optics A: Pure and Applied Optics 2 (4):279-283.

151. Rocha L, Dumarcher V, Denis C, Raimond P, Fiorini C, Nunzi JM (2001) Laser emission in periodically modulated polymer films. Journal of Applied Physics 89 (5):3067-3069.

152. Ubukata T, Isoshima T, Hara M (2005) Wavelength-programmable organic distributed-feedback laser based on a photoassisted polymer-migration system. Advanced Materials 17 (13):1630-1633.

153. Egami C, Kawata Y, Aoshima Y, Alasfar S, Sugihara O, Fujimura H, Okamoto N (2000) Two-stage optical data storage in azo polymers. Japanese Journal of Applied Physics 39 (3B):1558-1561.

154. Harada K, Itoh M, Yatagai T, Kamemaru SI (2005) Application of surface relief hologram using azobenzene containing polymer film. Optical Review 12 (2):130-134.

155. Ramanujam PS, Pedersen M, Hvilsted S (1999) Instant holography. Applied Physics Letters 74 (21):3227-3229.

156. Na SI, Kim SS, Jo J, Oh SH, Kim J, Kim DY (2008) Efficient polymer solar cells with surface relief gratings fabricated by simple soft lithography. Advanced Functional Materials 18 (24):3956-3963.

157. Gritsai Y, et al. (2008) 3D structures using surface relief gratings of azobenzene materials. Journal of Optics A: Pure and Applied Optics 10 (12):125304.

158. Neumann J, Wieking KS, Kip D (1999) Direct laser writing of surface reliefs in dry, self-developing photopolymer films. Applied Optics 38 (25):5418-5421.

159. Li XT, Natansohn A, Rochon P (1999) Photoinduced liquid crystal alignment based on a surface relief grating in an assembled cell. Applied Physics Letters 74 (25):3791-3793.

160. Kim M-H, Kim J-D, Fukuda T, Matsuda H (2000) Alignment control of liquid crystals on surface relief gratings. Liquid Crystals 27 (12):1633-1640.

161. Parfenov A, Tamaoki N, Ohnishi S (2000) Photoinduced alignment of nematic liquid crystal on the polymer surface microrelief. Journal of Applied Physics 87 (4):2043-2045.
162. Parfenov A, Tamaoki N, Ohni-Shi S (2001) Photoinduced alignment of nematic liquid crystal on the polymer surface microrelief. Molecular Crystals and Liquid Crystals 359:487-495.
163. Kaneko F, Kato T, Baba A, Shinbo K, Kato K, Advincula RC (2002) Photo-induced fabrication of surface relief gratings in alternate self-assembled films containing azo dye and alignments of LC molecules. Colloid Surface A 198:805-810.
164. Ishow E, Brosseau A, Clavier G, Nakatani K, Pansu RB, Vachon J-J, Tauc P, Chauvat D, Mendonça CR, Piovesan E (2007) Two-Photon Fluorescent Holographic Rewritable Micropatterning. Journal of the American Chemical Society 129 (29):8970-8971.
165. Chen X, Liu B, Zhang H, Guan S, Zhang J, Zhang W, Chen Q, Jiang Z, Guiver MD (2009) Fabrication of fluorescent holographic micropatterns based on azobenzene-containing host-guest complexes. Langmuir 25 (18):10444-10446.
166. Ye YH, Badilescu S, Truong VV, Rochon P, Natansohn A (2001) Self-assembly of colloidal spheres on patterned substrates. Applied Physics Letters 79 (6):872-874.
167. Yi DK, Kim MJ, Kim DY (2002) Surface relief grating induced colloidal crystal structures. Langmuir 18 (6):2019-2023.
168. Yi DK, Seo E-M, Kim D-Y (2002) Fabrication of a Mesoscale Wire: Sintering of a Polymer Colloid Arrayed Inside a One-Dimensional Groove Pattern. Langmuir 18 (13):5321-5323.
169. Noel S, Batalla E, Rochon P (1996) A simple method for the manufacture of mesoscopic metal wires. J Mater Res 11 (4):865-867.
170. Kim SS, Chun C, Hong JC, Kim DY (2006) Well-ordered TiO2 nanostructures fabricated using surface relief gratings on polymer films. Journal of Materials Chemistry 16 (4):370-375.
171. Morikawa Y, Nagano S, Watanabe K, Kamata K, Iyoda T, Seki T (2006) Optical alignment and patterning of nanoscale microdomains in a block copolymer thin film. Advanced Materials 18 (7):883-886.

172. Liu B, Wang M, He Y, Wang X (2006) Duplication of Photoinduced Azo Polymer Surface-Relief Gratings through a Soft Lithographic Approach. Langmuir 22 (17):7405-7410.
173. Ye G, Li X, Wang X (2010) Diffraction grating of hydrogel functionalized with glucose oxidase for glucose detection. Chemical Communications 46 (22):3872-3874.
174. Lee S, Kang HS, Park JK (2011) High-resolution patterning of various large-area, highly ordered structural motifs by directional photofluidization lithography: Sub-30-nm line, ellipsoid, rectangle, and circle arrays. Advanced Functional Materials 21 (10):1770-1778.
175. Lee S, Shin J, Lee YH, Fan S, Park JK (2010) Directional photofluidization lithography for nanoarchitectures with controlled shapes and sizes. Nano Letters 10 (1):296-304.
176. Kravchenko A, Shevchenko A, Ovchinnikov V, Priimagi A, Kaivola M (2011) Optical Interference Lithography Using Azobenzene-Functionalized Polymers for Micro- and Nanopatterning of Silicon. Advanced Materials 23 (36):4174-4177.
177. Ikawa T, Kato Y, Yamada T, Shiozawa M, Narita M, Mouri M, Hoshino F, Watanabe O, Tawata M, Shimoyama H (2010) Virus-templated photoimprint on the surface of an azobenzene-containing polymer. Langmuir 26 (15):12673-12679.
178. Watanabe O, Ikawa T, Hasegawa M, Tsuchimori M, Kawata Y, Egami C, Sugihara O, Okamoto N (2000) Transcription of near-field induced by photo-irradiation on a film of azo-containing urethane-urea copolymer. Molecular Crystals and Liquid Crystals 345:629-634.
179. Ikawa T, Mitsuoka T, Hasegawa M, Tsuchimori M, Watanabe O, Kawata Y, Egami C, Sugihara O, Okamoto N (2000) Optical near field induced change in viscoelasticity on an azobenzene-containing polymer surface. Journal of Physical Chemistry B 104 (39):9055-9058.
180. Hasegawa M, Ikawa T, Tsuchimori M, Watanabe O, Kawata Y (2001) Topographical nanostructure patterning on the surface of a thin film of polyurethane containing azobenzene moiety using the optical near field around polystyrene spheres. Macromolecules 34 (21):7471-7476.

181. Hasegawa M, Keum C-D, Watanabe O (2002) Enhanced Photofabrication of a Surface Nanostructure on Azobenzene-Functionalized Polymer Films with Evaporated Gold Nanoislands. Advanced Materials 14 (23):1738-1741.

182. Keum CD, Ikawa T, Tsuchimori M, Watanabe O (2003) Photodeformation behavior of photodynamic polymers bearing azobenzene moieties in their main and/or side chain. Macromolecules 36 (13):4916-4923.

183. Fukuda T, Sumaru K, Kimura T, Matsuda H, Narita Y, Inoue T, Sato F (2001) Observation of optical near-field as photo-induced surface relief formation. Japanese Journal of Applied Physics 40 (8B):L900-L902.

184. Galarreta BC, Rupar I, Young A, Lagugné-Labarthet F (2011) Mapping hot-spots in hexagonal arrays of metallic nanotriangles with azobenzene polymer thin films. Journal of Physical Chemistry C 115 (31):15318-15323.

185. Hubert C, Rumyantseva A, Lerondel G, Grand J, Kostcheev S, Billot L, Vial A, Bachelot R, Royer P, Chang SH, Gray SK, Wiederrecht GP, Schatz GC (2005) Near-field photochemical imaging of noble metal nanostructures. Nano Letters 5 (4):615-619.

186. Camacho-Lopez M, Finkelmann H, Palffy-Muhoray P, Shelley M (2004) Fast liquid-crystal elastomer swims into the dark. Nature Materials 3 (5):307-310.

187. Bublitz D, Helgert M, Fleck B, Wenke L, Hvilsted S, Ramanujam PS (2000) Photoinduced deformation of azobenzene polyester films. Applied Physics B: Lasers and Optics 70 (6):863-865.

188. Ji HF, Feng Y, Xu XH, Purushotham V, Thundat T, Brown GM (2004) Photon-driven nanomechanical cyclic motion. Chemical Communications (22):2532-2533.

189. White TJ, Tabiryan NV, Serak SV, Hrozhyk UA, Tondiglia VP, Koerner H, Vaia RA, Bunning TJ (2008) A high frequency photodriven polymer oscillator. Soft Matter 4 (9):1796-1798.

190. White TJ, Serak SV, Tabiryan NV, Vaia RA, Bunning TJ (2009) Polarization-controlled, photodriven bending in monodomain liquid crystal elastomer cantilevers. Journal of Materials Chemistry 19 (8):1080-1085.

191. Serak S, Tabiryan N, Vergara R, White TJ, Vaia RA, Bunning TJ (2010) Liquid crystalline polymer cantilever oscillators fueled by light. Soft Matter 6 (4):779-783.

192. Chen M, Huang H, Zhu Y, Liu Z, Xing X, Cheng F, Yu Y (2010) Photodeformable CLCP material: study on photo-activated microvalve applications. Applied Physics A: Materials Science and Processing 102 (3):667-672.

193. Yamada M, Kondo M, Mamiya JI, Yu Y, Kinoshita M, Barrett CJ, Ikeda T (2008) Photomobile polymer materials: Towards light-driven plastic motors. Angewandte Chemie International Edition 47 (27):4986-4988.

194. Blair HS, Ivor Pogue H (1982) Photomechanical effects in polymers containing 6′-nitro-1,3,3-trimethyl-spiro-(2′H-1′-benzopyran -2,2′-indoline). Polymer 23 (5):779-783.

195. Blair HS, Pague HI, Riordan JE (1980) PHOTORESPONSIVE EFFECTS IN AZO POLYMERS. Polymer 21 (10):1195-1198.

196. Menzel H, Weichart B, Hallensleben ML (1992) Langmuir-Blodgett-films of photochromic polyglutamates - II. Synthesis and spreading behaviour of photochromic polyglutamates with alkylspacers and -tails of different length. Polymer Bulletin 27 (6):637-644.

197. Menzel H (1994) Langmuir-Boldgett-films of photochromic polyglutamates. 7. The photomechanical effect in monolayers of polyglutamate with azobenzene moieties in the side-chains. Macromolecular Chemistry and Physics 195 (12):3747-3757.

198. Seki T, Tamaki T (1993) Photomechanical effect in monolayers of azobenzene side-chain polymers. Chemistry Letters (10):1739-1742.

199. Seki T, Sekizawa H, Fukuda RI, Tamaki T, Yokoi M, Ichimura K (1996) Features of photomechanical response in monolayers composed of a charged amphiphilic azobenzene polymer. Polymer Journal 28 (7):613-618.

200. Seki T, Ichimura K, Fukuda RI, Tamaki T (1996) Photomechanical behaviour of monolayers of azobenzene derivatives. Thin Solid Films 284-285:365-367.

201. Seki T (2004) Dynamic photoresponsive functions in organized layer systems comprised of azobenzene-containing polymers. Polymer Journal 36 (6):435-454.

202. Seki T, Tanaka K, Ichimura K (1997) Photomechanical Response in Monolayered Polymer Films on Mica at High Humidity. Macromolecules 30 (20):6401-6403.

203. Seki T, Sekizawa H, Morino SY, Ichimura K (1998) Inherent and cooperative photomechanical motions in monolayers of an azobenzene containing polymer at the air-water interface. Journal of Physical Chemistry B 102 (27):5313-5321.
204. Kago K, Fürst M, Matsuoka H, Yamaoka H, Seki T (1999) Direct observation of photoisomerization of a polymer monolayer on a water surface by X-ray reflectometry. Langmuir 15 (7):2237-2240.
205. Seki T, Kojima JY, Ichimura K (2000) Multifarious photoinduced morphologies in monomolecular films of azobenzene side chain polymer on mica. Macromolecules 33 (7):2709-2717.
206. Kago K, Seki T, Schücke RR, Mouri E, Matsuoka H, Yamaoka H (2002) Nanostructure of a photochromic polymer/liquid crystal hybrid monolayer on a water surface observed by in situ x-ray reflectometry. Langmuir 18 (10):3875-3879.
207. Seki T, Fukuchi T, Ichimura K (2002) Role of hydrogen bonding in azobenzene-urea assemblies. The packing state and photoresponse behavior in Langmuir monolayers. Langmuir 18 (14):5462-5467.
208. Klajn R (2010) Immobilized azobenzenes for the construction of photoresponsive materials. Pure and Applied Chemistry 82 (12):2247-2276.
209. Liu C, Chun SB, Mather PT, Zheng L, Haley EH, Coughlin EB (2002) Chemically cross-linked polycyclooctene: Synthesis, characterization, and shape memory behavior. Macromolecules 35 (27):9868-9874.
210. Otero TF, Cortés MT (2003) Artificial muscles with tactile sensitivity. Advanced Materials 15 (4):279-282.
211. Fukushima T, Asaka K, Kosaka A, Aida T (2005) Fully plastic actuator through layer-by-layer casting with ionic-liquid-based bucky gel. Angewandte Chemie International Edition 44 (16):2410-2413.
212. Gao J, Sansiñena JM, Wang HL (2003) Tunable polyaniline chemical actuators. Chemistry of Materials 15 (12):2411-2418.
213. Merian E (1966) Steric Factors Influencing the Dyeing of Hydrophobic. Fibers. Textile Research Journal 36 (7):612-618.
214. Irie M (1990) Photoresponsive polymers. Advances in Polymer Science 94:26-67.

215. Smets GaD, F. (1974) Chemical reactions in solid polymeric systems. Photomechanical phenomena. Pure and Applied Chemistry 39 (1-2):225–238.
216. Matějka L, Dušek K, Ilavský M (1979) The thermal effect in the photomechanical conversion of a photochromic polymer. Polymer Bulletin 1 (9):659-664.
217. Matějka L, Ilavský M, Dušek K, Wichterle O (1981) Photomechanical effects in crosslinked photochromic polymers. Polymer 22 (11):1511-1515.
218. Matějka L, Dušek K (1981) Photochromic polymers: Photoinduced conformational changes and effect of polymeric matrix on the isomerization of photochromes. Die Makromolekulare Chemie 182 (11):3223-3236.
219. Yager KG, Barrett CJ (2006) Photomechanical surface patterning in azo-polymer materials. Macromolecules 39 (26):9320-9326.
220. Kim HK, Wang XS, Fujita Y, Sudo A, Nishida H, Fujii M, Endo T (2005) Photomechanical switching behavior of semi-interpenetrating polymer network consisting of azobenzene-carrying crosslinked poly(vinyl ether) and polycarbonate. Macromolecular Rapid Communications 26 (13):1032-1036.
221. Kim HK, Wang XS, Fujita Y, Sudo A, Nishida H, Fujii M, Endo T (2005) A rapid photomechanical switching polymer blend system composed of azobenzene-carrying poly(vinylether) and poly(carbonate). Polymer 46 (16):5879-5883.
222. Kim HK, Wang XS, Fujita Y, Sudo A, Nishida H, Fujii M, Endo T (2005) Reversible photo-mechanical switching behavior of azobenzene-containing semi-interpenetrating network under UV and visible light irradiation. Macromolecular Chemistry and Physics 206 (20):2106-2111.
223. Tanaka S, Kim HK, Sudo A, Nishida H, Endo T (2008) Anisotropic photomechanical response of stretched blend film made of polycaprolactone-polyvinyl ether with azobenzene group as side chain. Macromolecular Chemistry and Physics 209 (20):2071-2077.
224. Zhang C, Zhao X, Chao D, Lu X, Chen C, Wang C, Zhang W (2009) Rapid bending of a nonliquid crystal azobenzene polymer film and characteristics of surface relief grating. Journal of Applied Polymer Science 113 (2):1330-1334.
225. Kim HK, Shin W, Ahn TJ (2010) UV sensor based on photomechanically functional polymer-coated FBG. IEEE Photonics Technology Letters 22 (19):1404-1406.

226. Kim KT, Moon NI, Kim HK (2010) A fiber-optic UV sensor based on a side-polished single mode fiber covered with azobenzene dye-doped polycarbonate. Sensors and Actuators A: Physical 160 (1-2):19-21.

227. Li N, Ye G, He Y, Wang X (2011) Hollow microspheres of amphiphilic azo homopolymers: Self-assembly and photoinduced deformation behavior. Chemical Communications 47 (16):4757-4759.

228. Liu J, He Y, Wang X (2010) Influence of chromophoric electron-withdrawing groups on photoinduced deformation of azo polymer colloids. Polymer 51 (13):2879-2886.

229. Liu JH, Chiu YH (2010) Behaviors of self-assembled diblock copolymer with pendant photosensitive azobenzene segments. Journal of Polymer Science, Part A: Polymer Chemistry 48 (5):1142-1148.

230. Liu J, He Y, Wang X (2008) Azo polymer colloidal spheres containing different amounts of functional groups and their photoinduced deformation behavior. Langmuir 24 (3):678-682.

231. Liu J, He Y, Wang X (2009) Size-dependent light-driven effect observed for azo polymer colloidal spheres with different average diameters. Langmuir 25 (10):5974-5979.

232. Küpfer J, Nishikawa E, Finkelmann H (1994) Densely crosslinked liquid single-crystal elastomers. Polymers for Advanced Technologies 5 (2):110-115.

233. Wermter H, Finkelmann H (2001) Liquid crystalline elastomers as artificial muscles. e-Polymers (no. 013).

234. Gennes PGD, Hebert M, Kant R (1997) Artificial muscles based on nematic gels. Macromolecular Symposia 113:39-49

235. Ikeda T, Mamiya J, Yu YL (2007) Photomechanics of liquid-crystalline elastomers and other polymers. Angewandte Chemie International Edition 46 (4):506-528.

236. Elias AL, Harris KD, Bastiaansen CWM, Broer DJ, Brett MJ (2006) Photopatterned liquid crystalline polymers for microactuators. Journal of Materials Chemistry 16 (28):2903-2912.

237. Yang H, Ye G, Wang X, Keller P (2011) Micron-sized liquid crystalline elastomer actuators. Soft Matter 7 (3):815-823.

238. Li MH, Keller P, Li B, Wang X, Brunet M (2003) Light-Driven Side-On Nematic Elastomer Actuators. Advanced Materials 15 (7-8):569-572.

239. Finkelmann H, Nishikawa E, Pereira GG, Warner M (2001) A New Opto-Mechanical Effect in Solids. Physical Review Letters 87 (1):015501.

240. Hogan PM, Tajbakhsh AR, Terentjev EM (2002) uv manipulation of order and macroscopic shape in nematic elastomers. Physical Review E 65 (4):041720.

241. Cviklinski J, Tajbakhsh AR, Terentjev EM (2002) UV isomerisation in nematic elastomers as a route to photo-mechanical transducer. European Physical Journal E 9 (5):427-434.

242. Yu Y, Nakano M, Ikeda T (2004) Photoinduced bending and unbending behavior of liquid-crystalline gels and elastomers. Pure and Applied Chemistry 76 (7-8):1467-1477.

243. Nakano H (2010) Direction control of photomechanical bending of a photochromic molecular fiber. Journal of Materials Chemistry 20 (11):2071-2074.

244. Yoshino T, Kondo M, Mamiya J, Kinoshita M, Yu YL, Ikeda T (2010) Three-Dimensional Photomobility of Crosslinked Azobenzene Liquid-Crystalline Polymer Fibers. Advanced Materials 22 (12):1361-1363.

245. Kondo M, Yu Y, Ikeda T (2006) How Does the Initial Alignment of Mesogens Affect the Photoinduced Bending Behavior of Liquid-Crystalline Elastomers? Angewandte Chemie International Edition 45 (9):1378-1382.

246. Tabiryan N, Serak S, Dai XM, Bunning T (2005) Polymer film with optically controlled form and actuation. Optics Express 13 (19):7442-7448.

247. Van Oosten CL, Corbett D, Davies D, Warner M, Bastiaansen CWM, Broer DJ (2008) Bending dynamics and directionality reversal in liquid crystal network photoactuators. Macromolecules 41 (22):8592-8596.

248. Priimagi A, Shimamura A, Kondo M, Hiraoka T, Kubo S, Mamiya J, Kinoshita M, Ikeda T, Shishido A Location of the Azobenzene Moieties within the Cross-Linked Liquid-Crystalline Polymers Can Dictate the Direction of Photoinduced Bending. ACS Macro Letters. DOI: 10.1021/mz20056w.

249. Harris KD, Cuypers R, Scheibe P, van Oosten CL, Bastiaansen CWM, Lub J, Broer DJ (2005) Large amplitude light-induced motion in high elastic modulus polymer actuators. Journal of Materials Chemistry 15 (47):5043-5048.

250. Kondo M, Sugimoto M, Yamada M, Naka Y, Mamiya JI, Kinoshita M, Shishido A, Yu Y, Ikeda T (2010) Effect of concentration of photoactive chromophores on photomechanical properties of crosslinked azobenzene liquid-crystalline polymers. Journal of Materials Chemistry 20 (1):117-122.

251. Lee KM, Koerner H, Vaia RA, Bunning TJ, White TJ (2010) Relationship between the Photomechanical Response and the Thermomechanical Properties of Azobenzene Liquid Crystalline Polymer Networks. Macromolecules 43 (19):8185-8190.

252. Shimamura A, Priimagi A, Mamiya J-i, Ikeda T, Yu Y, Barrett CJ, Shishido A (2011) Simultaneous Analysis of Optical and Mechanical Properties of Cross-Linked Azobenzene-Containing Liquid-Crystalline Polymer Films. ACS Applied Materials & Interfaces. DOI: 10.1021/am200621j.

253. Bar-Cohen Y (2004) Electroactive polymer (EAP) actuators as artificial muscles: reality, potential, and challenges.

254. Mirfakhrai T, Madden JDW, Baughman RH (2007) Polymer artificial muscles. Materials Today 10 (4):30-38.

255. Yamada M, Kondo M, Miyasato R, Naka Y, Mamiya JI, Kinoshita M, Shishido A, Yu Y, Barrett CJ, Ikeda T (2009) Photomobile polymer materials - Various three-dimensional movements. Journal of Materials Chemistry 19 (1):60-62.

256. Naka Y, Mamiya J-i, Shishido A, Washio M, Ikeda T (2011) Direct fabrication of photomobile polymer materials with an adhesive-free bilayer structure by electron-beam irradiation. Journal of Materials Chemistry 21 (6):1681-1683.

257. Yin RY, Xu WX, Kondo M, Yen CC, Mamiya J, Ikeda T, Yu YL (2009) Can sunlight drive the photoinduced bending of polymer films? Journal of Materials Chemistry 19 (20):3141-3143.

258. Cheng F, Yin R, Zhang Y, Yen CC, Yu Y (2010) Fully plastic microrobots which manipulate objects using only visible light. Soft Matter 6 (15):3447-3449.

259. Cheng F, Zhang Y, Yin R, Yu Y (2010) Visible light induced bending and unbending behavior of crosslinked liquid-crystalline polymer films containing azotolane moieties. Journal of Materials Chemistry 20 (23):4888-4896.
260. Lee KM, Koerner H, Vaia RA, Bunning TJ, White TJ (2011) Light-activated shape memory of glassy, azobenzene liquid crystalline polymer networks. Soft Matter 7 (9):4318-4324.
261. Wu W, Yao L, Yang T, Yin R, Li F, Yu Y (2011) NIR-light-induced deformation of cross-linked liquid-crystal polymers using upconversion nanophosphors. Journal of the American Chemical Society 133 (40):15810-15813.
262. Chen M, Xing X, Liu Z, Zhu Y, Liu H, Yu Y, Cheng F (2010) Photodeformable polymer material: Towards light-driven micropump applications. Applied Physics A: Materials Science and Processing 100 (1):39-43.
263. Liu H, Zhu Y, Liu Z, Chen M (2010) Research of photo-induced bending thin film microactuators. Yadian Yu Shengguang/Piezoelectrics and Acoustooptics 32 (3):417-419.
264. van Oosten CL, Bastiaansen CWM, Broer DJ (2009) Printed artificial cilia from liquid-crystal network actuators modularly driven by light. Nature Materials 8 (8):677-682.
265. Palffy-Muhoray P (2009) Liquid crystals: Printed actuators in a flap. Nature Materials 8 (8):614-615.
266. Toda F (2002) Organic solid state reactions.
267. Tanaka K, Toda F (2000) Solvent-Free Organic Synthesis. Chemical Reviews 100 (3):1025-1074.
268. Kaupp G (1992) Photodimerization of Cinnamic Acid in the Solid State: New Insights on Application of Atomic Force Microscopy. Angewandte Chemie International Edition 31 (5):592-595.
269. Kaupp G (1992) Photodimerization of Anthracenes in the Solid State: New Results from Atomic Force Microscopy. Angewandte Chemie International Edition 31 (5):595-598.

270. Irie M, Kobatake S, Horichi M (2001) Reversible Surface Morphology Changes of a Photochromic Diarylethene Single Crystal by Photoirradiation. Science 291 (5509):1769-1772.

271. Koshima H, Ide Y, Ojima N (2008) Surface Morphology Changes of a Salt Crystal of 4-(2,5-Diisopropylbenzoyl)benzoic Acid with (S)-Phenylethylamine via Single-Crystal-to-Single-Crystal Photocyclization. Crystal Growth & Design 8 (7):2058-2060.

272. Kobatake S, Takami S, Muto H, Ishikawa T, Irie M (2007) Rapid and reversible shape changes of molecular crystals on photoirradiation. Nature 446 (7137):778-781.

273. Morimoto M, Irie M (2010) A diarylethene cocrystal that converts light into mechanical work. Journal of the American Chemical Society 132 (40):14172-14178.

274. Nakayama K, Jiang L, Iyoda T, Hashimoto K, Fujishima A (1997) Photo-Induced Structural Transformation on the Surface of Azobenzene Crystals. Japanese Journal of Applied Physics 36:3898-3902.

275. Ichimura K (2009) Reversible photoisomerisability and particle size changes of mill-dispersed azobenzene crystals in water. Chemical Communications (12):1496-1498.

276. Ichimura K (2010) Photoisomerisation behaviour of azobenzene crystals hybridised with silica nanoparticles by dry grinding. Chemical Communications 46 (19):3295-3297.

277. Nakano H, Tanino T, Shirota Y (2005) Surface relief grating formation on a single crystal of 4-(dimethylamino)azobenzene. Applied Physics Letters 87 (6):061910.

278. Nakano H (2008) Photoinduced surface relief grating formation on a (100) surface of a single crystal of 4-(dimethylamino)azobenzene. Journal of Physical Chemistry C 112 (41):16042-16045.

279. Nakano H (2010) Photoinduced surface relief grating formation for a single crystal of 4-aminoazobenzene. International Journal of Molecular Sciences 11 (4):1311-1320.

280. Nakano H, Seki S, Kageyama H (2010) Photoinduced vitrification near the surfaces of single crystals of azobenzene-based molecular materials with glass-forming ability. Physical Chemistry Chemical Physics 12 (28):7772-7774.

281. Koshima H, Ojima N, Uchimoto H (2009) Mechanical motion of azobenzene crystals upon photoirradiation. Journal of the American Chemical Society 131 (20):6890-6891.

282. Milam K, O'Malley G, Kim N, Golovaty D, Kyu T (2010) Swimming Photochromic Azobenzene Single Crystals in Triacrylate Solution. Journal of Physical Chemistry B 114 (23):7791-7796.

Chapter 2: Measuring the Photomechanical Effect in Thin Polymer Films of Azobenzene Using a Cantilever Based Sensor

As a first step to understanding the photomechanical effect exhibited by azobenzene polymers it is necessary to be able to take some fundamental measurements of the various azobenzene based systems and make direct comparisons between them. Numerous photomechanical systems have been presented in the literature, many with different chemical structures surrounding the core azobenzene group. Quantitative comparison of these systems as well as rational design and optimization of their performance can then supplant experimental trial and error. Thus, it is important to discover chemical design parameters common to all azobenzene based systems. This chapter seeks to provide a basis from which such common design parameters can be established. A cantilever based sensor system is used to make some basic measurements of multiple azobenzene based polymeric systems to understand how properties are affected by structure.

2.1 Abstract

The efficiency of the photomechanical effect in thin films of three azobenzene based polymers PDR1A, PDR13A and PMMA-co-PDR1A was determined using a cantilever based sensor. The polymers were coated on cantilevers of both silicon and mica, and under irradiation with visible light the resulting cantilever bending was measured to provide estimates of change in surface stress, photomechanical energy transduction per unit volume, and thus resulting photomechanical efficiency. This photomechanical effect was shown to be robust, repeatable, and measurable for all the polymers studied, even when the thickness of the driving layer was small compared to the thickness of the cantilever; PDR1A exerted the largest forces and PMMA-co-PDR1A the greatest efficiency. With 30 μm thick mica cantilevers coated with PDR1A, the photo-isomerization results in fast and significant cantilever bending ranging from 50-313 μm, changes in surface stresses ranging from 96 to 568 N/m and an efficiency of 0.0011%.

This demonstrates the ability of these thin polymer layers to act as strong light-driven 'artificial muscles' for larger mechanical systems, and demonstrates the utility of the cantilever sensor platform to quantitative characterization of the photomechanical effect of azobenzene based polymers.

2.2 Introduction

As a result of reversible photoisomerization from the thermally stable *trans* (E) to meta stable *cis* (Z) states (Fig. 2.1a), azobenzene molecules are capable of inducing powerful changes to a variety of properties in its host material [1-9]. Composed of two phenyl rings connected by an azo (-N=N-) linkage, azobenzene is an aromatic chromophore capable of facile modification with a variety of molecular architectures. Tuning the physical and chemical amplification of the geometric shape change can reversibly alter various material properties such as switchable phase changes [1], phase separation [2] (or reversal of phase separation [3]), solubility changes [4, 5], as well as applications in surface patterning and photonics [6-9].

The photon adsorption and subsequent isomerization by azobenzene chromophores can also result in a significant macroscopic mechanical deformation of the host material defined as the photomechanical effect. This effect was first proposed by Merian in 1966 [10] when he observed that a nylon filament fabric dyed with an azobenzene derivative shrank upon photo-irradiation. This effect was postulated to involve the photochemical structural change of the azobenzene group absorbed on the nylon fibers, yet the structural complexity and small observed shrinkage (0.1 %) made it difficult to draw firm conclusions as to the true mechanism. Following this interesting observation, however, much effort was made to find new photomechanical systems with an enhanced efficiency [11, 12]. Most recently, the photoinduced expansion of thin films of acrylate polymers containing azobenzene chromophores was tracked directly in real time by our group, using a variety of techniques including *in situ* single wavelength ellipsometry, Atomic Force Microscopy (AFM), and *in situ* Neutron Reflectometry [9, 13-17]. An initial expansion of the azobenzene polymer films was found to be irreversible with an extent of relative expansion observed of 1.5–4 % in films of thickness ranging from 25 to 140 nm, and then a subsequent and reversible expansion was observed with repeated irradiation cycles, achieving a relative extent of expansion of 0.6–1.6 %.

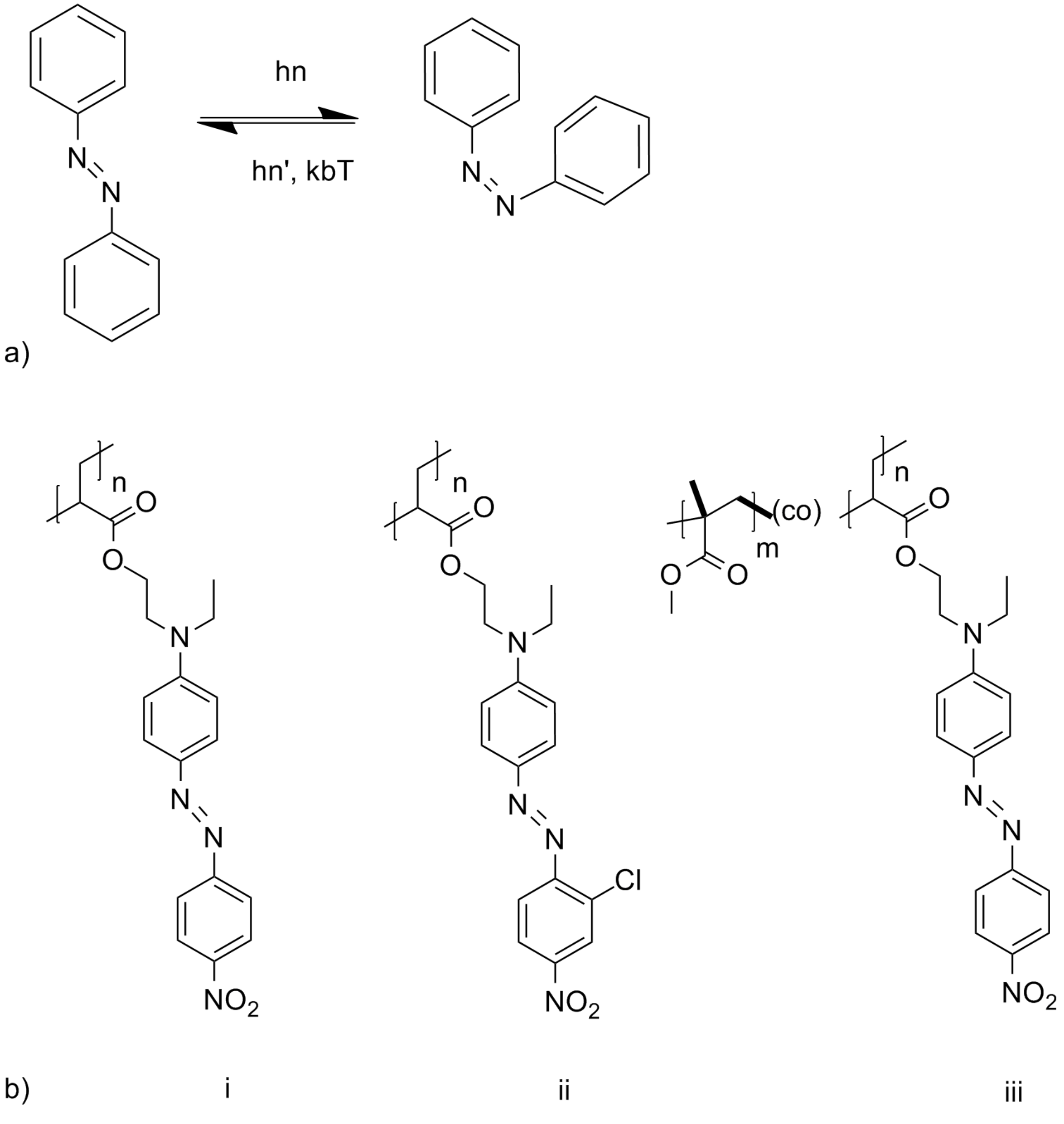

Figure 2.1: a) The *trans-cis* isomerization of azobenzene, b) the polymers (i) Poly Disperse Red 1 Acrylate (PDR1A), (ii) Poly Disperse Red 13 Acrylate (PDR13A) and (iii) Poly Methyl Methacrylate –co-Poly Disperse Red 1 Acrylate (PMMA-co-PDR1A).

Azobenzene polymers thus have promising applications as photo-actuators by virtue of their ability to control expansion and contraction with light through the photomechanical effect. This effect has been optimized for self-assembled monolayers, and has been used for example to induce bending of a coated microcantilever [19]. In related experiments, it has been shown that azo-colloids can also be permanently photo-deformed into ellipsoids [20, 21]. This photomechanical deformation can be used to create a novel class of photo-functional materials with promising applications in light-driven robotics as reported by Ikeda, Barrett and coworkers [13, 22-29], as well as others [30-35]. Many of these applications in robotics are based upon freestanding films of azobenzene based materials and films on flexible substrates, capable of macroscopic motions such as bending, rolling and walking [28]. These films have also been engineered to form plastic motors [26], robotic arms [33], and other devices powered by light [29-32, 34]. Despite the tremendous progress and numerous applications of azobenzene based materials there has been very little attention devoted to characterization of the photo-mechanical forces and efficiency of the photo-mechanical materials behind these applications. There is also a desire to explore the extent to which the azo polymers can function as driving layers in small amounts, transducing the light energy to much larger inert levers, thus functioning as high-efficiency light-driven ‘artificial muscles’.

Herein we seek to address the need and method to evaluate the force generation and efficiency of a series of photo-mechanical azo materials as well as demonstrate a new versatile technique for the future characterization of the photomechanical effects of new photo-functional materials. For the first time, we use a well characterized flexible substrate to recover full mechanical characterization of the photomechanical layers driving the motion as measured by adapting a microcantilever-based sensor system, and demonstrate the utility of these thin azo layers to drive actuation of support structures many times thicker.

2.3 Experimental

2.3.1 Materials

Poly-Disperse Red 1 acrylate (PDR1A) as shown in Fig. 2.1b was synthesized according to previously published methodology [17] with 10 % wt. AIBN (Aldrich) and polymerization at 62 °C for 4 days (Mw 3K). The synthesized polymer was used only for coating the silicon cantilevers. The polymers poly-Disperse Red 1 acrylate (PDR1A) and Poly Methyl Methacrylate–co-Poly Disperse Red 1 Acrylate (PMMA-co-PDR1A) and Poly-Disperse Red 13 acrylate (PDR13A) were purchased from Aldrich.

2.3.2 Coatings

To coat the silicon cantilevers (MikroMasch CSC12/tipless/no Al), PDR1A was dissolved in a minimum amount of tetrahydrofuran (THF) or methylelene chloride and painted using solvent resistant paintbrush bristles onto the cantilevers. The cantilevers were then left to air dry for at least two hours before use. To make the mica cantilevers, mica sheets (25 mm x 50 mm x 0.15 mm, SPI, V1 grade) were first cleaved to a thickness of approx. 30 μm using GEM® Scientific Blades. The sheets were then cleaned by cleaving layers off the top using adhesive tape. Films of PDR1A, PDR13A or PDR1MA were then spin-cast at 4000 rpm for 90 seconds with their respective polymer concentration 10 mg/ml in tetrahydrofuran (THF). The films were annealed under vacuum for 8 h at 90 °C. Finally cantilevers of dimensions in the order of 6 mm x 2 mm x 30 μm were cut from the sheets. The cantilever coating thickness was then estimated by taking a UV-Vis absorbance of the sample and dividing by the absorbance coefficient of the polymer thin film assuming a beer-lambert absorption profile.

2.3.3 Bending

The silicon cantilever deflection was measured using the micromechanical cantilever sensor system characterized and published previously [36-40]. Cantilever deflection was induced with a diode pumped solid state 532 nm green pump laser (B&W tek, single mode comet 532 nm) at 100 mW/cm^2. Mica cantilever deflection was measured using a micromechanical cantilever sensor system similar to the previously described silicon sensor system. The system was modified to support the larger mica cantilevers and did not support a reference cantilever. In addition, the differential microcantilever-based sensor was operated in static mode with microcantilever defections measured using an optical beam, where a HeNe laser (JDSUniphase Model 1136P) operating at 633 nm was used as the probe beam while a mixed-gas Kr-Ar (Melles Griot Omnichrome series 43) at 514 nm was used as the pump beam. The probe beam was focused onto the cantilever using commercial focusing lens (Melles Griot). The position sensitive detector (PSD) (model 1L10, ON-TRAK Photonics, USA) was located 6.7 cm away from the cantilever. The pump beam was expanded using a 10X beam expander and focusing lens to achieve a 0.4 cm diameter. The photocurrents generated at the PSD terminals by the impinging light spot are converted into voltages by home-built precision transimpedance differential amplifiers. The output voltage, V_{pos}, is directly proportional to the absolute position of the light spot on the PSD, $S = V_{pos}/2$. A 16-bit analog-to-digital converter from National Instruments, card model # SCB 68, digitizes the signal which is finally stored on a computer with a LabView program. The cantilevers are depicted in Fig. 2.2 and the system is schematically depicted in Fig. 2.3.

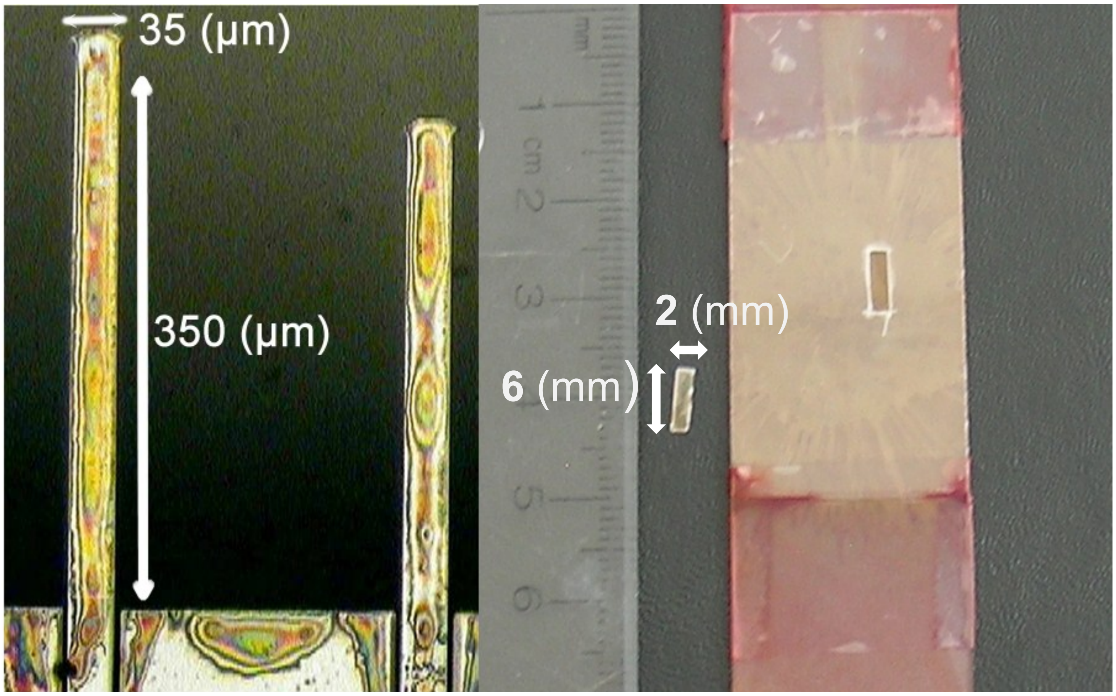

Figure 2.2: Photographs of the silicon (left) and mica (right) cantilevers and their dimensions.

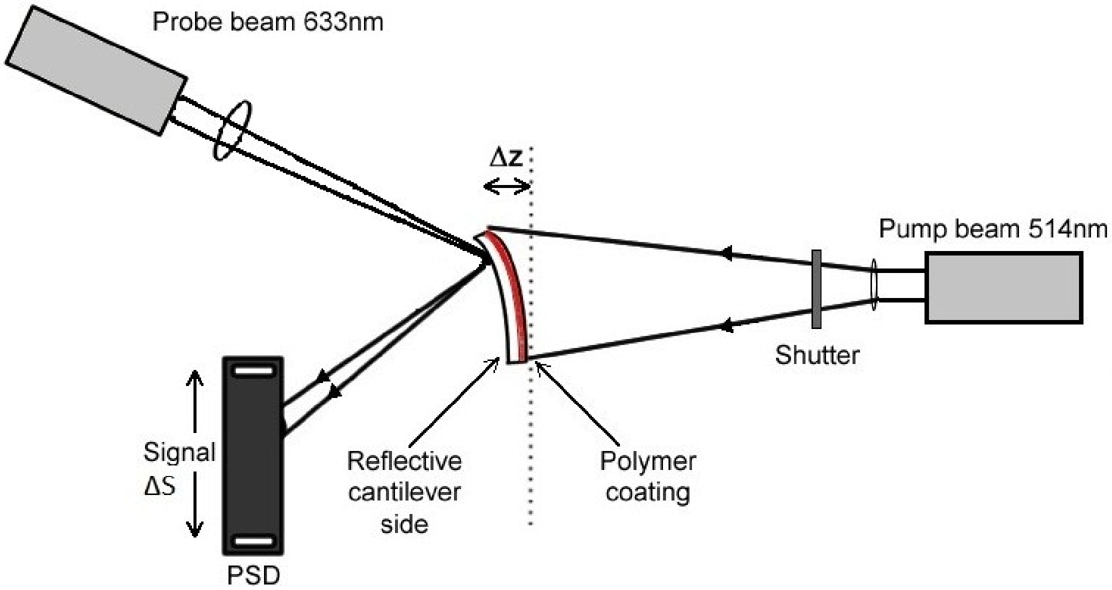

Figure 2.3: Schematic view of the cantilever bending in the sensor system. The polymer coating expands upon irradiation by the pump beam exerting a compressive surface stress upon the cantilever.

2.4 Results and Discussion

A microcantilever-based sensor, operated in a static mode can be used to transduce the photo-isomerization of the azobenzene coating into a measurable mechanical movement (bending of the free end of the cantilever). From the measured movement and induced surface stress the photo-mechanical force and efficiency of azobenzene polymer coatings can then be calculated. As the deflection of the microcantilever (Δz) for small deflections is linearly proportional to the acquired signal it can be calculated through the relationship

$$\Delta z = C_{cal}\Delta S \tag{2.1}$$

Where the calibration constant C_{cal} has been characterized as $C_{cal} = (3.42 \pm 0.07)\times10^{-6}$ m/V for the silicon cantilevers and detector system [40]. It can also be determined geometrically (equation (2.2)) as was done for the mica cantilevers [40],

$$(\Delta z) \cong \frac{l_{eff}}{2L}\Delta S \tag{2.2}$$

Where l_{eff} is the effective length of the microcantilever and L the distance between the microcantilever and the position sensitive detector. The effective length of the microcantilever is defined as the length at which the laser beam hits the microcantilever [40]. The change in surface stress ($\Delta\sigma$) which is in turn directly proportional to the microcantilever deflection (Δz) can then be calculated using the following relationship [40]:

$$(\Delta\sigma) = \frac{4}{3(1-\upsilon)}\frac{l}{wt}k\frac{l_{eff}}{4L}\Delta S\left(\frac{l}{l_{eff}}\right)^2 \tag{2.3}$$

Where υ represents the Poisson's ratio (0.06418 for the silicon cantilevers) [40]. *l, w, t, k*, represent the length, width, thickness, and spring constant of the microcantilever; and l_{eff} and L, the effective length and the distance between the microcantilever and PSD, respectively. The 4/3 factor accounts for the difference in cantilever beam curvature resulting from a uniform surface stress, as opposed to a concentrated load applied at the tip.

For the silicon cantilevers an example of the deflection and corresponding change in surface stress is presented below in Fig. 2.4 as a plot of deflection & photomechanical stress against time. These initial samples were irradiated at a high beam power (≈ 100 mW/cm^2) for varying lengths of time. The initial photo-response (cantilever deformation and photoisomerization) was observed to occur within a few seconds of pump beam exposure, can be maintained with the presence of the pump beam for a significant amount of time (> 200 s,), and is repeatable over many cycles.

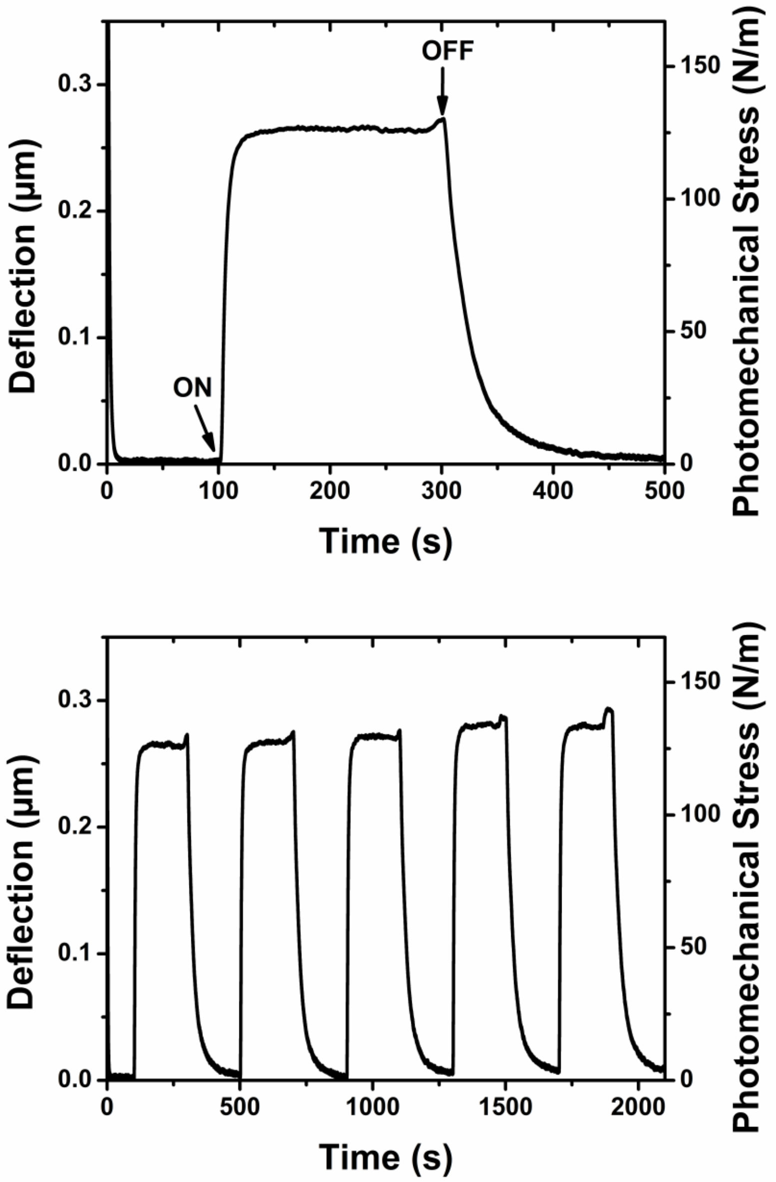

Figure 2.4: Top: Deflection (μm) and Photomechanical stress (N/m) plots of a silicon cantilever coated with PDR1A where the positive deflection is defined as a compressive stress exerted by the coating causing cantilever bending towards the probe beam (Fig. 2.3). Sample is irradiated for 200 s then allowed to relax for 200 s. Bottom: Repeat pump and relaxation cycles of sample.

Over multiple samples photomechanical deformation of the cantilevers was observed to vary significantly with deformations ranging from 0.2 μm to 0.8 μm (corresponding to surface stress changes of 110 N/m to 340 N/m). In addition to the deflections and surface stress changes, the relaxation profiles showed some variation between samples of polymer dissolved in different solvents (THF vs. Methylene chloride). Many of these variations were primarily attributable to the coating technique. The painting of a single side of the cantilevers was unable to produce consistently thick, uniform, and completely dry (solvent free) films of similar polymer content. Thus variables such as concentration, thickness, solvent content as well as film processing could not be replicated to a high degree using the silicon cantilevers. The bending with silicon however, demonstrated the ability of obtaining large deflections and using the sensor system to measure the photomechanical response of PDR1A. Challenges with uniform and reproducible cantilever coating were overcome by making larger mica cantilevers, upon which the polymer films would be amenable to various coating techniques especially spin casting, allowing a better control of the properties of the polymer coating.

The deflection and surface stress change of the cantilever were estimated using equations 2 and 3 respectively. The spring constant of the mica cantilevers was estimated using (Eq. 2.4)

$$(k) \cong \frac{wt^3E}{4Lo^3} \tag{2.4}$$

where *w, t, E, Lo* are the width, thickness, Young's Modulus, and length of the cantilever, and the Poisson's ratio of the cantilever taken as 0.44 [41]. Using the mica cantilevers and reproducible spin cast polymer coatings a more consistent photomechanical response was observed across multiple cantilever samples. Thus, we investigated three variables that may affect the extent of the photomechanical effect in azobenzene polymers, namely, the power of the pump beam, chemical modifications of the polymer main chain or chromophore, and the presence of solvent upon the photomechanical response and demonstrate the general applicability of the measurement system for various azobenzene based materials and conditions. The cantilevers of mica were coated with the polymers PDR1A, PDR13A and PMMA-co-PDR1A. In addition, to test the effect of solvent presence, a cantilever coated with PDR1A was not oven-dried after spin casting but the "wet" sample was immediately tested.

Due to the manual cutting of the mica, there were small variations in the dimensions of the cantilevers (and thus spring constant). Therefore, the results cannot be easily compared using the deflection of the cantilevers but by comparing changes in surface stress which accounts for the variations in the physical dimensions and spring constant of the cantilevers.

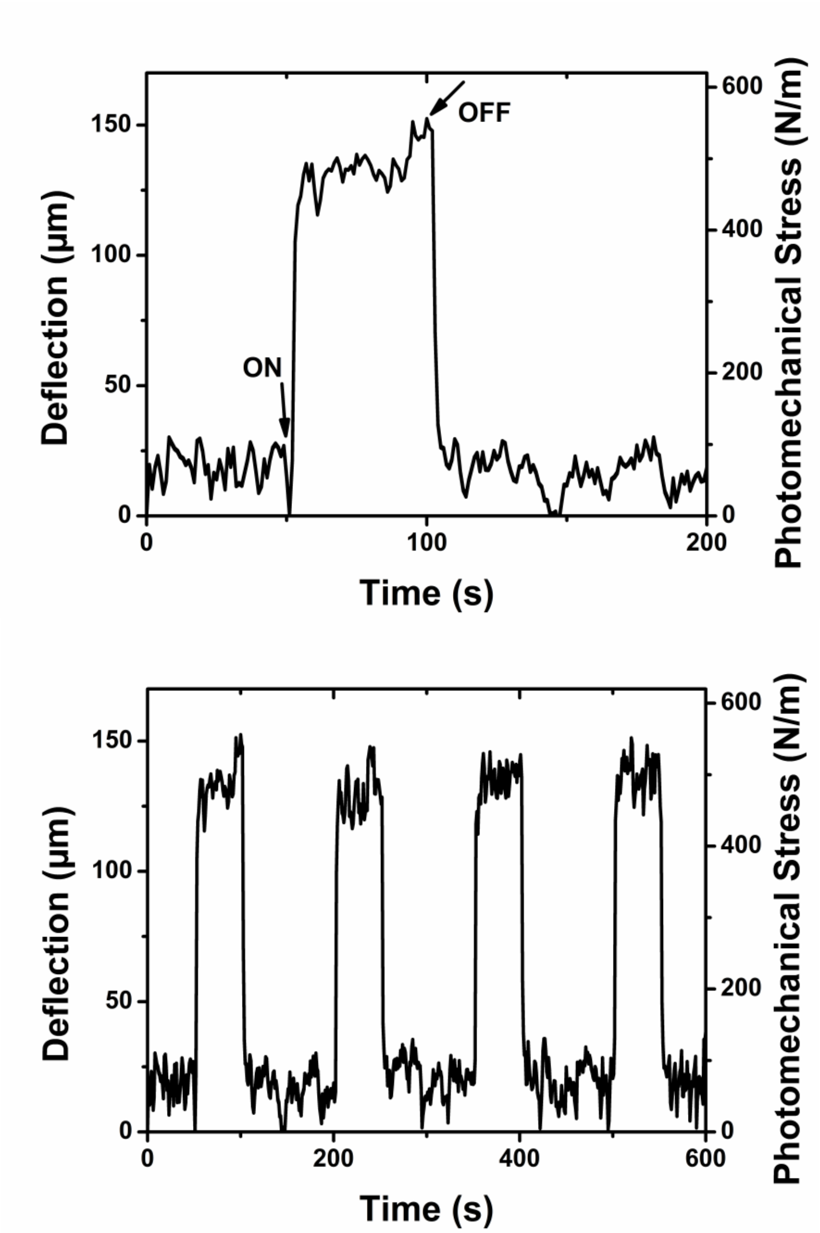

Figure 2.5: Top: Deflection (µm) and photomechanical stress (N/m) plots of a mica cantilever coated with PDR1A and irradiated at 80 mW/cm^2. Sample is irradiated for 50 s then allowed to relax for 100 s. Bottom: Repeat pump and relaxation cycles of sample.

A sample output of the mica cantilever is presented in Fig. 2.5 and a compilation of the change in surface stress at pump beam irradiation of all the above samples is presented in Fig. 2.6 as a plot of the changes in surface stress to pump beam power. The pump beam power was limited to a maximum of 100 mW/cm^2 to avoid thermal effects on the cantilever, photo-damage, and dye photo-bleaching.

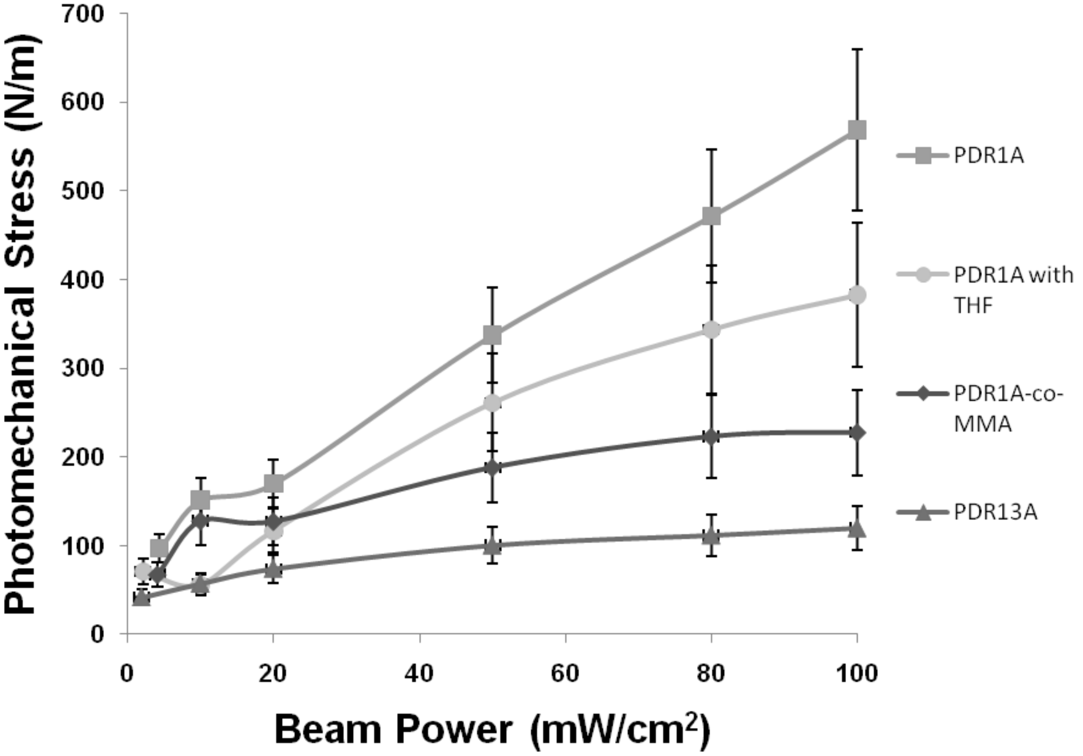

Figure 2.6: Surface stress changes of mica cantilevers coated with PDR1A, PDR1A with solvent, PDR13A, and PMMA-co-PDR1A to increasing pump beam power.

Finally the photomechanical efficiency of the samples was determined. The energy input was based upon the absorbed light of the sample at a beam power of 100 mW/cm^2 and the time taken to achieve equilibrium (maximum stable response). An absorption coefficient of 4.3 µm^{-1} at 514 nm [14] was used. The output photomechanical energy is determined using equation 2.5 [37] that describes the energy (E_k) stored in a uniformly stressed cantilever due to a chemical reaction can be determined by

$$\left(E_k\right) = \frac{4}{3(1-\upsilon)} k \frac{1}{2} \Delta z^2 \tag{2.5}$$

Where υ represents the Poisson's ratio (0.44) [41], k the spring constant and Δz the cantilever deflection [37].

In addition the film volume and thus photomechanical energy produced per cubic millimetre of film coating was also calculated by assuming that light absorption and photo-isomerization occurred throughout the 100 nm thick film coating. This assumption is based upon the materials possessing a Beer-Lambert absorption profile and the samples absorption coefficient. The results of the above calculations are tabulated in Table 2.1.

Polymer	**Energy Absorbed (mJ)**	**Photo-mechanical energy (nJ)**	**Film volume (mm^3) $*10^{-3}$**	**Efficiency (%)**	**Photo-mechanical energy per unit volume (nJ/mm^3)**
PDR1A	273	1247	1.63	0.0011	766
PDR13A	25	59	1.27	0.0005	46
PMMA-co-PDR1A	34	251	1.13	0.0017	223
PDR1A with THF	142	847	1.32	0.0014	640

Table 2.1: Summary of the photomechanical energy, efficiency and energy exerted per unit volume of film calculated from the photomechanical response of mica coated cantilevers at a beam power of 100 mW/cm^2.

The resulting data (Fig. 2.6) showed an increasing photomechanical response with beam power as has been elsewhere observed due to a greater *trans-cis* conversion of the azobenzene polymers. We also observed significant cantilever bending (up to hundreds of μm) and large surface stress exerted by the polymer coating upon the cantilever by the various film coatings. PDR1A measured the highest response followed by the solvent containing sample, the co-polymer and PDR13A in both the photomechanical energy and energy per unit volume. The presence of solvent within the coating, chemical modification of the chromophore and polymer main chain all reduce the surface stress exerted by the polymer with the lowest response due to chemical modification of the azobenzene chromophore. In addition, the surface stress changes observed by the silicon cantilevers are similar to those seen exerted on the mica cantilevers.

In the case of the solvent (THF) containing sample, the reduction in surface stress is likely due to the solvent occupying volume within the film that can be easily rearranged to accommodate the internal change of volume associated with the *trans-cis* isomerization of the chromophore, reducing the stress exerted by the film on the cantilever. The process is however, slightly more efficient as borne out by a higher calculated efficiency of the wet samples over the dry ones. In the case of main chain modification, as anticipated, coatings of PMMA-co-PDR1A did not enhance the photomechanical response, as the copolymer contains only 15 mol % chromophore and has less azobenzene compared to PDR1A but possesses a greater efficiency than PDR1A. The chemical modification of the azobenzene chromophore (PDR13A) had the largest impact on the reduction of the photomechanical effect compared with previous changes. This was expected in that this modification directly affects the isomerization of the chromophore. Further work would be needed to understand and relate the impact of chemical modification on the photomechanical effect as it has the greatest impact on both the efficiency and photomechanical energy of the material.

2.5 Conclusions

In conclusion, we have demonstrated that the photomechanical effect of azobenzene based polymer coatings is large and measurable. In addition the photomechanical stress and efficiency of the system can be characterized using this cantilever based sensor system. We have shown that this sensor can be used to understand and characterize the various factors influencing the photomechanical effect, as this knowledge is crucial to the optimization and development of applications exploiting the photomechanical effect of azobenzene polymers.

2.6 References

1. Aoki Ki, Nakagawa M, Ichimura K (2000) Self-Assembly of Amphoteric Azopyridine Carboxylic Acids: Organized Structures and Macroscopic Organized Morphology Influenced by Heat, pH Change, and Light. Journal of the American Chemical Society 122 (44):10997-11004.
2. Kadota S, Aoki K, Nagano S, Seki T (2005) Photocontrolled Microphase Separation of Block Copolymers in Two Dimensions. Journal of the American Chemical Society 127 (23):8266-8267.
3. Effing JJ, Kwak JCT (1995) Photoswitchable Phase Separation in Hydrophobically Modified Poly(acrylamide)/Surfactant Systems. Angewandte Chemie International Edition in English 34 (1):88-90.
4. Yamamoto H, Nishida A, Takimoto T, Nagai A (1990) Photoresponsive peptide and polypeptide systems. VIII. Synthesis and reversible photochromism of azo aromatic poly(L-ornithine). Journal of Polymer Science Part A: Polymer Chemistry 28 (1):67-74.
5. Arai K, Kawabata Y (1995) Changes in the sol-gel transformation behavior of azobenzene moiety-containing methylcellulose irradiated with UV light. Macromolecular Rapid Communications 16 (12):875-880.
6. Yager KG, Barrett CJ (2001) All-optical patterning of azo polymer films. Current Opinion in Solid State and Materials Science 5 (6):487-494.
7. Yager KG, Barrett CJ (2008) Amorphous Azobenzene Polymers for Light-Induced Surface Patterning. Smart Light-Responsive Materials. John Wiley & Sons, Inc.
8. Yager KG, Barrett CJ (2008) Azobenzene Polymers for Photonic Applications. Smart Light-Responsive Materials. John Wiley & Sons, Inc.
9. Yager KG, Barrett CJ (2006) Photomechanical surface patterning in azo-polymer materials. Macromolecules 39 (26):9320-9326.
10. Merian E (1966) Steric Factors Influencing the Dyeing of Hydrophobic. Fibers. Textile Research Journal 36 (7):612-618.
11. Irie M (1990) Photoresponsive polymers. In: New Polymer Materials, vol 94. Advances in Polymer Science. Springer Berlin / Heidelberg, pp 27-67.

12. Smets G, Blauwe FD (1974) Chemical reactions in solid polymeric systems. Photomechanical phenomena. Pure Appl Chem 39:225-238.
13. Barrett CJ, Mamiya JI, Yager KG, Ikeda T (2007) Photo-mechanical effects in azobenzene-containing soft materials. Soft Matter 3 (10):1249-1261.
14. Tanchak OM, Barrett CJ (2005) Light-induced reversible volume changes in thin films of azo polymers: The photomechanical effect. Macromolecules 38 (25):10566-10570.
15. Yager KG, Barrett CJ (2006) Novel photo-switching using azobenzene functional materials. Journal of Photochemistry and Photobiology A: Chemistry 182 (3):250-261.
16. Yager KG, Tanchak OM, Barrett CJ, Watson MJ, Fritzsche H (2006) Temperature-controlled neutron reflectometry sample cell suitable for study of photoactive thin films. Review of Scientific Instruments 77 (4).
17. Yager KG, Tanchak OM, Godbout C, Fritzsche H, Barrett CJ (2006) Photomechanical effects in azo-polymers studied by neutron reflectometry. Macromolecules 39 (26):9311-9319.
18. Tabiryan N, Serak S, Dai XM, Bunning T (2005) Polymer film with optically controlled form and actuation. Optics Express 13 (19):7442-7448.
19. Ji HF, Feng Y, Xu X, Purushotham V, Thundat T, Brown GM (2004) Photon-driven nanomechanical cyclic motion. Chemical Communications 10 (22):2532-2533.
20. Li Y, He Y, Tong X, Wang X (2005) Photoinduced deformation of amphiphilic azo polymer colloidal spheres. Journal of the American Chemical Society 127 (8):2402-2403.
21. Li Y, He Y, Tong X, Wang X (2006) Stretching effect of linearly polarized Ar+ laser single-beam on azo polymer colloidal spheres. Langmuir 22 (5):2288-2291.
22. Yu Y, Nakano M, Ikeda T (2003) Directed bending of a polymer film by light. Nature 425 (6954):145.
23. Kondo M, Miyasato R, Naka Y, Mamiya J, Kinoshita M, Yu Y, Barrett CJ, Ikeda T (2009) Photomechanical properties of azobenzene liquid-crystalline elastomers. Liquid Crystals 36 (10-11):1289-1293.

24. Kondo M, Sugimoto M, Yamada M, Naka Y, Mamiya JI, Kinoshita M, Shishido A, Yu Y, Ikeda T (2010) Effect of concentration of photoactive chromophores on photomechanical properties of crosslinked azobenzene liquid-crystalline polymers. Journal of Materials Chemistry 20 (1):117-122.
25. Naka Y, Mamiya JI, Shishido A, Washio M, Ikeda T (2011) Direct fabrication of photomobile polymer materials with an adhesive-free bilayer structure by electron-beam irradiation. Journal of Materials Chemistry 21 (6):1681-1683.
26. Yamada M, Kondo M, Mamiya JI, Yu Y, Kinoshita M, Barrett CJ, Ikeda T (2008) Photomobile polymer materials: Towards light-driven plastic motors. Angewandte Chemie - International Edition 47 (27):4986-4988.
27. Yamada M, Kondo M, Miyasato R, Mamiya JI, Kinoshita M, Yu Y, Barrett CJ, Ikeda T (2009) Photoresponsive behavior of laminated films composed of a flexible plastic sheet and a crosslinked azobenzene liquid-crystalline polymer layer with different initial alignment of mesogens. Molecular Crystals and Liquid Crystals 498:65-73.
28. Yamada M, Kondo M, Miyasato R, Naka Y, Mamiya JI, Kinoshita M, Shishido A, Yu Y, Barrett CJ, Ikeda T (2009) Photomobile polymer materials - Various three-dimensional movements. Journal of Materials Chemistry 19 (1):60-62.
29. Yoshino T, Kondo M, Mamiya JI, Kinoshita M, Yu Y, Ikeda T (2010) Three-dimensional photomobility of crosslinked azobenzene liquid-crystalline polymer fibers. Advanced Materials 22 (12):1361-1363.
30. White TJ, Koval JJ, Tondiglia VP, Natarajan LV, Vaia RA, Serak S, Grozhik V, Tabirian N, Bunning TJ Polarization dependent photoactuation in azobenzene LC polymers. In, San Diego, CA, 2007. Liquid Crystals XI.
31. White TJ, Serak SV, Tabiryan NV, Vaia RA, Bunning TJ (2009) Polarization-controlled, photodriven bending in monodomain liquid crystal elastomer cantilevers. Journal of Materials Chemistry 19 (8):1080-1085.
32. White TJ, Tabiryan NV, Serak SV, Hrozhyk UA, Tondiglia VP, Koerner H, Vaia RA, Bunning TJ (2008) A high frequency photodriven polymer oscillator. Soft Matter 4 (9):1796-1798.

33. Cheng F, Yin R, Zhang Y, Yen CC, Yu Y (2010) Fully plastic microrobots which manipulate objects using only visible light. Soft Matter 6 (15):3447-3449.
34. Chen M, Huang H, Zhu Y, Liu Z, Xing X, Cheng F, Yu Y (2010) Photodeformable CLCP material: study on photo-activated microvalve applications. Applied Physics A: Materials Science and Processing:1-6.
35. Chen M, Xing X, Liu Z, Zhu Y, Liu H, Yu Y, Cheng F (2010) Photodeformable polymer material: Towards light-driven micropump applications. Applied Physics A: Materials Science and Processing 100 (1):39-43.
36. Beaulieu LY, Godin M, Laroche O, Tabard-Cossa V, Grütter P (2006) Calibrating laser beam deflection systems for use in atomic force microscopes and cantilever sensors. Applied Physics Letters 88 (8).
37. Godin M, Tabard-Cossa V, Grütter P, Williams P (2001) Quantitative surface stress measurements using a microcantilever. Applied Physics Letters 79 (4):551-553.
38. Beaulieu LY, Godin M, Laroche O, Tabard-Cossa V, Grütter P (2007) A complete analysis of the laser beam deflection systems used in cantilever-based systems. Ultramicroscopy 107 (4-5):422-430.
39. Godin M, Laroche O, Tabard-Cossa V, Beaulieu LY, Grütter P, Williams PJ (2003) Combined in situ micromechanical cantilever-based sensing and ellipsometry. Review of Scientific Instruments 74 (11):4902-4907.
40. Tabard-Cossa V, Godin M, Beaulieu LY, Grütter P (2005) A differential microcantilever-based system for measuring surface stress changes induced by electrochemical reactions. Sensors and Actuators, B: Chemical 107 (1 SPEC. ISS.):233-241.
41. Mugele F, Salmeron M (2000) Dynamics of layering transitions in confined liquids. Physical Review Letters 84 (25):5796-5799.

Chapter 3: Measuring Photo-Induced Softening of Azobenzene Systems by Nanoidentation

In the previous chapter, the photomechanical energy, efficiency, and surface stress changes of azobenzene polymers resulting from the photomechanical effect were measured through cantilever bending. The experiments measured the energy that thin films of these polymers are capable of exerting and allowed a comparison of multiple azobenzene polymers. Another well-known aspect of the photomechanical effect is micron scale surface mass transport, used for applications in photopatterning and nanofabrication. Despite numerous applications and studies, the exact mechanism underlying surface mass transport in azobenzene polymers is still not well understood. There have been suggestions in the literature that photosoftening and photo-induced viscosity changes play a large role in enabling this effect. Thus, nanoindentation experiments described in this chapter are conducted to investigate *in situ* changes to the mechanical properties of these polymers under irradiation.

3.1 Abstract

Nanoindentation studies on thin films of the widely-used azo polymer pDR1A demonstrate a significant light-induced softening upon visible-light irradiation. This photo-induced softening effect due to *trans-cis-trans* photoisomerization of the azobenzene units can be further enhanced via supramolecular functionalization of the azo dye to the backbone as compared to covalently-functionalized polymers. Specifically, the strain-rate sensitivities of such a hydrogen bonded complex, p4VP(DY7)$_{0.5}$, increases by more than 120 % upon 532 nm irradiation whereas the increase for pDR1A is 80 %. These results confirm a photo-softening contribution to the mechanisms of light-induced surface patterning of azo polymers and the photo-mechanical effect, and the finding that photo-softening is more significant in the supramolecular complex than in the covalently-functionalized polymer reveals the potential of noncovalent functionalization strategies in designing materials to optimize these efficient photomechanical responses and effects.

3.2 Introduction

Azobenzene-containing polymers have the unique ability to undergo micron-scale mass transport upon irradiation with non-uniform light field or interference pattern [1-3]. The origin of this fascinating photomechanical effect has been associated with rapid *trans-cis-trans* photoisomerization cycles of azobenzene upon irradiation, which can generate sufficient forces to, e.g., deform single crystals[4] or to give rise to surface patterns with modulation depths as large as twice the initial sample thickness[5,6]. Such single-step photoinduced surface patterns have application potential way beyond conventional diffractive optical elements[7,8], and in recent years azo-polymer surface patterns have been used in soft lithography and replica molding[9,10], photochemical imaging[11,12], and as a nanofabrication tool[13,14], to mention but a few potential directions. However, despite extensive research since the discovery of the phenomenon in 1995, complete understanding of the outlying mechanism has not yet been achieved. Understanding the relation between the mechanical properties of the materials, their changes upon light irradiation, and the surface deformation in different material systems is an important goal for rational design of photodeformable/photomechanical material systems with pre-tailored properties to meet the requirements of a specific application.

The efforts on understanding the SRG formation have focused either on explaining the nature of the driving force [15] or modelling the viscoelastic flow of the polymeric material during the formation of surface pattern [16], but none of the current models are able to combine the two to explain the whole process. Almost all the models describing the viscoelastic flow assume that the viscosity of the polymeric material is reduced from its bulk value close to the value of the molten polymer during the light illumination [16]. However, it has been shown that the temperature rise of the polymer due to light intensities typically used in the grating inscription is only in the range of few kelvins [17], and also that the SRG formation ceases when the glass transition temperature is approached [18]. These observations then suggest a photo-induced origin of the required viscosity decrease. Indeed, photoinduced changes in the mechanical properties (*e.g.* softening of the material) of azo-polymer thin films upon light irradiation have been studied via several experiments.

Among the first quantitative studies on the topic in 2000, Srikhirin and Nehrer reported that azobenzene-doped polymers tend to soften upon irradiation with visible light,[19] due to continuous *trans-cis-trans* cycling of the azobenzene units. Conversely, UV irradiation (which drives the molecules from *trans*- to *cis*-form) appeared to harden the material. Later in 2005, a similar observation from the same group was made in azobenzene-functionalized side-chain polymers.[20] However, the light-induced softening in these systems was shown to be minor compared to the case of heating the polymer film in the dark.[21] In crosslinked azobenzene-containing amorphous and liquid-crystalline polymer networks, UV irradiation has also been reported to decrease the elastic modulus, *i.e.*, to soften the material system, in contrast to the non-crosslinked systems previously reported.[22,23]

In 2005, Karageorgiev and co-workers showed using an AFM-based load-penetration curves that the absolute values for elastic modulus and photoinduced viscosity of the pDR1M polymer can be calculated and the latter decreased many orders of magnitudes under light illumination [24]. They also clearly distinguished between the light-and heat-induced processes by showing that irradiation with linearly polarized light led to the viscoelastic flow only in the direction perpendicular to the light polarization. They address the photoplastization to the segmental softening of the polymer as opposed to the more profound isotropy in the fluidic state.

Recently, depth-sensing indentation called nanoidentation has proven to be a very powerful technique for measuring mechanical properties of materials. Continuous development of indentation equipment offers nowadays a possibility to measure the properties of thin films with high accuracy in the thickness range of hundreds of nanometers. Also, nanoindentation doesn't require the measurement of the spring constant and modeling of the tip shape, which makes it advantageous compared to AFM-based techniques [25]. Indeed, very interesting results of the photoplasticity of chalcogenide glasses have been shown by nanoindentation [26].

In this work, we explore the mechanical properties of a well-known covalent side-chain azo polymer, pDR1A (see Fig. 1a) and a hydrogen-bonded polymer-azobenzene complex, P4VP(DY7)0.5 (Fig. 1b) by nanoindentation. Like many supramolecular polymer systems [27-30], the latter has recently proven very efficient material for SRG formation even though (i) the chromophore DY7 is non-polar, and (ii) its absorption at 488 nm used to inscribe the gratings is quite negligible. Herein, we study the load-depth curves of these two SRG materials with nanoindentation both in dark and under light illumination, and their strain-rate sensitivities are calculated and compared. We demonstrate that amazingly, the supramolecular complex based on nonpolar DY7 dye leads to more pronounced photoinduced viscosity decrease than the conventional and provenly efficient DR1-based acrylate. This suggests that supramolecular materials can not only efficiently compete but may surpass the performance of conventianal covalently-bonded side-chain polymers, when designing the future photomobile materials.

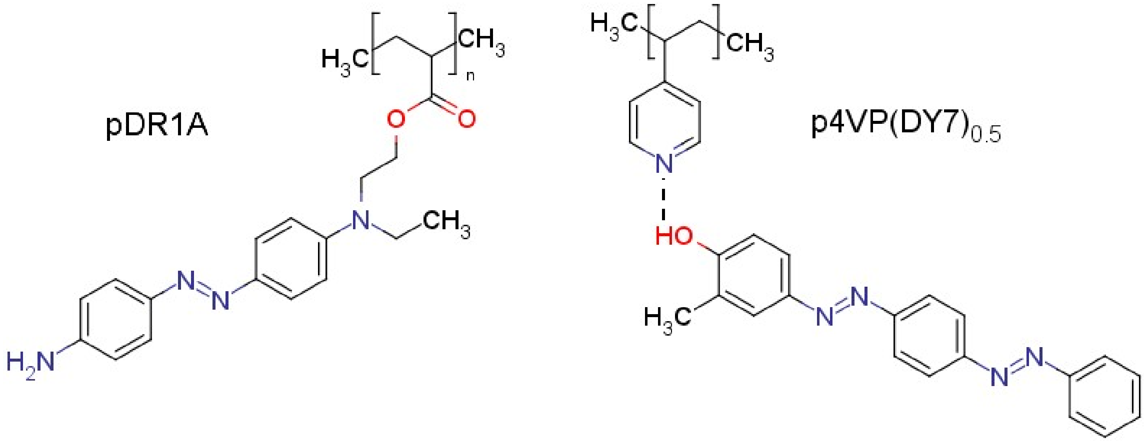

Figure 11: Structures of (a) pDR1a polymer and (b) P4VP(DY7)0.5 polymer-azobenzene complex.

To compare the photoinduced effects on the mechanical properties of these material, we follow the determination of the strain-rate sensitivity, m, introduced by by Mayo and Nix [31]:

$$m = \left(\frac{d[\log \sigma]}{d[\log \dot{\varepsilon}]}\right) \tag{1}$$

Experimentally, the strain-rate sensitivity can then be determined by measuring the strain-rates, $\dot{\varepsilon}$, at certain value of the stress, σ, (at constant depth) and by varying loading-rates. The stress is defined by:

$$\sigma = \frac{P}{A} \tag{2}$$

Where P equals the applied loading force and the projected contact area A at the depth h is calculated by

$$A = C_0h^2 + C1h + C_2h^{\frac{1}{2}} + C_3h^{\frac{1}{4}} \ldots \tag{3}$$

Where the constants C0−C3 depend on the tip geometry
Strain-rate $\dot{\varepsilon}$ can be written in the form

$$\dot{\varepsilon} = \left(\frac{1}{h}\right)\left(\frac{dh}{dt}\right) = \frac{d(\ln h)}{dt} \tag{2}$$

In all the calculations, the depth was replaced by plastic depth as defined in the reference [32].

3.3 Materials and Methods

Poly Disperse Red 1 Acrylate was purchased from Aldrich and used as received. For preparing the hydrogen-bonded complexes, Poly(4-vinylpyridine) (P4VP, Polymer Source, Inc.,Mn=5100g/mol, Mw=5400 g/mol) and Disperse Yellow 7 (DY7, Sigma-Aldrich, 95%) were dissolved in tetrahydrofuran (THF). After being stirred for 24 hours, the stock solutions were mixed to obtain the complexation degree of 0.5, indicating that, on average, every second repeat unit of the polymer is occupied by a chromophore. This solution was then stirred 24 hours before the use.

This particular degree of complexation was chosen, because it has been proven to be the most efficient in SRG formation and the formation of hydrogen-bonding between the constituents has been confirmed by FTIR studies [29].

Films of Poly Disperse Red 1 Acrylate (PDR1A) and Poly 4-Vinyl Pyridine were prepared by spin coating (1000rpm, 750rpm respectively) from solutions of tetrahydrofuran (THF) onto 1cm by 1cm squares of silicon <100> single crystal wafers. The films were annealed under vacuum for 12hrs at 120 °C. The film thicknesses were measured after the indentation experiments using an Ambios XP200 Profiler and were found to be 8mm and 24mm for PDR1A and P4VP(DY7)$_{0.5}$ respectively.

The indentation experiments were performed on a Hysitron Ubi3 indenter (Minneapolis, MN) with a load and displacement resolution of 0.1 mN and 0.2nm respectively. A blunted Berkovitch diamond indenter tip (radius 850nm) was used. The tip area function was calibrated on a fused quartz sample as done in protocols described by the instrument manufacturer based upon the methodology in [33]. Individual indents were separated from each other by at least 20 mm which was several times the average indentation width. A peak indentation load of 500 mN was used for all indents with the loading rates of 500 mN/s, 166.66 mN/s, 50 ms, 10 mN/s and 1mN/s. A solid state 532nm (B & W Tek) laser was used to irradiate the samples with linearly polarized light using a beam power of 15mW/cm^2.

3.4 Results and Discussion

Figure 3.2a shows an example of a typical nanoindentation experiment in dark and under 532 nm light illumination, when load and depth are recorded simultaneously. In this Figure, it is seen that light causes polymer to flow more under the pressure of the nanoindenter compared to the same sample kept in darkness, suggesting that creep might be the dominant light-induced effect on the mechanical properties of this polymer. Figure 2b shows the same depth data plotted against time thus confirming, that when the loading rate is kept constant, the nanoindenter penetrates significantly deeper, when the material is illuminated.

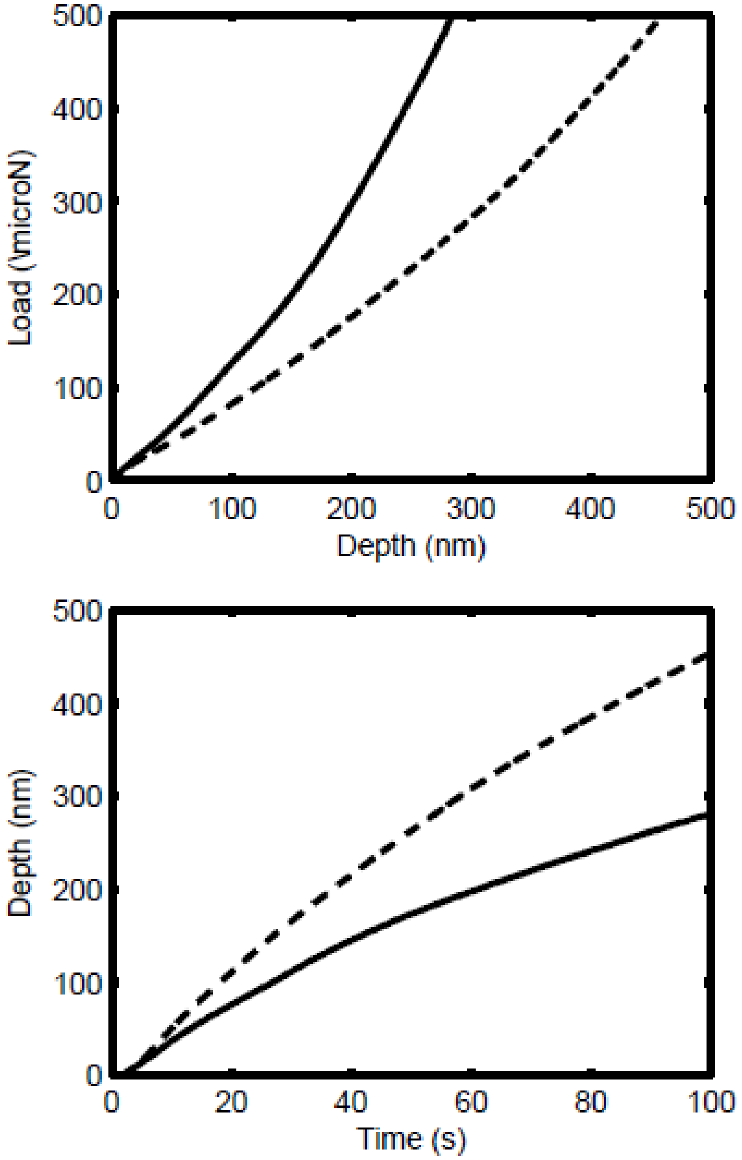

Figure 12: (a) The used nanoindenter load as a function of the penetration depth and (b) the depth as a function of time for loading rate of 5 mN/s, under the illumination of 532 nm light (dashed line) and in darkness (solid line)

For calculating strain-rate sensitivity, the stress and the strain-rate at the depth of 150 nm was determined. The load value for calculating indenter stress (eq. 2) at 150nm was taken from the linear regression of the load against depth curve between the depths 125 and 175nm to avoid minor point-to-point variations in the data. The indentation strain rate (eq. 4) was calculated over the 125-175nm interval as the slope of a regression in a plot of ln(h) over time. The average of the resulting stress strain-rate data pairs for all loading rates were then graphed on a logarithmic scale in Fig. 3a for pDR1a polymer and in Fig. 3b for P4VP(DY7)$_{0.5}$ polymer-azobenzene complex. Strain-rate sensitivities, obtained from the linear regression of these plots were then collected to the Table 1.

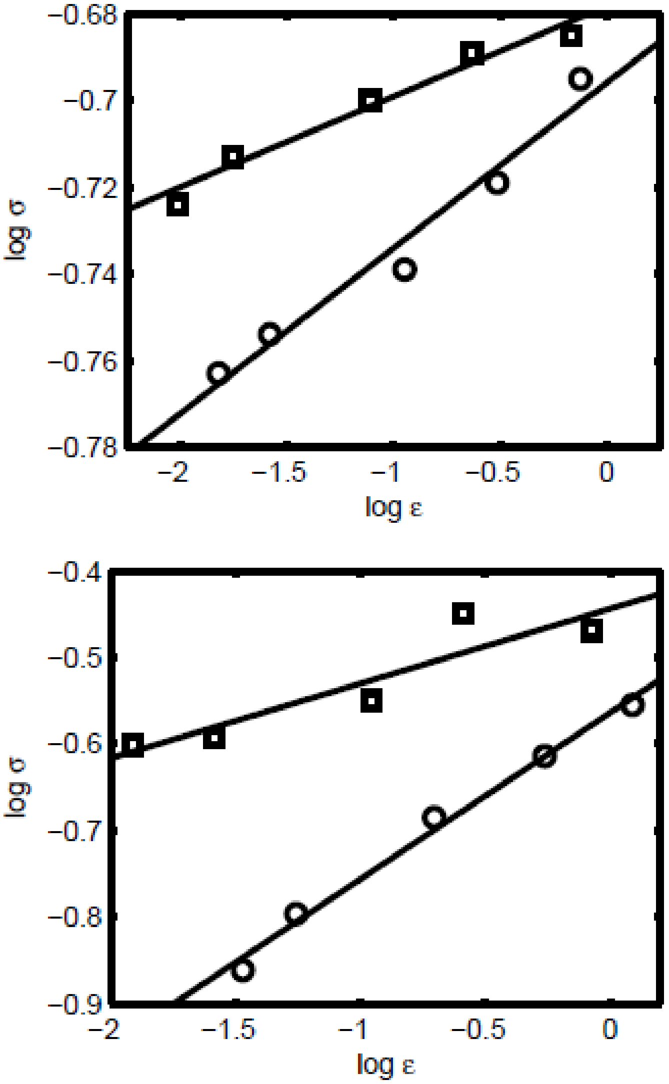

Figure 13: The stress strain-rate data pairs at the depth of 150 nm for (a) pDR1a and (b) P4VP(DY7)0.5 under 532 nm light illumination (open circles) and in darkness (open squares).

As can be seen from the linear fittings in Table 1, the strain-rate sensitivity for the polymers under light illumination increases 81% for pDR1A and 123% for P4VP(DY7)$_{0.5}$ thus proving that (i) photoinduced softening takes place in both materials and (ii) for these illumination conditions the polymer-azobenzene complex is more light-sensitive than the conventional polymer. At this point, more studies are required to explain, what molecular standpoints could explain the difference. In general, the Tg of the polymers is known to increase with increasing cohesive energy density [34] and the fact that under the illumination the azo molecules are constantly changing their conformation between trans and cis is apparently decreasing this energy. To confirm that, it would be tempting to measure the glass transition temperature directly under the light illumination.

Table 3.1: The values of fitted strain-rate sensitivities for both materials under the illumination of 532 nm light and in darkness.

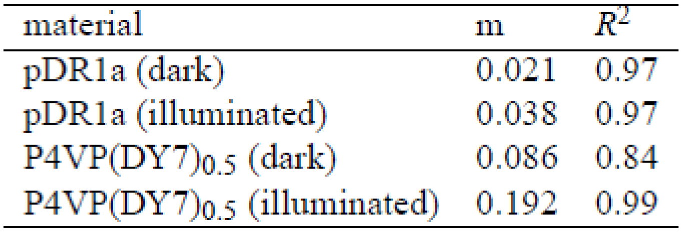

material	m	R^2
pDR1a (dark)	0.021	0.97
pDR1a (illuminated)	0.038	0.97
$P4VP(DY7)_{0.5}$ (dark)	0.086	0.84
$P4VP(DY7)_{0.5}$ (illuminated)	0.192	0.99

The P4VP(DY7)0.5 complex has also the advantage that the single chromophores are more apart from each other than in the homopolymer pDR1a chain. This certainly allows more free space for a single dye molecule to isomerize and might thus increase the cis-concentration in the photostationary state. In general, there are many more additional factors affecting the cis concentration, such as the the quantum yields of the photoisomerization reactions as well as the rate of the thermal cis-trans reaction, and it would be interesting to try to find, if there is any correlation between the steady-state cis concentration and the amount of obtained photoinduced softening.

One should note that, in addition to photoinduced softening, the used linearly polarized light also introduces photoinduced birefringence into the material. Photo-orientation effect is known to be more pronounced in pDR1a and thus the higher induced order might play a role in why there is less photosoftening observed in pDR1a polymer. Also, the intramolecular interactions between the adjacent DR1-based chromophores are more significant compared to the intermolecular interactions of DY7 dyes due to the non-polar nature of the latter ones.

Recently, this polarization-controllable photoinduced softening has been exploited for high resolution photofluidization lithography [35]. This measurement technique provides an excellent base for the insitu exploration of the mechanical properties of azobenzene-based polymers under light illumination and the direct comparison of different materials, as shown in this letter. Much more fundamental research is needed to truly understand the effect of the molecular structure on the photoinduced mechanical properties in order to find the optimal materials for different future applications and to finally solve the mystery behind SRG formation process.

3.5 References

1. Rochon P, Batalla E, Natansohn A (1995) OPTICALLY INDUCED SURFACE GRATINGS ON AZOAROMATIC POLYMER-FILMS. Appl Phys Lett 66 (2):136-138.
2. Kim DY, Tripathy SK, Li L, Kumar J (1995) LASER-INDUCED HOLOGRAPHIC SURFACE-RELIEF GRATINGS ON NONLINEAR-OPTICAL POLYMER-FILMS. Appl Phys Lett 66 (10):1166-1168.
3. Bian SP, Williams JM, Kim DY, Li LA, Balasubramanian S, Kumar J, Tripathy S (1999) Photoinduced surface deformations on azobenzene polymer films. J Appl Phys 86 (8):4498-4508.
4. Nakano H, Tanino T, Shirota Y (2005) Surface relief grating formation on a single crystal of 4-(dimethylamino)azobenzene. Appl Phys Lett 87 (6).
5. Zettsu N, Ogasawara T, Mizoshita N, Nagano S, Seki T (2008) Photo-Triggered Surface Relief Grating Formation in Supramolecular Liquid Crystalline Polymer Systems with Detachable Azobenzene Unit. Advanced Materials 20 (3):516-521.
6. Priimagi A, Saccone M, Cavallo G, Shishido A, Pilati T, Metrangolo P, Resnati G (2012) Submitted. Adv Opt Mater.
7. Emoto A, Uchida E, Fukuda T (2012) Optical and Physical Applications of Photocontrollable Materials: Azobenzene-Containing and Liquid Crystalline Polymers. Polymers 4 (1):150-186.

8. Mahimwalla Z, Yager K, Mamiya J-i, Shishido A, Priimagi A, Barrett C (2012) Azobenzene photomechanics: prospects and potential applications. Polym Bull:1-40.

9. Liu B, Wang M, He Y, Wang X (2006) Duplication of Photoinduced Azo Polymer Surface-Relief Gratings through a Soft Lithographic Approach. Langmuir 22 (17):7405-7410.

10. Na S-I, Kim S-S, Jo J, Oh S-H, Kim J, Kim D-Y (2008) Efficient Polymer Solar Cells with Surface Relief Gratings Fabricated by Simple Soft Lithography. Advanced Functional Materials 18 (24):3956-3963.

11. Hubert C, Rumyantseva A, Lerondel G, Grand J, Kostcheev S, Billot L, Vial A, Bachelot R, Royer P, Chang S-h, Gray SK, Wiederrecht GP, Schatz GC (2005) Near-Field Photochemical Imaging of Noble Metal Nanostructures. Nano Letters 5 (4):615-619.

12. Haggui M, Dridi M, Plain J, Marguet S, Perez H, Schatz GC, Wiederrecht GP, Gray SK, Bachelot R (2012) Spatial Confinement of Electromagnetic Hot and Cold Spots in Gold Nanocubes. ACS Nano 6 (2):1299-1307.

13. Kravchenko A, Shevchenko A, Ovchinnikov V, Priimagi A, Kaivola M (2011) Optical Interference Lithography Using Azobenzene-Functionalized Polymers for Micro- and Nanopatterning of Silicon. Advanced Materials 23 (36):4174-4177.

14. Lee S, Kang HS, Park J-K (2012) Directional Photofluidization Lithography: Micro/Nanostructural Evolution by Photofluidic Motions of Azobenzene Materials. Advanced Materials 24 (16):2069-2103.

15. Barrett CJ, Rochon PL, Natansohn AL (1998) Model of laser-driven mass transport in thin films of dye-functionalized polymers. Journal of Chemical Physics 109 (4):1505-1516.

16. Geue TM, Saphiannikova MG, Henneberg O, Pietsch U, Rochon PL, Natansohn AL (2002) Formation mechanism and dynamics in polymer surface gratings. Physical Review E - Statistical, Nonlinear, and Soft Matter Physics 65 (5):052801/052801-052801/052804.

17. Yager KG, Barrett CJ (2004) Temperature modeling of laser-irradiated azo-polymer thin films. J Chem Phys 120 (2):1089-1096.

18. Veer PU, Pietsch U, Rochon PL, Saphiannikova M (2008) Temperature dependent analysis of grating formation on azobenzene polymer films. Molecular Crystals and Liquid Crystals 486:66/[1108]-1178/[1120].
19. Srikhirin T, Laschitsch A, Neher D, Johannsmann D (2000) Light-induced softening of azobenzene dye-doped polymer films probed with quartz crystal resonators. Appl Phys Lett 77 (7):963-965.
20. Mechau N, Saphiannikova M, Neher D (2005) Dielectric and Mechanical Properties of Azobenzene Polymer Layers under Visible and Ultraviolet Irradiation. Macromolecules 38 (9):3894-3902.
21. Mechau N, Neher D, Borger V, Menzel H, Urayama K (2002) Optically driven diffusion and mechanical softening in azobenzene polymer layers. Appl Phys Lett 81 (25):4715-4717.
22. Kim H-K, Wang X-S, Fujita Y, Sudo A, Nishida H, Fujii M, Endo T (2005) Reversible Photo-Mechanical Switching Behavior of Azobenzene-Containing Semi-Interpenetrating Network under UV and Visible Light Irradiation. Macromolecular Chemistry and Physics 206 (20):2106-2111.
23. Shimamura A, Priimagi A, Mamiya J-i, Ikeda T, Yu Y, Barrett CJ, Shishido A (2011) Simultaneous Analysis of Optical and Mechanical Properties of Cross-Linked Azobenzene-Containing Liquid-Crystalline Polymer Films. ACS Applied Materials & Interfaces 3 (11):4190-4196.
24. Karageorgiev P, Neher D, Schulz B, Stiller B, Pietsch U, Giersig M, Brehmer L (2005) From anisotropic photo-fluidity towards nanomanipulation in the optical near-field. Nat Mater 4 (9):699-703.
25. VanLandingham MR, Villarrubia JS, Guthrie WF, Meyers GF (2001) Nanoindentation of polymers: an overview. Macromolecular Symposia 167 (1):15-44.
26. Trunov ML (2008) Photoplastic effect in non-crystalline materials: A nanoindentation study. Journal of Physics D: Applied Physics 41 (7).

27. Koskela JE, Vapaavuori J, Hautala J, Priimagi A, Faul CFJ, Kaivola M, Ras RHA (2011) Surface-Relief Gratings and Stable Birefringence Inscribed Using Light of Broad Spectral Range in Supramolecular Polymer-Bisazobenzene Complexes. The Journal of Physical Chemistry C 116 (3):2363-2370.
28. Priimagi A, Vapaavuori J, Rodriguez FJ, Faul CFJ, Heino MT, Ikkala O, Kauranen M, Kaivola M (2008) Hydrogen-Bonded Polymer−Azobenzene Complexes: Enhanced Photoinduced Birefringence with High Temporal Stability through Interplay of Intermolecular Interactions. Chemistry of Materials 20 (20):6358-6363.
29. Vapaavuori J, Priimagi A, Kaivola M (2010) Photoinduced surface-relief gratings in films of supramolecular polymer-bisazobenzene complexes. Journal of Materials Chemistry 20 (25):5260-5264.
30. Vapaavuori J, Valtavirta V, Alasaarela T, Mamiya J-I, Priimagi A, Shishido A, Kaivola M (2011) Efficient surface structuring and photoalignment of supramolecular polymer-azobenzene complexes through rational chromophore design. Journal of Materials Chemistry 21 (39):15437-15441.
31. Mayo MJ, Nix WD (1988) A micro-indentation study of superplasticity in Pb, Sn, and Sn-38 wt% Pb. Acta Metallurgica 36 (8):2183-2192.
32. Doerner MF, Nix WD (1986) A method for interpreting the data from depth-sensing indentation instruments. . Journal of Materials Research 1:601-609
33. Oliver WC, Pharr GM (1992) An Improved Technique for Determining Hardness and Elastic-Modulus Using Load and Displacement Sensing Indentation Experiments. Journal of Materials Research 7 (6):1564-1583.
34. Gedde U (1995) Polymer Physics Chapman & Hall, London.
35. Lee S, Kang HS, Park J-K (2011) High-Resolution Patterning of Various Large-Area, Highly Ordered Structural Motifs by Directional Photofluidization Lithography: Sub-30-nm Line, Ellipsoid, Rectangle, and Circle Arrays. Advanced Functional Materials 21 (10):1770-1778.

Chapter 4: Conclusions and Future Work

4.1 Conclusions

This thesis describes novel measurements of the photomechanical effect and seeks to provide a basis for characterization and understanding of the structure-property relationship of azobenzene polymers that are the primary drivers of this effect. A thorough review of the photomechanical effect including surface mass transport and photoinduced motions and modulations for a host of azobenzene based materials is presented in Chapter 1. This includes the significance and current applications of the photomechanical effect in photo-patterning, nanofabrication, actuation, and robotics, demonstrating the need to better understand and characterize the photomechanical effect in order to design of new materials and systems for new and existing applications of azobenzene materials.

To this end, a cantilever based sensor system was adapted to measure the changes in surface stress, photomechanical energy, efficiency, and energy per unit volume of multiple azobenzene based materials. These measurements are used to demonstrate the ability of these thin polymer layers to act as strong light-driven 'artificial muscles' for larger mechanical systems and the utility of the cantilever sensor platform to quantitatively characterize the photomechanical effect of azobenzene based polymers. The experiments demonstrated robust, repeatable and measurable photomechanical effect exhibited by all studied polymers through fast and significant cantilever bending. It was shown that PDR1A exerted the largest forces and PMMA-co-PDR1A the greatest efficiency. The utility of the cantilever sensor platform as a means to compare and understand changes in material response to chemical modifications and changes in film processing of the azobenzene based polymers was demonstrated.

Finally indentation experiments were performed to investigate photosoftening of azobenzene polymers under irradiation. Material creep was characterized by calculation of the strain rate sensitivity *m*, of the two polymers for the dark and illuminated states. The experiments show a significant change in material creep between the dark and illuminated states of both materials. The measured strain rate sensitivity *m* increases by 81 % for PDR1A and 123 % for P4VP(DY7)$_{0.5}$ between the dark and illuminated states respectively. The results correlate with previous data that demonstrates P4VP(DY7)$_{0.5}$ is a highly efficient material to form surface relief gratings and exhibit surface mass transport. The results also highlight the potential of supramolecular strategies in the design of materials with efficient photomechanical response.

4.2 Future Work

This thesis has demonstrated the measurement of photomechanical properties of azobenzene polymers through a modified cantilever based sensor. The sensor system is capable of quantitatively measuring the photomechanical effect for a range of azobenzene based polymers. Future work could focus on a detailed quantification of the structure-property-processing relationship of azobenzene polymers and their photomechanical response. Such data would be a necessary basis to identify and predict chemical substituents and processing conditions necessary to tailor the photomechanical effect for specific applications. For example the results of Chapter 2 demonstrated a marked decrease in photomechanical response of PDR13A from PDR1A highlighting the large impact an *ortho* substitution with chlorine can have upon the photomechanical response. Investigations seeking to identify other substituents capable of similarly increasing or decreasing the material's photomechanical response could be conducted with a carefully chosen set of systematically modified polymers. This would thus enhance our general understanding of the photomechanical effect and correlate the nature of the substituents (e.g. stearically hindered, electron donating, electron withdrawing etc.) to material response. The experimental data in Chapter 2 also suggest that processing conditions of the thin films, in this case the presence of solvent, can affect material response. Other related conditions such as choice of solvent, polymer molecular weight, film thickness, temperature and humidity to name a few, might be similarly important in modifying the photomechanical response.

Finally the nanoindentation experiments demonstrate the ability to probe the mechanical properties of azobenzene polymers under irradiation. Future studies similar to those proposed for the cantilever based sensor system could focus on understanding the effect of molecular structure upon the photoinduced mechanical properties with a view towards solving the mystery behind SRG formation in azobenzene based polymers and designing new materials for applications in nanofabrication. The materials could also be tested using dynamic mechanical analysis (DMA) to measure the polymer's storage and loss moduli and thus derive the viscosity of the azo materials in the dark and under irradiation.